MODELING AND OPTIMIZATION OF SHALE GAS WATER MANAGEMENT SYSTEMS

Alba Carrero Parreño

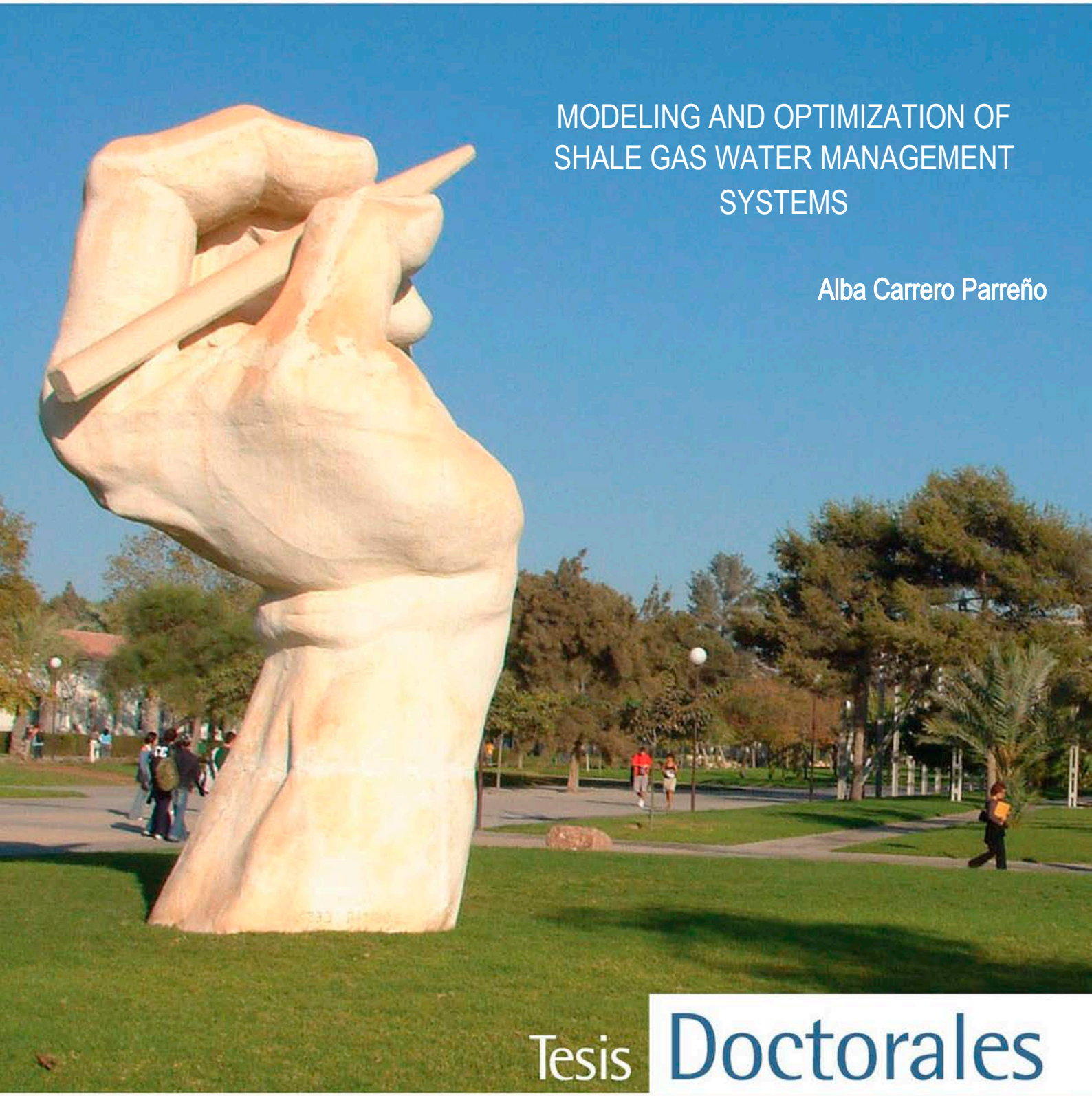

Universitat d'Alacant
Universidad de Alicante

DEPARTAMENTO DE INGENIERÍA QUÍMICA
ESCUELA POLITÉCNICA SUPERIOR

MODELING AND OPTIMIZATION OF SHALE GAS WATER MANAGEMENT SYSTEMS

ALBA CARRERO PARREÑO

Tesis presentada para aspirar al grado de
DOCTORA POR LA UNIVERSIDAD DE ALICANTE

MENCIÓN DE DOCTORA INTERNACIONAL
DOCTORADO EN INGENIERÍA QUÍMICA

Dirigida por:
JUAN ANTONIO REYES LABARTA
RAQUEL SALCEDO DÍAZ

Esta tesis ha recibido financiación de la Unión Europea, programa de Investigación e Innovación Horizonte 2020 bajo el acuerdo de subvención Nº640979

Universitat d'Alacant
Universidad de Alicante
ESCUELA POLITÉCNICA SUPERIOR
Instituto Universitario de Ingeniería de Procesos Químicos

Dr. JUAN ANTONIO REYES LABARTA y Dra. RAQUEL SALCEDO DÍAZ, Catedrático y Profesora Titular del Departamento de Ingeniería Química de la Universidad de Alicante

CERTIFICAN:

Que Dña. ALBA CARRERO PARREÑO, Ingeniera Química, ha realizado bajo nuestra dirección, en el Instituto de Ingeniería de los Procesos Químicos/Dpto. de Ingeniería Química de la Universidad de Alicante, el trabajo que con el título "MODELING AND OPTIMIZATION OF SHALE GAS WATER MANAGEMENT SYSTEMS" constituye su memoria para aspirar al grado de Doctora en Ingeniería Química, reuniendo a nuestro juicio las condiciones necesarias para ser presentada y juzgada por el tribunal correspondiente.

Y para que conste a los efectos oportunos, firmo el presente Certificado en Alicante, Noviembre de 2018.

Fdo. Dr. Juan A. Reyes Labarta

Fdo. Dra. Raquel Salcedo Díaz

Contents

List of tables **7**

List of figures **9**

Abstract **13**

Resumen **17**

Thesis Outline **23**

Esquema de la tesis **25**

Chapter 1. Introduction **27**

1.1 Shale gas extraction 29

1.2 Water quality from hydraulic fracturing 31

1.3 Wastewater management strategies 33

1.4 Mathematical Programming 36

1.5 Environmental analysis 40

Chapter 2. Published papers **45**

Chapter 2.1 Optimal Pretreatment System of Flowback Water from Shale Gas Production **47**

Abstract 47

2.1.1 Introduction 48

2.1.2 Problem Statement 49

2.1.3 Mathematical Programming Model 52

2.1.4 Case Studies 61

2.1.5 Conclusions 66

Chapter 2.2 Holistic Planning Model for Sustainable Water Management in the Shale Gas Industry **69**

Abstract 69

Annexes. Unpublished papers **71**

Annex 1. Optimization of Multistage Membrane Distillation System for Treating Shale Gas Produced Water **73**

Abstract 73

A.1.1 Introduction 73
A.1.2 Problem Statement 76
A.1.3 Mathematical Programming Model 78
A.1.4 Case Studies 86
A.1.5 Conclusions 94
Annex 2. Economic and Environmental Strategic Water Management in the Shale Gas Industry: An Assessment from the Viewpoint of Cooperative Game Theory 99
Abstract 99
A.2.1 Introduction 100
A.2.2 Cooperative game theory: Overview 101
A.2.3 Problem Statement 104
A.2.4 Case studies and discussion 105
A.2.5 Conclusions 117
Chapter 3. Conclusions and Future Works 119
3.1 Conclusions summary 119
3.2 Research contributions 122
3.3 Future Research 122
3.4 Conclusiones 125
Chapter 4. Scientific Contributions 129
4.1 Journal Articles 129
4.2 Book Chapters 130
4.3 Conferences 131
4.4 Research Stay 132
4.5 Award 132
Appendices 133
References 145

List of tables

Table 1.1 Composition data of several randomly flowback water from Barnett and Appalachian Plays....28

Table 1.2 Salinity of the flowback water from various shales expressed in terms of total dissolved solids (TDS)....29

Table 1.3 Mathematical programming model classification....33

Table 2.1.1 Removal factors of component c in equipment t....48

Table 2.1.2 Cost correlations for estimation of capital investment of water pretreatment systems....53

Table 2.1.3 Constraints on outlet water concentration for the case studies....56

Table 2.1.4 Optimal results obtained for the different pretreatment scenarios....56

Table A.1.1 Input data....87

Table A.1.2 Optimal costs (kUS$ $year^{-1}$) of MDS under different recycle connections....89

Table A.1.3 Treated water cost to desalinate shale gas water using MEE-MVR or MDS (US$·$m^{-3}$ shale gas water)....94

Table A.2.1 Characteristic function of each coalition for the three-player games focus in (a) the maximization of gross profit (k$) and (b) minimization of LCIA (points)....111

Table A.2.2 Marginal benefit (k$) of each player estimating the profit allocation based on Shapley value and the Core solution concept....113

Table A.2.3 Environmental impact reduction (%) in the cooperative game case compared to the non-cooperative case for each player, estimating the environmental impact allocation based on the Shapley value and the Core solution concept....114

Table A.2.4 Iteration process of row generation algorithm for eight-player games....115

Table B.1 Process variables for the optimal solution of the MDS model and values obtained from the simulation....131

List of figures

Figure 1.1 U.S. shale gas production with projections to 2050. Total U.S. shale gas production reaches 925 billion cubic meters (bcm) in 2050, over 99.5 % higher than in 2018.....24

Figure 1.2 World shale gas resources (in trillion cubic feet).....25

Figure 1.3 Alternatives for the management of shale gas flowback water: disposal, sent to pretreatment system and reuse the pretreated water or sent to desalination treatment to discharge the water or recycle for other uses.....30

Figure 1.4 Forecast of flowback and produced water generation and water demand over time.....31

Figure 1.5 Generalized Disjunctive Programming solutions methods.....35

Figure 1.6 Life Cycle Assessment framework.....36

Figure 1.8 Relationship between LCI parameters (left), midpoint indicator (middle), and endpoint indicator (right) in ReCiPe 2008.....38

Figure 2.1.1 Multistage superstructure for water pretreatment system (WPS) of flowback water from shale gas production.....43

Figure 2.1.2 Graphical representation of the different case studies.....55

Figure 2.1.3 Effect of the inlet water composition on the total annualized cost (TAC): (a) Case I - Scenarios 1–4; (b) Case II - Scenarios 5–8; and, (c) Case III – Scenarios 9-12.....59

Figure A.1.1 Multistage Membrane Distillation superstructure for treating produced water from shale gas production.....77

Figure A.1.2 Multistage Membrane Distillation superstructure for treating produced water from shale gas production.....78

Figure A.1.3 Direct Contact Membrane Distillation module with heat recovery.....80

Figure A.1.4 Optimal solution of the multistage membrane distillation system (MDS) with heat integration obtained for the base case study.....88

Figure A.1.5 Fractional contribution of various cost elements for the optimal solution of the base case study.....89

Figure A.1.6 Effect of the number of membrane stages in serires on the process cost.....90

Figure A.1.7 Effect of steam cost on the total process cost for the optimal solution of the base case study.....91

Figure A.1.8 Comparative effect of produced water salinity and water recovery on water treatment cost and freshwater cost of the multistage membrane distillation system.....92

Figure A.2.1 Pareto set of solutions (blue circles) for the bi-objective problem that maximizes the gross profit and minimizes life-cycle impact assessment (LCIA) for a cooperative shale gas water management.....106

Figure A.2.2 Disaggregated water-related cost contribution (left axis) and total shale gas revenue (right axis) for cases A, B, C, D & E of shale water management strategies of a three companies (i.e., wellpads, players).....107

Figure A.2.3 Fracturing schedule obtained (a) maximizing revenues, (b) minimizing environmental impacts, and (c) established in advance for each company that maximized its revenue according to shale gas price forecast.....108

Figure A.2.4 Optimal solution of: (a) cooperative with a fixed fracturing schedule (Case C), (b) cooperative (Case D), and (c) non-cooperative (Case E) for shale water management strategies of three companies (i.e., wellpads, players).....109

Figure A.2.5 Environmental impact of the different life cycle stages using ReCiPe Endpoint (H,A) in points/m^3 gas.....110

Figure A.2.6 Comparison between case studies A, B, C, D and E using ReCiPe Endpoint (H,A). a) Comparison between the main impact categories. b) Comparison between subcategories.....110

Figure A.2.7 Geometrical interpretation of the Core and Shapley value to allocate environmental impacts for a three player games.....113

Figure A.2.8 Optimal water-related cost of each player in eight-player games (cooperating and in the absence of cooperation).....115

Figure A.2.9 Optimal shale water management solution of the cooperative game theory of eight companies (i.e., wellpads, players).....116

Figure A.2.10 Comparison of the total environmental impact using ReCiPe Endpoint (H,A) when companies cooperate and in the absence of cooperation.....116

Figure A.2.11 Comparison between the two case studies using ReCiPe Endpoint (H,A). a) Comparison between the main impact categories. b) Comparison between subcategories.....117

Figure B.1 Membrane distillation system process flow diagram in Aspen HYSYS® of the optimal solution for the base case.....131

Figure D.1 Supply chain network of shale gas water management operations.....135

Abstract

Shale gas has emerged as a potential resource to transform the global energy market. Nevertheless, gas extraction from tight shale formations is only possible after horizontal drilling and hydraulic fracturing, which generally demand large amounts of water. Part of the ejected fracturing fluid returns to the surface as flowback water, containing a variety of pollutants. Thus, water reuse and water recycling technologies have received further interest for enhancing overall shale gas process efficiency and sustainability. Thereby, the objectives of this thesis are:

- Develop mathematical models to treat flowback and produced water at various salinities and flow rates, decreasing the high environmental impact due to the freshwater withdrawal and wastewater generated during shale gas production at minimum cost.
- Develop mathematical programming models for planning shale gas water management through the first stage of the well's life to promote the reuse of flowback water by optimizing simultaneously all operations belonging several wellpads.

Within the first objective, we developed medium size generalized disjunctive-programming (GDP) models reformulated as mixed integer non-linear programming problems (MINLPs). First, we focused on flowback water pretreatment and later, in wastewater desalination treatment. Particularly, an emergent desalination technology, Membrane Distillation, has been studied. All mathematical models have been implemented using GAMS® environment.

First, we introduce a new optimization model for wastewater from shale gas production including a superstructure with several water pretreatment alternatives. The mathematical model is formulated via GDP to minimize the total annualized cost. Hence, the superstructure developed allows identifying the optimal pretreatment sequence with minimum cost, according to inlet water composition and wastewater desired destination (i.e., water reuse as fracking fluid or desalination in thermal or membrane techonologies). As each destination requires specific composition constraints, three case studies illustrate the applicability of the proposed approach. Additionally, four distinct flowback water compositions are evaluated for the different target

conditions. The results highlight the ability of the developed model for the cost-effective water pretreatment system synthesis, by reaching the required water compositions for each specified destination.

Regarding desalination technologies, a rigorous optimization model with energy recovery for the synthesis of multistage direct contact membrane distillation (DCMD) system has been developed. The mathematical model is focused on maximizing the total amount of water recovered. The outflow brine is fixed close to salt saturation conditions (300 $g \cdot kg^{-1}$) approaching zero liquid discharge (ZLD). A sensitivity analysis is performed to evaluate the system's behavior under different uncertainty sources such as the heat source availability and inlet salinity conditions. The results emphasize the applicability of this promising technology, especially with low steam cost or waste heat, and reveal variable costs and system configurations depending on inlet conditions.

Within the second objective, large-scale multi-period water management problems, and collaborative water management models have been studied.

Thus, to address water planning decisions in shale gas operations, in a first stage a new non-convex MINLP optimization model is presented that explicitly takes into account the effect of high concentration of total dissolved solids (TDS) and its temporal variations in the impaired water. The model comprises different water management strategies: direct reuse, treatment or send to Class II disposal wells. The objective is to maximize the "sustainability profit" to find a compromise solution among the three pillars of sustainability: economic, environmental and social criteria. The solution determines freshwater consumption, flowback destination, the fracturing schedule, fracturing fluid composition and the number of tanks leased at each time period. Because of the rigorous determination of TDS in all water streams, the model is a nonconvex MINLP model that is tackled in two steps: first, an MILP model is solved on the basis of McCormick relaxations for the bilinear terms; next, the binary variables that determine the fracturing schedule are fixed, and a smaller MINLP is solved. Finally, several case studies based on Marcellus Shale Play are optimized to illustrate the effectiveness of the proposed formulation.

Later, a simplified version of the shale gas water management model developed in the previous work has been used to study possible cooperative strategies among companies. This model allows increasing benefits and reduces costs and environmental impacts of water management in shale gas

production. If different companies are working in the same shale zone and their shale pads are relatively close (under 50 km), they might adopt a cooperative strategy, which can offer economic and environmental advantages. The objective is to compute a distribution of whatever quantifiable unit among the stakeholders to achieve a stable agreement on cooperation among them. To allocate the cost, profit and/or environmental impact among stakeholders, the Core and Shapley value are applied. Finally, the impact of cooperation among companies is shown by two examples involving three and eight players, respectively. The results show that adopting cooperative strategies in shale water management, companies are allowed to improve their benefits and to enhance the sustainability of their operations.

The results obtained in this thesis should help to make cost-effective and environmentally-friendly water management decisions in the eventual development of shale gas wells.

Resumen

El gas de esquisto se ha convertido en un recurso con un gran potencial, transformando el mercado energético global. El desarrollo de la extracción de gas ha generado un crecimiento continuo en la producción de gas natural, que se espera que aumente en los próximos años. El gas de esquisto representó, en el 2000, el 8% de la producción total de gas natural de Estados Unidos. Éste valor aumentó a 49,8% en 2015, y se espera que represente tres cuartas partes (75,2%) de la producción para 2050.

La extracción de este gas, el cual se encuentra en formaciones rocosas compactas, es solo posible con la combinación de dos técnicas: la perforación horizontal y la fractura hidráulica. El problema reside en que estas técnicas requieren una gran cantidad de agua. Además, parte del agua inyectada para fracturar la formación rocosa y extraer el gas, vuelve a la superficie conteniendo gran cantidad de contaminantes. Así, la reutilización del agua contaminada para fracturar nuevos pozos, y el uso de tratamientos de desalinización han recibido un mayor interés en estos últimos años, mejorando la eficiencia y la sostenibilidad del proceso global. Por ello, los objetivos de esta tesis son:

- Desarrollar modelos matemáticos para tratar el agua procedente de la extracción del gas de esquisto, disminuyendo así el alto impacto ambiental debido a las aguas contaminadas generadas y al uso del agua dulce.
- Desarrollar modelos matemáticos para planificar la gestión del agua de gas de esquisto durante la primera etapa de vida del pozo, para fomentar la reutilización del agua contaminada al optimizar de forma simultánea todas las operaciones de varios pozos.

Con respecto al primer objetivo, se ha desarrollado modelos de tamaño mediano de programación disyuntiva generalizada reformulados como un problema de programación no lineal entera mixta. Primero, nos enfocamos en el pretratamiento del agua de retorno, y después en el tratamiento de desalinización. En particular, se ha estudiado una técnica emergente de desalinización, la destilación por membrana. Todos los modelos matemáticos de esta tesis han sido implementados y resueltos utilizando GAMS®.

En primer lugar, se presenta un nuevo modelo de optimización para el pretratamiento de las aguas residuales que provienen de la producción de gas de esquisto. Para ello, se define una superestructura que incluye los siguientes pretratamientos: filtro, electrocuagulación, floculación sedimentación, filtro granular, flotación, ultrafiltración, filtro de cartucho, y, filtro prensa. La función objetivo de este modelo matemático es minimizar el coste total anualizado permitiendo identificar la secuencia óptima de pretratamiento con un coste mínimo, de acuerdo con la composición del agua de entrada y el destino deseado del agua residual, es decir, la reutilización del agua como fluido de fractura o vertido al medio ambiente. Como cada destino requiere restricciones de composición específicas, tres casos de estudio ilustran la aplicabilidad del problema propuesto. Adicionalmente, se evalúan cuatro composiciones de agua de retorno para los diferentes objetivos. Las configuraciones óptimas obtenidas son muy similares, o incluso iguales, para los diferentes casos de estudio: filtro, electrocoagulación, y sedimentación. Los resultados destacan la capacidad del modelo desarrollado para la síntesis de un pretratamiento óptimo para alcanzar las composiciones de agua requeridas para cada destino especificado.

En cuanto a los tratamientos de desalinización, se ha desarrollado un modelo riguroso incluyendo recuperación de energía para el diseño de un sistema de destilación multi-etapa de membranas por contacto directo. Este modelo matemático tiene como objetivo minimizar costes a la vez que maximiza la cantidad de agua recuperada. Por ello, la salmuera de salida se fija cerca de las condiciones de saturación de la sal (300 $g \cdot kg^{-1}$) acercándose a la descarga cero de líquido. Adicionalmente, se han realizado diferentes análisis de sensibilidad para evaluar el comportamiento del sistema bajo diferentes fuentes de incertidumbre, como la disponibilidad de la fuente de calor y las condiciones de entrada. Los resultados destacan la aplicación de esta prometedora tecnología para el tratamiento del agua de retorno que proviene de la extracción del gas de esquisto, especialmente cuando se puede utilizar vapor de bajo coste o calor residual. El coste del tratamiento varía significativamente según el coste de la energía, ya que representa más del 50% del coste total anualizado. Por ejemplo, el coste por metro cúbico de agua tratada para el caso base (salinidad de entrada 200 $g \cdot kg^{-1}$) es de 23.0 US$ por metro cúbico cuando el coste de la energía es alto; 8.3 US$ por metro cúbico cuando el coste de la energía es bajo; y 2.8 US$ por metro cúbico cuando la energía proviene del calor residual de la producción de gas de esquisto. Además, debido a la incertidumbre de la salinidad del agua producida, el

modelo también se verifica mediante un análisis de sensibilidad realizado variando la concentración de sales de 150 a 250 $g \cdot kg^{-1}$. Los resultados revelan que la configuración óptima y el coste del tratamiento dependen significativamente de la salinidad de entrada. Tanto el número de etapas de membrana como el coste total disminuyen a medida que aumenta la salinidad de entrada. Para el valor más bajo de salinidad aplicado en el análisis (es decir, 150 $g \cdot kg^{-1}$), se obtiene un coste de 11.5 US$ por metro cúbico con una configuración compuesta por cuatro etapas. Por el contrario, para el valor de salinidad más alto (es decir, 250 $g \cdot kg^{-1}$), tanto el coste como el número de membranas en el sistema disminuyen a 4.4 US$ por metro cúbico y dos etapas, respectivamente. Aunque el coste total es menor cuando la concentración de entrada es mayor, se debe tener en cuenta que el flujo de permeado obtenido disminuye, lo que implica que solo se recupera una pequeña fracción de la enorme cantidad de aguas residuales producida durante la extraccion del gas. Por tanto, aunque la destilación por membrana puede presentar numerosas ventajas económicas en áreas remotas donde se dispone de calor residual o energía térmica de baja calidad, aún son necesarios más análisis en el laboratorio y pruebas a escala piloto para hacer que esta tecnología sea comercialmente atractiva para los procesos de desalinización de aguas residuales de gas de esquisto.

En cuanto al segundo objetivo, se han desarrollado modelos multi-periodo a gran escala para la gestión integral del agua. En primer lugar, para abordar las decisiones de planificación en las operaciones de gas de esquisto, se desarrolla un nuevo modelo no-convexo de optimización que tiene en cuenta el contenido de sales disueltas. El modelo comprende diferentes estrategias de gestión del agua: reutilización directa, tratamiento y descarga al medio ambiente o envío a pozos de eliminación. El objetivo es maximizar un "beneficio sostenible" para encontrar una solución de compromiso entre los tres pilares de la sostenibilidad: criterios económicos, ambientales y sociales. La solución determina el consumo de agua fresca, el destino del agua de retorno, el programa de fracturación, la composición del fluido de fracturación y el número de tanques alquilados en cada período de tiempo. Este modelo a gran escala se puede resolver eficazmente usando envolventes convexas de McCormick para los términos bilineales, permitiendo así calcular buenos puntos iniciales para el problema general. Para mostrar la efectividad de la formulación propuesta, se han resuelto varios casos de estudio basados en Marcellus Play. Los resultados revelan que la reutilización del agua de retorno es obligatoria para obtener una solución de compromiso entre los tres pilares

de la sostenibilidad: criterios económicos, ambientales y sociales. Además, la solución manifiesta que el nivel de sales en el agua reutilizada no es un obstáculo para poder usar el agua contaminada de retorno como fluido de fracturamiento en nuevas operaciones. Con respecto a las alternativas de gestión de aguas residuales, también se ha demostrado que instalar tratamientos de desalinización en cada asociación de pozos es la solución más rentable. Finalmente, cabe señalar que el impacto más alto tanto económico como ambiente es debido al transporte del agua.

A continuación, se ha utilizado una versión simplificada del modelo matemático desarrollado en el trabajo descrito anteriormente para estudiar posibles estrategias de cooperación entre las diferentes compañías de producción de gas de esquisto, permitiendo aumentar los beneficios y reducir tanto los costes como los impactos ambientales asociados a la extracción del gas. Si diferentes compañías están trabajando en la misma zona y los pozos están relativamente cerca, la cooperación incluye la posibilidad de compartir los costes de transporte de agua dulce y el agua reciclada entre diferentes pozos, reduciendo así la demanda total de agua dulce y los costes de transporte y tratamiento. El objetivo es calcular una distribución de cualquier unidad cuantificable (coste, impacto ambiental, beneficio, etc.) entre las partes interesadas, para lograr un acuerdo estable de cooperación entre ellos. Para hacer esto, utilizamos dos conceptos principales usados en la teoría juegos cooperativos: núcleo del juego y el valor de Shapley. Para mostrar el impacto de la cooperación entre empresas en esta aplicación, se presentan dos diferentes ejemplos que involucran tres y ocho participantes, respectivamente. El ejemplo formado por tres jugadores muestra el compromiso existente entre maximizar el beneficio y minimizar los impactos ambientales en un juego cooperativo y no cooperativo. La asignación de beneficios y de impacto ambiental se realiza utilizando el concepto de núcleo del juego y el valor de Shapley. Luego, se analiza un ejemplo compuesto por ocho jugadores con el objetivo de minimizar el coste total de la gestión del agua. En este caso, el coste de asignación se logra utilizando el algoritmo de generación de filas. Los resultados obtenidos con ambos ejemplos revelan ahorros de alrededor del 30-50% cuando todas las empresas trabajan juntas en lugar de trabajar de forma independiente. El mayor ahorro económico se debe al aumento de la cantidad de agua reutilizada, que reduce al mismo tiempo la extracción de agua del medio ambiente y el transporte.

Dado que el gas de esquisto se ha convertido en una energía puente esencial en la transición de combustibles fosiles hasta lograr la implementación total de

energía renovables, los resultados obtenidos en esta tesis ayudaran a tomar decisiones rentables y respetuosas con el medio ambiente en la gestión del agua que proviene de la explotación de pozos de gas de esquisto.

Thesis Outline

This thesis has been developed in the research group COnCEPT at the Institute of Chemical Processes Engineering of the University of Alicante from October 2015 to November 2018, within the European research project *ShaleXenviromenT - Maximizing the EU shale gas potential by minimizing its environmental footprint* (No. 640979), led by University College London. Part of the specific research finding obtained by working package (08) led by the University of Alicante are summarized in this thesis.

C**hapter 1** introduces the problem of water usage and contamination associated with shale gas extraction. Additionally, a brief overview of mathematical programming and environmental impacts are also included. Within the first objective, we developed medium size GDP models reformulated as MINLPs. First, we focused in flowback water pretreatment (**Chapter 2.1**) and in wastewater desalination treatment, concretely membrane distillation (MD) (**Annex 1**). Within the second objective, large-scale multi-period water management problems (**Chapter 2.2**), and collaborative water management models (**Annex 2**) are developed. **Chapter 3** summarizes the main findings and highlights the main novelties introduced by this thesis. Finally, in **Chapter 4** all the scientific contributions of the candidate are enumerated. The scientific contributions that comprise this thesis, which represent **chapters 2.1-2.2** and **Annexes 1-2,** respectively, are the following:

1. Carrero-Parreño, A.; Onishi, V.C.; Salcedo-Diaz, R.; Ruiz-Femenia, R.; Fraga, E.S.; Caballero, J.A.; Reyes-Labarta, J.A.; Optimal Pretreatment System of Flowback Water from Shale Gas Production. *Industrial & Engineering Chemistry Research*. **2017**. 56(15). p. 4386-4398.
2. Carrero-Parreño, A.; Onishi, V.C.; Ruiz-Femenia, R.; Salcedo-Diaz, R.; Caballero, J.A.; Reyes-Labarta, J.A.; Optimization of Multistage Membrane Distillation System for Treating Shale Gas Water. *Desalination*. **Under review (July 14, 2018).**
3. Carrero-Parreño, A.; Reyes-Labarta, J.A.; Salcedo-Diaz, R.; Ruiz-Femenia, R.; Onishi, V.C.; Caballero, J.A.; Grossman, I.E.; Holistic Planning Model for Sustainable Water Management in the Shale Gas Industry. *Industrial & Engineering Chemistry Research*. **2018.** 57(39).p. 13131-13143

4. Carrero-Parreño, A.; Quirante, N.; Ruiz-Femenia, R.; Reyes-Labarta, J.; Salcedo-Díaz, R.; Caballero, J.A.; Economic and Environmental Strategic Water Management in the Shale Gas Industry: An Assessment from the Viewpoint of Cooperative Game Theory. *ACS Sustainable Chemistry & Engineering*. **Under review (September 20, 2018).**

Esquema de la tesis

Esta tesis ha sido desarrollada en el grupo de investigación COnCEPT en el Instituto de Ingeniería Química de la Universidad de Alicante desde Octubre 2015 a Noviembre 2018, dentro del proyecto Europeo *ShaleXenviromenT - Maximizing the EU shale gas potential by minimizing its environmental footprint* (No. 640979), dirigido por la universidad University College London.

El **Capítulo 1** intoduce los problemas mediambientales que tiene asociado la extracción del gas de esquisto. Además, también se incluye un resumen de las técnicas matemáticas de programación aplicadas. Dentro del primer objetivo, se desarrollan modelos medianos de optimización de programación no lineal entera mixta. Primero nos enfocamos en el pretratamiendo del agua (**Capítulo 2.1**) y porteriormente en su desalinización, utilizando principalmente destilación por membranas (**Anexo 1**). Dentro del segundo objetivo, se desarrollan modelos matemáticos multiperíodo (**Capítulo 2.2**) y modelos cooperativos para la gestión del agua. Finalmente, en el **Capítulo 3** se describen las conclusiones y las contribuciones científicas del doctorando.

Los artículos que constituyen esta tesis, que representan los **capítulos 2.1-2.2** (artículos publicados) y **Anexos 1-2** (artículos en revisión), son los siguientes:

1. Carrero-Parreño, A.; Onishi, V.C.; Salcedo-Diaz, R.; Ruiz-Femenia, R.; Fraga, E.S.; Caballero, J.A.; Reyes-Labarta, J.A.; Optimal Pretreatment System of Flowback Water from Shale Gas Production. Industrial & Engineering Chemistry Research. 2017. 56(15). p. 4386-4398.
2. Carrero-Parreño, A.; Reyes-Labarta, J.A.; Salcedo-Diaz, R.; Ruiz-Femenia, R.; Onishi, V.C.; Caballero, J.A.; Grossman, I.E.; Holistic Planning Model for Sustainable Water Management in the Shale Gas Industry. *Industrial & Engineering Chemistry Research*. **2018.** 57(39).p. 13131-13143
3. Carrero-Parreño, A.; Onishi, V.C.; Ruiz-Femenia, R.; Salcedo-Diaz, R.; Caballero, J.A.; Reyes-Labarta, J.A.; Optimization of Multistage Membrane Distillation System for Treating Shale Gas Water. *Desalination*. **Under review (July 14, 2018).**
4. Carrero-Parreño, A.; Quirante, N.; Ruiz-Femenia, R.; Reyes-Labarta, J.; Salcedo-Díaz, R.; Caballero, J.A.; Economic and Environmental Strategic

Water Management in the Shale Gas Industry: An Assessment from the Viewpoint of Cooperative Game Theory. *ACS Sustainable Chemistry & Engineering*. **Under review (September 20, 2018).**

Chapter 1

Introduction

Natural gas is gaining importance in meeting the world's energy demand. In recent years, the development of shale gas extraction has generated a continuous natural gas production growth, which is expected to increase in the coming years (see **Figure 1.1)**. Shale gas accounted for about 8% of total U.S. natural gas production in 2000, but this value had increased to 49.8% in 2015, and it is expected that three-quarters (75.2%) of the U.S. production will be supplied by shale gas extraction by 2050.[1] This fast increase in natural gas production from shale formations is due to the improvements made in the extraction techniques, such as horizontal drilling and hydraulic fracturing.[2–4]

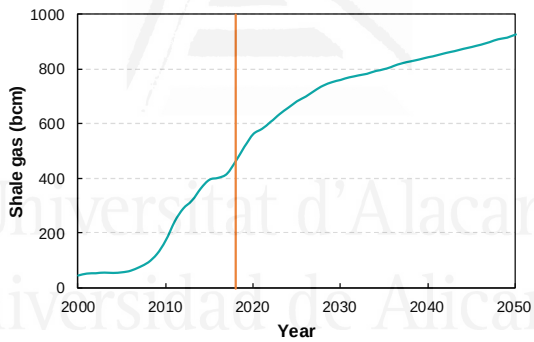

Figure 1.1 U.S. shale gas production forecast. Total U.S. shale gas production reaches 925 billion cubic meters (bcm) in 2050, over 99.5% higher than in 2018.[1]

As a result of such rapid growth, shale gas production has significantly altered the worldwide energy scenario for any foreseeable future.[5,6] However, public attention started in 2007 when the "U.S. Gas Committee" increased its estimates of U.S. gas reserves by 45%, from 32.7 trillion cubic meters to 47.4 trillion cubic meters.[7] Since 2007, the fast development of shale gas in the U.S. has led to a significant drop in the U.S. domestic gas prices. Between 2004 and 2009 the average natural gas price was $6.68 per thousand cubic feet. In 2011, according to Energy Information Administration (EIA), the average wellhead price was $3.95 per thousand cubic feet and February 2012 it went down to $2.46.[8]

Currently, only the United States, Canada, China, and Argentina have commercial production of shale gas.[1] Mexico and Algeria are expected to contribute to the projected growth. Additionally, following the fast growing of shale gas production in the U.S., an increasing interest in shale gas is developing in many European countries.[9] **Figure 1.2** shows the shale gas resources around the world.

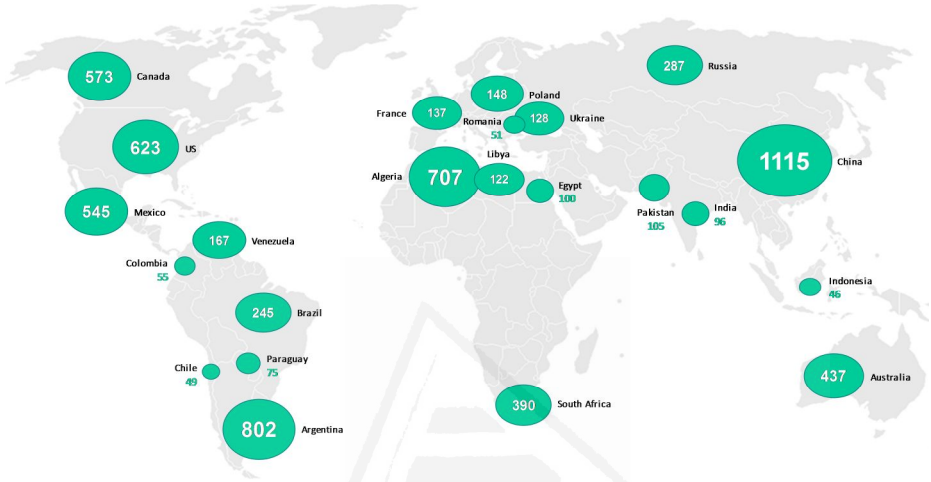

Figure 1.2 World shale gas resources (in trillion cubic feet).[10]

Shale gas production offers important benefits: (1) Replacing coal and petroleum with natural gas will go a long way towards addressing climate change since natural gas produces the lowest CO_2 emissions, concretely 50% less than coal, and none of the toxic pollutants that we find in coal or petroleum. In fact, in the U.S., thanks to the switch from coal to natural gas, the emissions in 2015 was 12% below 2005 levels[10]; (2) It is an essential bridging technology given the transition from fossil fuels to achieve full implementation of renewables, which will still take a few decades. This is especially true given the challenges with the variability of wind and solar energy, and storage of electricity; (3) According to EIA projections, energy consumption shows large growth of natural gas,a large decrease in coal, and significant growth in renewable, but still below natural gas consumption[1]; (4) Shale gas production is helping the U.S. to become energy independent. EIA contemplates that if shale production accelerates, the U.S. could achieve complete energy independence by 2022.[11]

All these benefits make shale gas production very attractive; nevertheless, there is a substantial political and public objection to the hydraulic fracturing process. Mainly, concerns have focused on the possible environmental impacts

of the process. The three major concerns are methane emissions, seismicity activity and, water consumption and contamination due to inappropriate water management. Methane leaks could be easily reduced with tight environmental regulations, and measurement and control.[12] Seismicity activity can be avoided using sustainable water management instead of deep well injection, which potentially contributes to induce earthquakes.[13]

In case of water, cost-efficient water management strategies such as reuse and recycle and, treatment can have a large impact on reducing water consumption and contamination. We introduce in **Section 1.1** the hydraulic fracturing process including freshwater consumption. The water quality that comes from hydraulic fracturing is detailed in **Section 1.2**. Then, **Section 1.3** describes different shale gas water management strategies. **Section 1.4** defines mathematical programming models and the optimization approaches to solve them. The explanation of environmental impact assessment methodologies is given in detail in **Section 1.5**.

1.1 Shale gas extraction

Contrary to conventional gas production where the gas is trapped in the highly permeable reservoir rock, shale basins are characterized by their low-permeability, which hampers gas displacement through rock formations.[14,15] Horizontal drilling and hydraulic stimulation techniques are necessary to release natural gas trapped into shale reservoirs. Both technologies were developed independently, but their combination has had a key impact on shale gas production in the U.S. Without their combination, shale gas production would not be economically feasible. The natural gas would not flow from the formation at high enough rates to justify the cost of drilling.[16]

The horizontal drilling had its origins in the 1940s, but it was in the latter 1970s and 1980s when the first horizontal wells were drilled.[17] While in vertical drilling operators drill the wellbore straight down into the ground, in horizontal drilling once they drill vertically until the desired depth (about 150 meters above the target formation), they gradually turn 90 degrees to continue drilling laterally (between 300 and 1500 meters).[16] As shale gas reservoirs occur in continuous accumulations over large geographic areas, operators drill multiple horizontal wells on every single vertical well. Due to the low permeability of shale formations, horizontal drilling alone is not enough to induce sufficient natural gas, therefore the combination with hydraulic fracturing is crucial.[18] Hydraulic fracturing has not been used exclusively for unconventional gas production, and it has been previously

applied in the oil and gas industry in order to stimulate the hydrocarbon productions when the production declines.

Unconventional well development includes exploration, wellpad construction, well drilling and construction, well treatment and completion (i.e., stimulation) and production. Well drilling and construction typically take between five days to two months, depending on well depth and how familiar operators are with the specific formation.[16] After the well is drilled, the well completion process involves: cleaning the well to remove drilling fluids, perforating the casing that lines the producing formation, inserting the producing tubing, installing the surface wellhead and stimulating the well (i.e., hydraulic fracturing). During the stimulation phase, a fracturing fluid is injected into a well in multiple stages (from eight to twenty-three depending on the lateral length) at high pressure (480–680 bar) and high flow rates (up to 0.3 $m^3 \cdot s^{-1}$).[16,19] Later in the well lifetime, the process can be repeated for re-stimulation as the production declines.[20]

The fracturing fluid is a mixture of base fluid and additives. Normally, it consists of more than 90% of water and 9% propping agent (the most common is sand) and less than 1% of functional additives.[16,21] Additives, including friction reducers, surfactants, corrosion inhibitors, flow improvers, etc, depend on the formation geology and are constantly evolving as operators determine the most effective composition to use for each fracturing job. There are two typical water-based fracturing fluids: slickwater fracturing and gel fracturing. Gel fracturing fluid contains less total base fluid but more additives and proppant. Therefore, it is more complex and sensitive to the quality of the base fluid. Generally, gel fracturing fluid is only used to fracture liquid rich formations.[16]

The challenge with water use is that a large volume of it is required in a short period of time for drilling and stimulation processes (i.e., hydraulic fracturing). It is estimated that well drilling requires from 298 to 383 $m^3 \cdot well^{-1}$ while hydraulic fracturing around 7571–37854 m^3 (2–10 million US gallons) of water per well.[16] The conventional sources for water used in hydraulic fracturing include surface water, groundwater, treated wastewater, and cooling water. The most common one is surface water such as lakes or rivers. The issues commonly faced by water acquisition include seasonal variation in water availability, permitting complexity, and access near the drilling site.

1.2 Water quality from hydraulic fracturing

During the exploration, three types of water can be differentiated: drilling fluid, flowback water, and produced water. The drilling fluid is a heavy, viscous fluid mixture that is used to carry rock cuttings to the surface and to lubricate and cool the drill bill. This water is typically managed onsite and recycled during the drilling operation. After all the stages are fractured, the pressure at the wellhead is released which allows recover between 10-70% of the injected water.[16] This water is called *flowback water* and consists of a portion of the fluid injected combined with the formation water. Typically, volumes range from about 1500 to 4500 m^3 per well per week[22], depending on the type of the well and the formation. Higher volumes of flowback water are generated at the beginning of the process in the first two weeks. The flowrates decrease as the well goes into the production phase. During the production phase, wells produce crude oil, condensates, and/or natural gas and water. This water is called *produced water* and consists of formation water that continues generating throughout the lifetime of the well. The rates again vary depending on the formation but range from less than one cubic meter to 112 m^3 per well per week.[16]

Chemical and physical properties of shale gas wastewater are strongly dependent on different factors, including the shale formation geology, geographic location, contact time between the fracking fluid and rock, as well as the inlet water composition used to fracture the well. Shale gas flowback water usually contains high concentrations of total dissolved solids (TDS), scaling ions such as Ca^{2+}, Mg^{2+} and Ba^{2+}, total organic carbon (TOC) and total suspended solids (TSS), which includes oils, greases, fuels and additives associated with the drilling and hydro-fracturing processes.[23–25] **Table 1.1** presents usual flowback water compositions from several shale gas wells in Barnett and Appalachian plays.

Table 1.1 Composition data of several randomly flowback water from Barnett and Appalachian Plays*

Parameter	Well 1	Well 2	Well 3	Well 4
TDS	200006	54230	110847	9751
TSS	3220	881	1530	168
TOC	200	89	138	38
Fe	92	60	105	40
Ca	14680	4800	3600	241
Mg	4730	1707	899	49
Ba	98	112	127	1
Oil & Grease	0	0	18	0

* Data extracted from reference[26], all values are given in $mg{\cdot}L^{-1}$

The main problem associated with the wastewater produced in shale gas extraction is the high salinity, especially in produced water. Contrary to the quantity of wastewater, which decreases with time, TDS increases. The concentration of TDS in flowback water can range from 8000 $mg \cdot L^{-1}$ to 200000 $mg \cdot L^{-1}$. Produced water can reach up 250000 $mg \cdot L^{-1}$.[16] In addition, this concentration usually presents high geographic variability. **Table 1.2** shows typical TDS values for different USA formations and some available European locations.

Table 1.2 Salinity of the flowback water from various shales expressed in terms of Total Dissolved Solids (TDS).

Shale	Average TDS ($mg \cdot L^{-1}$)	Maximum TDS ($mg \cdot L^{-1}$)
Fayetteville	13000	20000
Woodford	30000	40000
Barnett	80000	> 150000
Marcellus	120000	> 280000
Haynesville	110000	> 200000
Lebien(b)	~16000	~70000
Lubocino	~17000	---
Bowland	130000	---
Germany(a)	100000	180000

(a) Data on specific location is not available.
(b) Data obtained by correlation.

Total suspended solids (TSS) are fine particles with sizes typically lower than 5 µm. Part of the TSS comes from the proppant added to the fracking fluid, usually silica and quartz sand.

The organic compounds (TOC) mainly come from the formulation of the fracturing fluid itself. These organic chemicals emerge at the surface with the flowback water at concentrations initially in the order of 500 $mg \cdot L^{-1}$ and decrease sharply during the first days after the hydraulic fracturing operation.

Hardness is the concentration of scale-forming ions such as calcium, magnesium, barium, strontium, aluminum, or manganese. As can be seen in **Table 1.1**, they are present at variable concentrations and typically up to the order of thousands of milligrams per liter. The major contributions to hardness are Ca^{2+} and Mg^{2+}.[27]

Oil and grease may be present in produced water in free emulsified or dissolved form. Produced shale gas water could contain small amounts of radioactive materials found naturally in shale formations. Some radioactive

isotopes found are uranium, thorium, and radium (Ra-226 and Ra-228). Radium isotopes are the most important due to their higher solubility.[28] Fortunately, in wastewater from shale gas, Normally Occurring Radioactive Materials (NORM) is, in general, very far away from the limits of dangerous concentrations. For example, Almond et al.[28] studied the radioactivity in flowback water from three areas: The Bowland shale in the UK; the Silurian shale in Poland and the Barnett shale in the U.S. They conclude that in the worst-case scenario it did not surpass the 1% exceedance exposure greater than 1 mSv that is the allowable annual exposure in the UK. However, the radiation per energy produced was lower for shale gas than for conventional oil and gas production, nuclear power production or electricity generated through burning coal. When NORM is important, Silva et al.[29] described feasible alternatives for precipitation and removal of radioactive materials.

1.3 Wastewater management strategies

Current water management strategies include disposal of wastewater via Class II disposal wells, transfer to a centralized water treatment facility (CWT), treatment in onsite portable treatment, or direct reuse in drilling subsequent wells. **Figure 1.3** schematically shows the set of all alternatives for shale gas flowback water management.

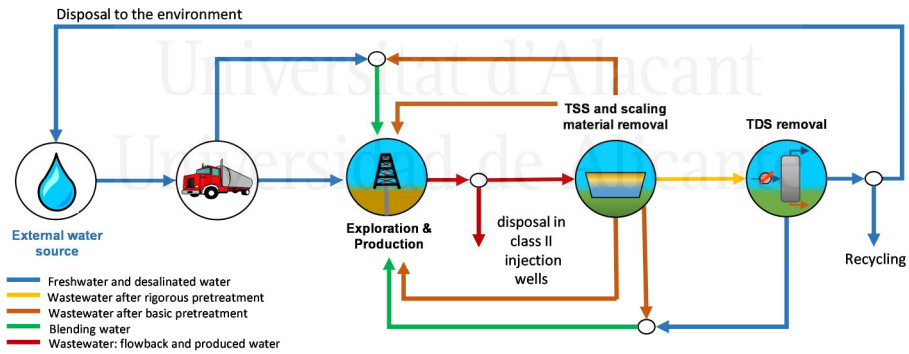

Figure 1.3 Alternatives for the management of shale gas flowback water: disposal, sent to the pretreatment system and reuse the pretreated water or sent to desalination treatment to discharge the water or recycle for other uses.

Direct reuse (after basic treatment) in drilling subsequent wells is currently the most popular option due to its operational simplicity for contractors.[30] The reused flowback is called *impaired water*. This water management option has been possible due to the development of salt-tolerant friction reducers additive.[16,31,32] Previous friction reducers were not compatible with salt-water,

therefore they were not able to control friction pressure losses and associated pump pressure. Moreover, this practice has the potential to decrease the environmental issues associated with shale gas water management such as transportation, direct disposal or treatment. However, friction reducers expenses increase with the concentration of TDS. Additionally, as the number of drilled wells decrease, this practice becomes less attractive. Specifically, as can be seen in **Figure 1.4**, the volume of fracturing fluid required to fracture new wells may be less than the volume of water generated by producing wells in the area. Consequently, operators must find a viable, sustainable and bearable wastewater management alternative when wastewater generation exceeds the water demand for fracturing.

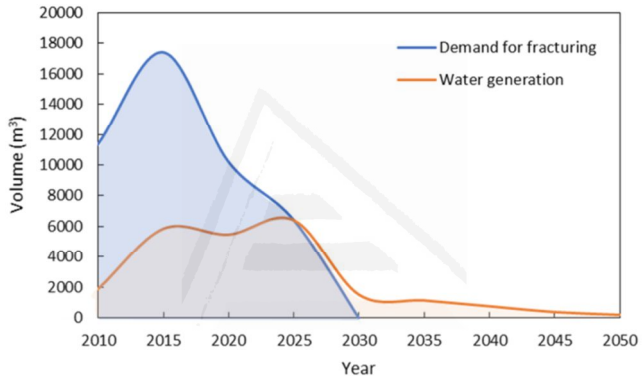

Figure 1.4 Forecast of flowback and produced water generation and water demand over time.[16]

Disposal includes deep well injection into Class II disposal wells, surface wastewater discharge, and evaporation ponds. Disposal in Class II disposal wells has been the most common. This practice has been especially true in the Barnett shale where such disposal sites are available locally and the cost of disposal is relatively cheap at \$1-\$3 bbl^{-1} (\$8.3-\$25.1 m^{-3}). However, in other shales in the U.S., there are no Class II sites and it is necessary to transport the wastewater long distances to be injected. For example, wastewater from Marcellus has been transported by trucks to Ohio and Indiana at a cost around \$4-\$19 bbl^{-1} (\$33.5 - \$159 m^{-3}). Moreover, this solution is not environmentally responsible, apart from represents an environmental drawback in freshwater preservation, there are some concerns related to induce seismicity. For instance, it is known that deep well injection significantly contributes to the generation of seismic activity, being more important than hydraulic fracturing itself in terms of potential risks to induce earthquakes.[13]

Surface water discharge was used in the Marcellus shale area. However, in August 2010 limit surface discharge from Oil and Gas operations was restricted to be less than 500 $mg \cdot L^{-1}$ in TDX (among other specific constituents such as chlorides, sulfates, barium, and strontium) in response to concerns about increasing total dissolved solids (TDS) concentrations in the receiving waters.

Evaporation ponds use the natural water cycle driven by solar energy to evaporate water. It can be a viable option in relatively warm, dry climates with high evaporation rates, level terrain, and low land costs. They are typically economical and employed only for smaller concentrate flows. However, this practice can lead to salt damage to soil and vegetation due to drifting. Therefore, in general, direct disposal is not considered a reasonable option due to environmental regulations and potential public health and safety concerns.[33] Thus, effective water treatment technologies must be developed for desalinating high-salinity produced water.

Different desalination processes can be used for removing TDS contents from shale gas flowback water, e.g. membrane and thermal-based technologies. Obviously, each of these processes should operate under specific water composition constraints for preventing damage and/or to avoid impacting equipment performance. Therefore, water pretreatment systems (WPS) play an important role. They includes several well-established water pretreatment alternatives (e.g., filtration, coagulation, flocculation, dissolved air flotation - DAF, electrocoagulation, softening, sedimentation, membrane treatments, etc.) to remove mainly TSS, oil and grease, and scaling component to avoid decreasing of equipment efficiency.

Regarding desalination technologies, reverse osmosis (RO) is the most universally applicable treatment to desalinate water. Nevertheless, this pressure driven technology can only treat water with TDS concentrations below 40000 - 45000 $mg \cdot L^{-1}$.[14,34] With a higher concentration of salts, RO is not able to overcome the high osmotic back pressure created.[35] Other membrane-based technologies, that are being investigated for this type of water, are forward osmosis[36] and electrodialysis (electrically driven membrane separation technology).[37] On the other hand, regarding thermal technologies, we can find multistage flash (MSF) and multiple-effect evaporation (MEE) with/without mechanical vapor recompression (MVR), that are extensively used in industry due to their applicability to high-salinity conditions and need for simpler pretreatment processes.[38,39] Finally, membrane distillation (MD) is an emerging technology that can be included within the membrane and

thermal technologies. This technology is now under investigation due to the great potential its presents, especially in shale gas operations.[14]

1.4 Mathematical Programming

Mathematical programming techniques are briefly described in this section since they are applied throughout this thesis. There are different options to design chemical processes and their optimal configuration: hierarchical decisions,[40] and superstructure optimization. In this work, we use the superstructure optimization because it maintains all the advantages of the rigorous mathematical programming with minor drawbacks. In this approach, a systematic representation is developed, in which all the alternatives considered as a candidate for the optimal solution and their interconnections are embedded. This representation is called *superstructure*.

Mathematical model formulations

The superstructure is modeled as a mathematical programming problem. Generally, it is described by linear and/or non-linear equations involving continuous, integer, and binary variables. The general formulation can be stated as follows:

$$\begin{aligned} \min\ & z = f(x,y) \\ s.t.\ & h(x,y) = 0 \\ & g(x,y) \leq 0 \\ & x \in X \subseteq \mathbb{R} \\ & y \in \{0,1\} \end{aligned} \tag{1.1}$$

where z the objective function to be minimized, h are the equality constraints that represent physical operation model and/or, mass and energy balances in the problem and g are the inequality constraints that represent bounds and limitations. x are continuous variables which generally correspond to state or design variables (e.g., flow, temperature, concentration, etc.) and y are binary variables. They are restricted to take 0-1 values to define the selection of an item or an action. In this work, the objective is typically to minimize cost or maximize revenue. Depending on the equations and variables involved in the mathematical programming model, it is classified as linear, nonlinear, mixed-integer linear, and mixed-integer nonlinear programming model (see **Table 1.3**). Note that superstructure optimization always involve binary variables since it implies choices.

Table 1.3 Mathematical programming model classification.

Formulation	Equations		Variables	
	Linear	**Nonlinear**	**Continuous**	**Binary**
Linear Programming (LP)	x		x	
Nonlinear programming (NLP)	x	x	x	
Mixed-integer Linear Programming (MILP)	x		x	x
Mixed-integer nonlinear Programming (MINLP)	x	x	x	x

Based on the disjunctive programming proposed by Balas[41], Raman and Grossmann[42,43] developed the Generalized Disjunctive Programming (GDP), which is an alternative approach to the traditional algebraic mixed-integer programming formulation. This formulation is a more intuitive and structured alternative for modelling discrete-continuous optimization problems compared to MINLP. Additionally, the logic structure allows finding the solution to the problem more efficiently.

GDP is a very useful framework for modeling superstructure problems since there will be conditional tasks or equipment that might be selected or not in the final flowsheet (i.e., optimal solution). The decisions are normally associated as to whether certain equipment is included or not in a process flowsheet. The conditional constraints that define the equipment and/or task are represented with disjunctions and assigned a Boolean variable that represents its existence (i.e., the Boolean variable takes a value of 'true'). In general, as in mixers and splitters only mass and energy balances are applied, they are considered permanent. These constraints do not involve any type of discrete decision. A GDP problem can be defined by the following form:

$$
\begin{aligned}
&\min z = f(x) + \sum_{k \in K} c_k \\
&s.t \quad g(x) \le 0 \\
&\bigvee_{i \in D_k} \begin{bmatrix} Y_{k,i} \\ r_{k,i}(x) \le 0 \\ c_k = \gamma_{k,i} \end{bmatrix} \qquad k \in K \\
&\underline{\vee}_{i \in D_k} Y_{k,i} \qquad\qquad k \in K \\
&\Omega(Y) = Verdad \\
&x \in \mathbb{R}^n;\ c_k \in \mathbb{R}^n \\
&Y_{k,i} \in \{Verdad,\ Falso\}, i \in D_k, k \in K
\end{aligned}
\tag{1.2}
$$

Where z is the objective function value and c_k is the cost associated with to the term k in the disjunction. x are the continuous variables and g the set of global constraints. Each disjunction, $\in K$, contains $i \in D_k$ terms, connected by an OR operator. If the disjunction $Y_{k,i}$ is true, then the cost, $c_k = \gamma_{k,i}$, and the constraints that define the equipment, $r_{k,i}(x) \leq 0$, are active, otherwise, they are ignored.

Solution methods

Different solution methods are applied depending on the model formulation. LP models are solved mainly using the simplex method[44] and the interior-point method[45]. In NLP models, we can differentiate between two different problems depending on its convexity. Note that a function is convex if the straight-line segment between any two points on the graph of the function lies above or on the graph. It should be highlighted that if the problem is convex, global solutions are always guaranteed, using global or local optimization solvers. However, for nonconvex NLPs, global optimality is only guaranteed with global solvers. Some examples of local solver are CONOPT[46], IPOPT[47], SNOPT[48], and KNITRO. Global solvers such as BARON[49], ANTIGONE[50] and SCIP[51] require finite upper and lower bounds on the nonlinear expressions to obtain the global optimum. The main methods used for NLP commercial solvers are Newton's method, the successive quadratic programming (SQP) algorithm[52], the reduced gradient method[53] and interior point method[54].

MILP problems are typically solved using branch and bound algorithms[53]. Some of the commercial solvers are CPLEX[55], Gurobi[56], and XPRESS-MP[57]. For MINLP models, decomposition algorithms are usually adapted where each iteration alternates between a MILP master problem and NLP subproblems for convergence. Branch and bound algorithm[58] is not usually effective for this type of problems because solving the NLP subproblems can be costly since they cannot be easily updated as in the case of the MILP. Thus, other decomposition algorithms are also used, such as Generalized Benders Decomposition[57], Outer Approximation[59] (DICOPT), and Extended Cutting Plane[60] (ECP).

To solve the GDP problem, we can apply direct solution methods and reformulation methods as shown in the scheme presented in **Figure 1.5.**

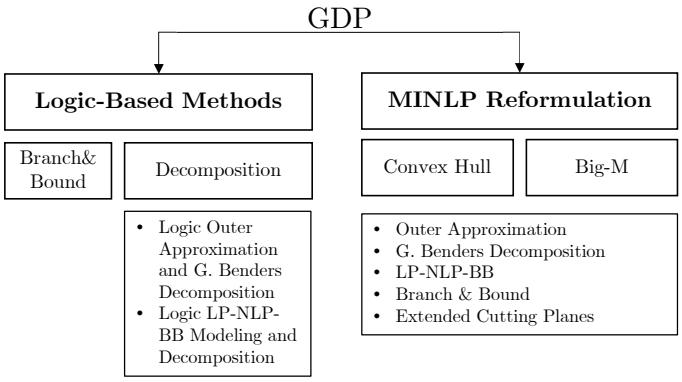

Figure 1.5 Generalized Disjunctive Programming solutions methods.

The two direct solution methods are Branch and Bound proposed by Lee and Grossmann[61] and Logic Based-Outer-Approximation method by Turkay and Grossmann[62].

However, the most direct approach, which is used in this work, consists of reformulating the problem into a MINLP to take advantage of the existing MINLP solvers. To that end, there are basically two alternatives[63], the big-M and the convex hull reformulations. The Big-M and convex hull reformulation of the GDP problem can be expressed as follows **Eqs. (1.3-1.4)**:

$$
\begin{aligned}
&\min z = f(x) + \sum_{k \in K} c_k y_{k,i} \quad \text{(Big-M)} \\
&s.t \quad g(x) \le 0 \\
&\quad r_{k,i}(x) \le M(1 - y_{k,i}) \quad i \in D_k, k \in K \\
&\quad \sum_{i \in D_k} y_{ik} = 1 \qquad k \in K \\
&x \in \mathbb{R}^n;\ c_k \in \mathbb{R}^n \\
&y_{k,i} \in \{0,1\}
\end{aligned}
\tag{1.3}
$$

$$
\begin{aligned}
&\min z = f(x) + \sum_{k \in K} c_k y_{k,i} \quad \text{(Convex Hull)} \\
&s.t \quad g(x) \le 0 \\
&\quad x = \sum_{i \in D_k} v^{i,k} \qquad k \in K \\
&\quad y_{k,i} r_{k,i}(v^{i,k} / y_{k,i}) \le 0 \quad i \in D_k, k \in K \\
&\quad y_{k,i} x^{lo} \le v^{i,k} \le y_{k,i} x^{up} \qquad i \in D_k, k \in K \\
&\quad \sum_{i \in D_k} y_{ik} = 1 \qquad k \in K \\
&x \in \mathbb{R}^n;\ c_k \in \mathbb{R}^n; v^{i,k} \in \mathbb{R}^n \\
&y_{k,i} \in \{0,1\}
\end{aligned}
\tag{1.4}
$$

In these formulations, the binary variable $y_{k,i}$ equals to 1 when the Boolean variable is True, and therefore, the disjunction constraints are enforced. The equation $\sum_{i \in D_k} y_{ik} = 1$ ensures that only one term is selected per disjunction.

In the case of Big-M reformulation, when $y_{k,i} = 0$ and the parameter M is significantly large, the associated constraint becomes redundant. In the convex hull reformulation, the size of the problem increases, with respect to the Big-M reformulation, by introducing a new set of disaggregated variables, $\nu^{i,k}$, and new constraints. The constraint $y_{k,i} x^{lo} \leq \nu^{i,k} \leq y_{k,i} x^{up}$ guarantees that when the binary variables take the value of 1, the disaggregated variable lies within the variables bounds.

The constraints of a disjunction are represented by $y_{k,i} r_{k,i}(\nu^{i,k} / y_{k,i}) \leq 0$, therefore the constraint is enforced when the term is active. In linear constraints, $\mathrm{A}^{k,i} x \leq a^{k,i}$, the perspective function is $\mathrm{A}^{k,i} \cdot \nu^{k,i} \leq a^{k,i} \cdot y_{k,i}$. In nonlinear constraints, the following approximation is used to avoid singularities.

$$y_{k,i} r_{k,i}(\nu^{i,k} / y_{k,i}) = \left((1-\varepsilon) y_{k,i} + \varepsilon\right) r_{k,i}\left(\frac{\nu^{i,k}}{\left((1-\varepsilon) y_{k,i} + \varepsilon\right)_t}\right) - \varepsilon r_{k,i}(0)(1 - y_{k,i}) \tag{1.5}$$

where ε is a small finite number.

Note that, although using the convex hull reformulation the number of variables increases, the relaxation is at least as tight and generally tighter than with Big-M when the discrete domain is relaxed. This is very important since MILP/MINLP solver efficiency relies on the quality of these relaxations. As a general rule, for discrete-continuous optimization models formulated as GDP problems, the hull reformulation should be used always for linear and non-linear but convex constraints. In the case of non-convex constraints, the selection of the best alternative is case-dependent, both the big-M and hull reformulations render non-convex terms.

A comprehensive review of discrete-continuous optimization models through generalized disjunctive programming can be found in the work presented by Trespalacios and Grossmann[64].

1.5 Environmental analysis

Despite the fact that the economy is the driving force in most industries, sustainable development has gained much attention by applying sustainability indicators in the decision-making process.[65] The widely accepted technique for academia and industry is Life Cycle Assessment (LCA)[66], defined in the ISO

14040[67] and 14044[68], 2006. This technique considers environmental impacts associated with all the stages of a product's life from raw material extraction ("cradle") through materials processing, manufacture, distribution, use, repair and maintenance, and disposal ("grave") or recycling ("cradle"). Generally, LCA is divided into four phases: goal and scope definition, inventory analysis, impact assessment, and interpretation. **Figure 1.6** illustrates and defines each phase of LCA.

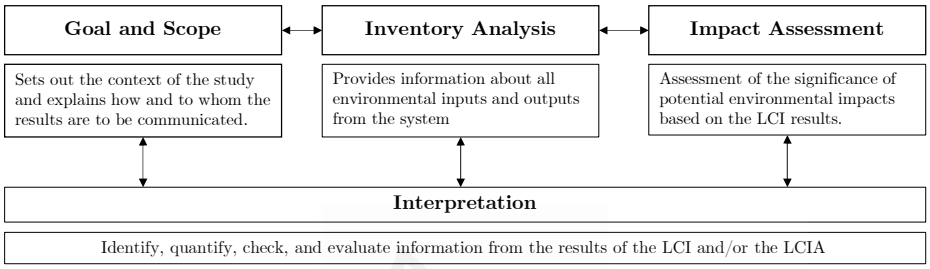

Figure 1.6 Life Cycle Assessment framework.

Two different indicators, Eco-cost[69] and ReCiPe 2008[70], for Life Cycle Impact Assessment (LCIA) have been used in this thesis. Eco-cost data allows "fast track" LCA calculation. Total eco-costs can be regarded as a robust indicator for cradle-to-cradle calculations in LCA for products and services in the theory of the circular economy[69]. The eco-cost method is based on data for emissions of seven toxic substances and four resource depletions. The twelve marginal prevention costs at midpoint level can be combined to 'endpoints' in three groups, eco-costs of human health, ecosystems, resource depletion, plus global warming as a separate group. This indicator is expressed in monetary terms, therefore it is especially advantageous for large models difficult to solve where the multi-objective optimization problem can be reduced to a single-objective. Additionally, the output of this calculation is easy to understand by instinct.

Recently, despite different approaches have being used to develop social LCA, they are still under development. Zore et al.[71] proposed a new metric, called sustainability profit, which includes economic, sustainable (eco-cost) and social indicators. As all the indicators are expressed in monetary terms, only one objective is necessary to consider the three pillars of sustainability in the decision-making process. This metric has been used in **Chapter 2.2** helping to find a sustainable solution in the large shale gas water management mathematical model.

A robust sustainable analysis has been done in **Annex 2**, when the mathematical model has been simplified regarding the solution obtained in **Chapter 2.2**, using in this case, the ReCiPe methodology to evaluate the LCA. This methodology addresses eighteen impact subcategories at the midpoint level: climate change, ozone depletion, terrestrial acidification, freshwater eutrophication, marine eutrophication, human toxicity, photochemical oxidant formation, particulate matter formation, terrestrial ecotoxicity, freshwater ecotoxicity, marine ecotoxicity, ionizing radiation, agricultural land occupation, urban land occupation, natural land transformation, water depletion, mineral resource depletion, and fossil fuel depletion; and three categories at the endpoint level: effect on human health, ecosystem quality and resource depletion.

Figure 1.7 illustrates the relations between the LCI parameter, the midpoint indicator, and the endpoint indicator.

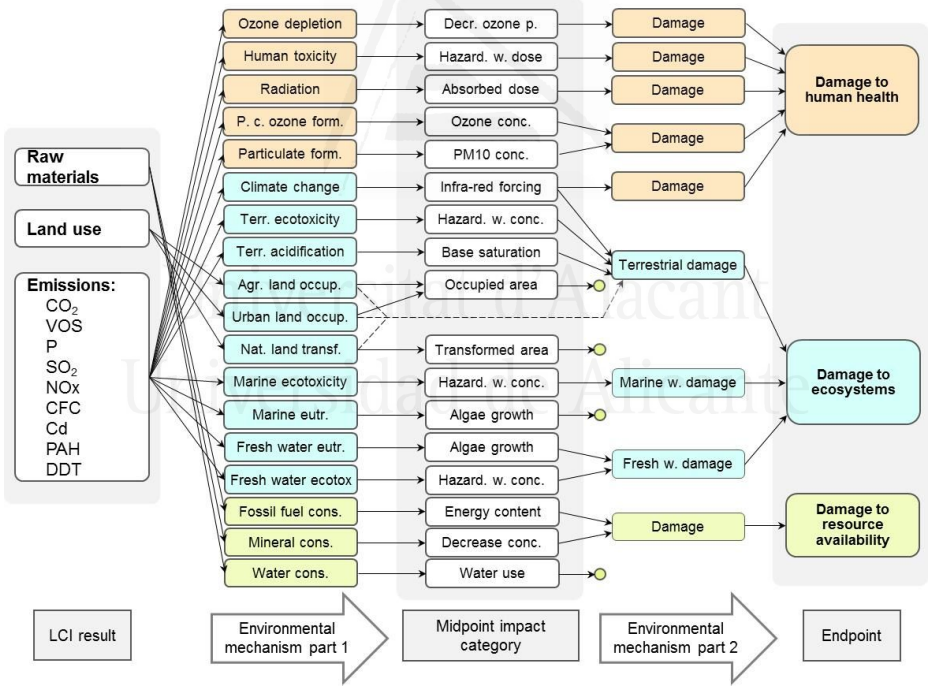

Figure 1.7 Relationship between LCI parameters (left), midpoint indicator (middle), and endpoint indicator (right) in ReCiPe 2008.

The results of this method are expressed in arbitrary "points", which makes difficulty its interpretation. Multi-objective optimization is required to consider both economic and sustainable decisions.

Finally, it should be mentioned that both eco-cost and ReCiPe present large uncertainties due to the different process of normalization and weighting.

Chapter 2

Published papers

I&EC research
Industrial & Engineering Chemistry Research

Article

pubs.acs.org/IECR

Chapter 2.1

Optimal Pretreatment System of Flowback Water from Shale Gas Production

Alba Carrero-Parreño,[†] Viviani C. Onishi,[*,†] Raquel Salcedo-Díaz,[‡,†] Rubén Ruiz-Femenia,[‡,†] Eric S. Fraga,[§] José A. Caballero,[‡,†] and Juan A. Reyes-Labarta[‡,†]

†Institute of Chemical Process Engineering and ‡Department of Chemical Engineering, University of Alicante, Ap. Correos 99, Alicante 03080, Spain

§Centre for Process Systems Engineering, Department of Chemical Engineering, University College London, London WC1E 7JE, U.K.

Received: October 18, 2016
Revised: March 10, 2017
Accepted: March 22, 2017
Published: March 22, 2017

DOI: 10.1021/acs.iecr.6b04016

Abstract

Shale gas has emerged as a potential resource to transform the global energy market. Nevertheless, gas extraction from tight shale formations is only possible after horizontal drilling and hydraulic fracturing, which generally demand large amounts of water. Part of the ejected fracturing fluid returns to surface as flowback water, containing a variety of pollutants. For this reason, water reuse and water recycling technologies have received further interest for enhancing overall shale gas process efficiency and sustainability. Water pretreatment systems (WPSs) can play an important role in achieving this goal. This work introduces a new optimization model for WPS simultaneous synthesis, especially developed for flowback water from shale gas production. A multistage superstructure is proposed for the optimal WPS design, including several water pretreatment

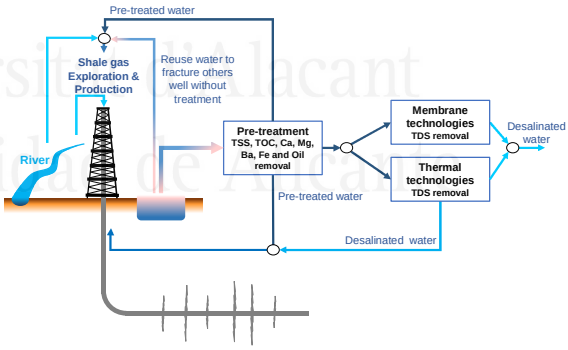

alternatives. The mathematical model is formulated via generalized disjunctive programming (GDP) and solved by reformulation as a mixed-integer nonlinear programming (MINLP) problem, to minimize the total annualized cost. Hence, the superstructure allows identifying the optimal pretreatment sequence with minimum cost, according to inlet water composition and wastewater-desired destination (i.e., water reuse as fracking fluid or recycling). As each destination requires specific composition constraints, three case studies illustrate the applicability of the proposed approach. Four distinct flowback water compositions are evaluated for the different target conditions. The results highlight the ability of the developed model for cost-effective WPS synthesis, by reaching the required water compositions for each specified destination.

2.1.1 Introduction

Water pretreatment systems (WPSs) of flowback water from shale gas production can be composed of several well-established water treatment alternatives (e.g., filtration, coagulation, flocculation, dissolved air flotation - DAF, electrocoagulation, softening, sedimentation, membrane treatments, etc.). Currently, there are different commercial processes for WPS, with their corresponding characteristics and limitations. An important review of the environmental risks and treatment strategies for the shale gas flowback water is addressed to Estrada and Bhamidimarri[17]. Michel et al.[34] have carried out an experimental research of a two-stage water treatment process for treating flowback water, composed by pretreatment and desalination. In the pretreatment step, the authors have considered the following sequence of treatment: filtration; pH adjustment; oxidation; and, sedimentation; while nanofiltration/RO has been performed at the desalination stage. The results obtained highlight the intensive pretreatment requirements before membrane-based desalination becomes possible. Also, Cho et al.[72] have investigated the use of anti-scalants to reduce scale formation in MD desalination of shale gas flowback water.

In the Process Systems Engineering (PSE) field, Beery et al.[73–75] have studied the application of life cycle assessment (LCA) together with a process design tool for seawater pretreatment aimed at RO desalination, including synthesis, simulation, and evaluation of costs and carbon footprint. The authors have proposed a knowledge-based algorithm—focused on previous laboratory experiments[76] —for the process flowsheet decision, considering several pretreatment technologies (e.g., pH adjustment, coagulation and flocculation,

sedimentation, granular filtration, and cartridge filtration). Notwithstanding, it should be emphasized that the seawater pretreatment processes have not been optimized, which can lead to non-optimal solutions.

To the best of our knowledge, there are no systematic mathematical modelling approaches for synthesizing the optimal set of alternatives for WPS, applied to shale gas production. Hence, this chapter introduces a new mathematical model for optimal WPS design for shale gas flowback water. The main novelties introduced comprise: (i) a collection of the main water pretreatment technologies used in shale gas industry within a more comprehensive multistage superstructure; (ii) a detailed cost analysis embracing all water pretreatment alternatives; and, (iii) global optimization of WPS design, considering a large range of feed water compositions and specific composition constraints for each wastewater-desired destination.

2.1.2 Problem Statement

Given is a shale gas flowback water stream with known inlet state (mass flowrate, density, temperature, and concentrations of TDS, TSS, TOC, Fe, Ca, Mg, Ba, and oil) target condition (defined by the wastewater-desired destination) and a set of water pretreatment technologies (strainer filter; hydrocyclone; electrocoagulation; flocculation; sedimentation; granular filtration; DAF; softening; ultrafiltration, cartridge filter; and, filter press) with their corresponding capital and operational costs. The objective is to identify the optimal sequence (minimum total annualized cost) of water pretreatment units that meet the final water specifications according to the desired treated water destination minimizing the capital and operational expenses.

It is worth mentioning that we have not taken into account the possible presence of Normally Occurring Radioactive Materials (NORM) such as uranium, thorium or radium (226Ra, 228Ra) due to in wastewater from shale gas NORM are, in general, very far away from the limits of dangerous concentrations.[28,29]

A knowledge-based superstructure composed of six stages is proposed for the optimal WPS design. In each stage, different water treatment technologies should be used to ensure the requirements on the final components concentrations specified by the wastewater-desired destination (i.e., water reuse or water recycling). Thus, the selection of the superstructure equipment was performed on a stage-by-stage heuristic basis, in order to safeguard the

workability of each upcoming stage. For instance, coagulation/flocculation should come before of sedimentation or dissolved air flotation. The later alternatives, mainly ultrafiltration, are also only possible after sedimentation/DAF/granular filtration. **Figure 2.1.1** displays the multistage superstructure proposed to solve the problem.

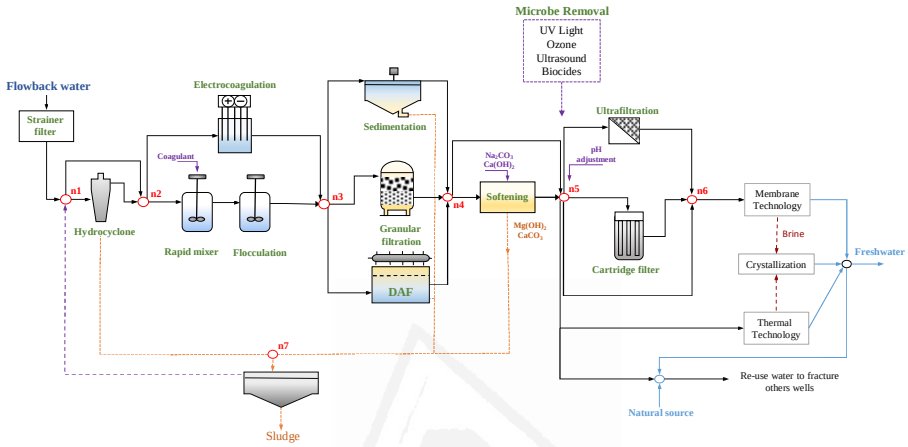

Figure 2.1.1. Multistage superstructure for water pretreatment system (WPS) of flowback water from shale gas production. The selection of the equipment in the superstructure was carried out on a stage-by-stage heuristic basis, in order to safeguard the workability of each upcoming stage (e.g., ultrafiltration is only possible after electrocoagulation/flocculation and sedimentation/filtration/flotation process).

The first stage of the superstructure is a strainer filter to remove larger particles and mud. In the second stage (node 1), the feed water stream can pass through the hydrocyclone or bypass. This decision depends on the inlet TSS composition. Hydrocyclones are important equipment for solid–liquid separation due to their simple design, low capital investment, low maintenance, and easy operation[77].

In the third stage (node 2), a decision should be made between coagulation and flocculation or electrocoagulation processes (EC). In general, the coagulation process is dominant due to its lower capital and operational costs in comparison with other available methods. In this process, coagulants are used to induce TSS and TOC growth, including metals salts (typically Fe and Al) and polymers. However, the EC process emerges as a potential technology for the pretreatment of shale gas flowback water, due to its ability to remove particles that are usually difficult to separate by other conventional treatments (including filtration and chemical treatments). Additionally, EC provides active cations without growing the salinity of the water.[78,79] The pH

control necessary for operating these units in different conditions is implicitly included in each unit operation.

The objective of the fourth stage (node 3) is to eliminate the particles/flocs formed in previous stages of the WPS. Three different water treatment alternatives are considered in this stage: sedimentation; granular filtration; and, DAF. Sedimentation is the cheapest option, but its efficiency is lower than granular filtration and DAF. Granular filtration is the most efficient option for TSS concentrations ranging from 50 to 100 mg L^{-1}.[80] Nevertheless, this process needs continuous backwashing to avoid decreasing of equipment efficiency. DAF is the usual method for eliminating oil and suspended solids.[81] In stage 5, there are two possibilities. The water could be treated by a softening process or it could pass through a bypass. These two alternatives are not exclusive, in other words a part can be treated, and the rest go through the bypass. The selection should be made based on the presence of scale forming cations (Ca, Mg, Ba, etc.). These contaminants can produce fouling in pipes by the increase in the temperature, promoting the diminution of the performance of the thermal technologies. The most common softening method is the cold lime-based process. In this case, lime ($Ca(OH)_2$) is added to remove Mg^{2+} and Ca^{2+} as calcium carbonate and magnesium hydroxide, respectively. Non-carbonated hardness is removed using soda ash (Na_2CO_3) Still, the pH should be adjusted to 4 to stabilize the scale forming cations.[82]

In stage 6 (node 5), the flowback water can be treated by ultrafiltration or a cartridge filter or it could pass through a bypass. This stage is considered in the superstructure because the water can be reused to fracture other wells, or it can be further treated for recycling by thermal or membrane-based desalination technologies. As membrane-based desalination methods are very sensitive to the feed composition, the last stage serves as a protection barrier against micro-particles that could foul and/or damage the membrane system elements.[83,84] Disinfection is critical for fracturing fluids since an excess of bacteria can produce equipment corrosion and cause the formation of sour (H_2S) fluids.[85] Bacteria can be destroyed using various technologies such as ultraviolet light, ozone, ultrasound or biocides.[86]

Some of the operations mentioned above produce a sludge with different solid concentrations (from a typical 45% w.w. in sedimentation to 5% w.w. in DAF). In order to recover as much water as possible to reach the objective of Zero Liquid Discharge (ZLD), the sludge is sent to a filter press and the water produced by filtration is returned to the WPS to be treated.

2.1.3 Mathematical Programming Model

The mathematical model is formulated using GDP and optimized as an MINLP problem, wherein binary variables represent the discrete decisions about the existence or selection of an equipment (water pretreatment technology) in a stage of the superstructure. It comprises the design equations for each water treatment technology, including mass balances at each node, sizing and costing equations, unit design equations, and the objective function (minimization of the total annualized cost). Due to the lack of correlations to predict the behavior of all components in each treatment unit, the aforementioned equipment's are mathematically modeled via short-cut models based on contaminants' removal ratios. In addition, outlet water conditions (i.e., wastewater obtained after the pretreatment sequence) should satisfy some requirements defined by its desired destination (i.e., water reuse or water recycling). Therefore, these composition requirements should be expressed as design constraints in the optimization model. Note that throughout the mathematical model description, lower case letters are used for variables and capital letters for parameters. The following data is assumed to be known:

$F^{feed,water}$	Water flow rate ($m^3 \cdot h^{-1}$)
S_c^{feed}	Concentration of contaminant c in feed stream ($kg \cdot m^{-3}$)
F_c^{feed}	Individual component c flowrate ($kg \cdot h^{-1}$)
u_t	Set of specific design parameters for equipment t (e.g. loading rate in sedimentation or DAF, etc.)
γ_t	Weight fraction of solids in outlet sludge stream for equipment t
$\alpha_{c,t}$	Removal factor of component c in equipment t
DT_t	Detention time (min) for coagulation, flocculation, electrocoagulation and softening.
ρ	Feed water density ($kg \cdot m^{-3}$)
LR_t	Loading rate of sedimentation, flotation, granular filtration and strainer filter ($m \cdot h^{-1}$)

Set definition

In order to clearly define the problem, we define the following index sets.

C = $\{c / c$ is a feed water component$\}$
[TDS; TSS; TOC; Fe; Ca; Mg; Ba; oil; H_2O]

N = $\{n / n$ is a node$\}$
[Nodes n1 to n7]

R = $\{r / r$ are the post-treatment desalination alternatives or water reuse$\}$
[MT = membrane treatment; TT = thermal treatment; WR = water reuse]

T = $\{t / t$ is a pre-treatment unit$\}$
[sf = strainer filter; hy = hydrocyclone; co = coagulation; flo = flocculation; ec = electrocoagulation; sd = sedimentation; gf = granular filtration; df = dissolved air flotation; sof = softening; uf = ultrafiltration; cf = cartridge filtration; pf = press filter; $b1$ = bypass 1; $b2$ = bypass 2]

$IN_{t,n}$ = $\{$outlet stream from a technology t is an input to node $n\}$

$OUT_{t,n}$ = $\{$inlet stream to technology t is an output from node $n\}$

SLU_t = $\{$sludge stream from technology t (if any) is an input to $pf\}$

Mass balance in the first stage

The mass balance in the first stage of the superstructure is defined by the following equation.

$$F_c^{feed} = f_{c,sf}^{in} \qquad \forall c \in C \tag{2.1.1}$$

Mass balances in the nodes (nodes 1-7)

The mass balances in the nodes 1 to 6 are given by the following equation.

$$\sum_{t \in IN_{t,n}} f_{c,t} = \sum_{t \in OUT_{t,n}} f_{c,t} \qquad \forall c \in C,\ n \in N \neq n7 \tag{2.1.2}$$

In node 4, the outlet flow could pass through both alternatives. Consequently, **Eq. (2.1.3)** must be added.

$$f_{c,t}^{out} \cdot \sum_{t \in IN_{t,n}} f_{c,t} = f_{c,t}^{in} \cdot \sum_{t \in OUT_{t,n}} f_{c,t} \qquad \forall\ c \in C,\ n \in N = n4 \tag{2.1.3}$$

The mass flowrate at the entrance of the filter press (node 7) is expressed by **Eq. (2.1.4)**.

$$f_{c,pf}^{in} = \sum_{t \in SLU_t} f_{c,t} \qquad \forall c \in C \tag{2.1.4}$$

Equipment design

The design equations related to a given pretreatment technology should be active only if the related equipment is selected in the WPS. Otherwise, the mass flowrates, equipment capacities, and all variables associated with the referred unit should be equal to zero. To this end, we define a Boolean variables Yt that takes the value «True» if the technology t is selected and «False» otherwise, and introduce the following disjunctions

$$\begin{bmatrix} Y_t \\ f_{c,t}^{in} = f_{c,t}^{out} + f_{c,t}^{slud} \quad \forall c \in C \\ \left(Sizing\ parameters\right)_t = f\left(f_t^{in}, u_t\right) \\ f_{H_2O,t}^{slud} = \dfrac{(1-\gamma_t)\cdot \sum_{c \neq H_2O\, t \in SLU_t} f_{c,t}}{\gamma_t} \\ f_{c,t}^{out} = (1-\alpha_{c,t})\cdot f_{c,t}^{in} \end{bmatrix} \veebar \begin{bmatrix} \neg Y_t \\ f_{c,t}^{in} = f_{c,t}^{out} = f_{c,t}^{slud} = 0 \quad \forall c \in C \\ \left(Sizing\ parameters\right)_t = 0 \end{bmatrix}$$

$$\forall t \in \{sf, hy, co, flo, ec, sof, uf, cf, pf\} \qquad (2.1.5)$$

$$0 \geq f_{c,t}^{in} \geq F_c^{UP}$$

$$\begin{bmatrix} Y_t \\ f_{c,t}^{in} = f_{c,t}^{out} + f_{c,t}^{slud} \quad \forall c \in C \\ \left(Sizing\ parameters\right)_t = f\left(f_t^{in}, u_t\right) \\ f_{H_2O,t}^{slud} = \dfrac{(1-\gamma_t)\cdot \sum_{c \neq H_2O\, t \in SLU_t} f_{c,t}}{\gamma_t} \\ \begin{bmatrix} Y1_t \\ f_{c,t}^{out} = (1-\alpha 1_{c,t})\cdot f_{c,t}^{in} \end{bmatrix} \veebar \begin{bmatrix} Y2_t \\ F_{c,t}^{out} = (1-\alpha 2_{c,t})\cdot f_{c,t}^{in} \end{bmatrix} \end{bmatrix} \veebar \begin{bmatrix} \neg Y_t \\ f_{c,t}^{in} = f_{c,t}^{out} = f_{c,t}^{slud} = 0 \quad \forall c \in C \\ \left(Sizing\ parameters\right)_t = 0 \end{bmatrix}$$

$$\forall t \in \{sd, df, gf\} \qquad (2.1.6)$$

$$0 \geq f_{c,t}^{in} \geq F_c^{UP}$$

In the left term of the disjunction given by **Eq. (2.1.5)** and **(2.1.6)**, the first equation represents the mass balance in the technology t, where, $f_{c,t}^{out}$ and $f_{c,t}^{slud}$ are the inlet, outlet and sludge flow of component c and technology t. The second one is the sizing equations to estimate the critical design parameters (usually the volume or area) of each unit. It depends on the inlet flowrate and specific design parameters «u_t» (e.g. detention times, loading rates, etc.). The design variables are required for the equipment sizing and estimation of capital investment.

The third equation calculates the water in the sludge stream. It is a function of the weight fraction of solids in the sludge stream (γ_t) for each technology. [29,87,88]

The relation between inlet and outlet mass flowrates is modeled by using removal factors ($\alpha_{c,t}$). These removal factors can be based on heuristics, manufactures recommendations and/or literature. See Beery et al.[76] for TSS removal by granular media filters (~93%); Fakhru'l-Razi et al.[89] for oil removal (~92%–97%), TOC (98%) and scale inhibition via coagulation, oil removal via DAF (99.3%–99.9%), and TOC (~98%) and oil (>99%) removal efficiencies by ultrafiltration; Houcine[90] for heavy metal removal through lime softening (>95%); Bilstad and Espedal[91] for oil removal via hydrocyclones (>90%). Additionally, in this work, the removal efficiencies for all components via filter press is considered equal to 90%.[89] A summary of all the removal factors can be found in **Table 2.1.1.** Clearly, these factors can be easily changed in the model.

Table 2.1.1 Removal factors of component c in equipment t**

(c)	Technologies (t)									
	Hy 54	**co -sd** 72	**ec-sd** 72	**co-gf** 72	**ec-gf** 72	**co-df** 7254	**ec-df** 7254	**uf, cf** 54	**sof** 74	**fp** 54
TSS	73	37.5	97.2	37.5	97.2	37.5	97.2	100		90
TOC		51	19	51	19	51	19	90		90
Fe		8	84	8	84	8	84	90		90
Ca			37				37		100	90
Mg									100	90
Ba									100	90
Oil						100	100	99		90

** Data extracted from references [89,92–94]

An embedded disjunction has been described in **Eq. (2.1.6)**, in order to include two different removal factors for sedimentation, DAF and granular filtration, depending on whether the flocs are formed by coagulation or electrocoagulation. The model is solved by reformulating the disjunctive representation of the problem as an MINLP model. To that end, we use a hull reformulation.[63] First, we define a set of binary variables (y_t) that will take the value 1 if the Boolean variable Y_t takes the value of «True» and zero otherwise. The equations form the reformulations of disjunctions **(2.1.5)** and the common part of **(2.1.6)** are the following:

$$
\begin{aligned}
& f_{c,t}^{in} = f_{c,t}^{out} + f_{c,t}^{slud} && \forall c \in C;\ \forall t \in T \\
& (Sizing\ parameter)_t = \left((1-\varepsilon)y_t + \varepsilon\right) f\left(\frac{f_t^{in}}{\left((1-\varepsilon)y_t + \varepsilon\right)}, u_t\right) - \varepsilon f(0)(1-y_t)\ \forall t \in T && \\
& f_{H_2O,t}^{slud} = \frac{(1-\gamma_t)\sum_{c|c\neq H_2O\ t\in SLU_t} f_{c,t}}{\gamma_t} && \forall t \in T \\
& \left.\begin{aligned} & f_{c,t}^{out} = (1-\alpha_{c,t}) f_{c,t}^{in};\quad f_{c,t}^{in} \le F_c^{UP} y_t \\ & f_{c,t}^{out} \le F_c^{UP} y_t;\quad f_{c,t}^{slud} \le F_c^{UP} y_t \end{aligned}\right\} && \forall c \in C;\ \forall t \in T \\
& f_{c,t}^{out} \ge 0;\ \ f_{c,t}^{in} \ge 0;\ y_t \in \{0,1\} &&
\end{aligned}
\tag{2.1.7}
$$

The second equation in **Eq. (2.1.7)** corresponds to the general hull reformulation. See Trespalacios and Grossmann[64] for a detailed explanation of this reformulation in the case of nonlinear equations. If the size equation is linear then the binary variables appear only multiplying constant terms.

For the embedded terms in disjunction **Eq. (2.1.6)** we need to define two new binary variables y1 and y2. The reformulation is as follows:

$$
\begin{aligned}
& y_t = y1_t + y2_t && \forall t \in \{sd, df, gf\} \\
& \left.\begin{aligned} & f_{c,t}^{out} = f1_{c,t}^{out} + f2_{c,t}^{out} \\ & f_{c,t}^{in} = f1_{c,t}^{in} + f2_{c,t}^{in} \\ & f1_{c,t}^{out} = (1-\alpha 1_{c,t})\, f1_{c,t}^{in} \\ & f2_{c,t}^{out} = (1-\alpha 2_{c,t})\, f2_{c,t}^{in} \\ & f1_{c,t}^{in} \le F_c^{UP} y1_t \\ & f1_{c,t}^{out} \le F_c^{UP} y1_t \\ & f2_{c,t}^{in} \le F_c^{UP} y2_t \\ & f2_{c,t}^{out} \le F_c^{UP} y2_t \end{aligned}\right\} && \forall t \in \{sd, df, gf\}\ \forall c \in C \\
& f_{c,t}^{out} \ge 0;\ \ f1_{c,t}^{out} \ge 0;\ \ f2_{c,t}^{out} \ge 0; && \\
& f_{c,t}^{in} \ge 0;\ \ f1_{c,t}^{in} \ge 0;\ \ f2_{c,t}^{in} \ge 0; && \\
& y_t \in \{0,1\}; y1_t \in \{0,1\};\ y2_t \in \{0,1\} &&
\end{aligned}
\tag{2.1.8}
$$

The equipment sizing equations of each technology are the following. The equipment volumes for coagulation, flocculation, electrocoagulation and softening processes, are calculated with **Eq. (2.1.9)**.

$$
v_t = \frac{DT_t}{\rho} \cdot \sum_{c\in C, t\in IN_{t,n}} f_{c,t} \qquad t \in \{co, flo, ec, sof\} \tag{2.1.9}
$$

In which DT_t is the detention time in minutes for equipment *t*. A detention time equal to 30 min is used to model the flocculation and electrocoagulation

units, while 5 and 15 min are considered for coagulation and electrocoagulation, respectively.[81,95,96] ρ indicates the feed water density considered as a parameter in the mathematical model.

Equipment for sedimentation, dissolved air flotation, granular filtration and filter press are typically designed by considering the loading rate (LR) for the equipment t . Data based on experience show that typical LR values are equal to 3 $m \cdot h^{-1}$ for sedimentation, 10 $m \cdot h^{-1}$ for dissolved air flotation, 10 $m \cdot h^{-1}$ for filter media, and 3 $m \cdot h^{-1}$ for filter press. The transversal area of these equipment is given by the next equation.

$$a_t = \frac{1}{\rho \cdot LR_t} \cdot \sum_{c \in C, t \in IN_{t,n}} f_{c,t} \qquad t \in \{sd, daf, gf, sf\} \tag{2.1.10}$$

There are many empirical models in literature for the design of hydrocyclones, the model proposed by Bradley[97] is used in this work.

$$d_{hy} = 0.01 \cdot \left(14 \frac{\rho_p - \rho}{4500 \cdot \tau}\right)^{0.33} \cdot \sum_{c \in C, t \in IN_{t,n}} \left(\frac{f_{c,t}}{\rho}\right)^{0.17} \tag{2.1.11}$$

In which d_{hy} is the hydrocyclone diameter, τ is the fluid dynamic viscosity and ρ_p is the particle density. The volume of the hydrocyclone can be calculated as follows.

$$v_{hy} = 1.096 \cdot d_{hy} - 0.346 \tag{2.1.12}$$

Design and specification constraints

Some separation technologies have constraints related to their performance, or the type of components they can deal with. In particular, granular filtration works more effectively when TSS concentration is lower than 100 $mg \cdot L^{-1}$.[76] Therefore, the following constraint should be added to the WPS model to avoid equipment clogging:

$$f_{TSS,gf}^{in} \leq \frac{0.1}{\rho} \cdot \sum_{c \in C} f_{c,gf} \tag{2.1.13}$$

Specification constraints are still necessary to ensure that the required composition is achieved for each desired destination (i.e., water reuse or desalination treatments such as thermal or membrane-based technologies). Note that the requirements for water reuse to fracture other wells are company dependent. As aforementioned, if membrane technologies are considered for the treatment (desalination) of the wastewater, it is essential to

reduce TSS, iron, oil and forming particles to avoid fouling problems.[72] In fact, membrane fouling can cause reduction in the treated flow, as well as an increase in the operating pressure, requiring expensive cleaning cycles. Additionally, membrane-based technologies are not able to treat water with TDS containing higher than 40000–45000 $mg \cdot L^{-1}$.[14,34] Thus, thermal technologies can be applied for water post-treatment with higher TDS contents, which can ensure the recycling water quality. However, the levels of scale forming ions should be reduced to prevent equipment problems caused by temperature changes. Moreover, the presence of oil should also be decreased to prevent equipment inefficiency. In general, these specification constraints can be expressed as follows.

$$f_{c,t}^{out} \le \frac{Z_r}{\rho} \cdot \sum_{c \in C} (f_{c,r}^{in} + f_{freshwater}) \qquad \forall r \in \{WR\} \tag{2.1.14}$$

$$f_{c,t}^{out} \le \frac{Z_r}{\rho} \cdot \sum_{c \in C} f_{c,r}^{in} \qquad \forall r \in \{MT, TT\} \tag{2.1.15}$$

In which Z_r is the upper bound for the amount of TDS, scale-forming ions or oil allowed for each water post-treatment alternative. Obviously, this constant can assume different values that depend on the component and wastewater-desired destination.

Logical relationships

In the multistage superstructure shown in **Figure 2.1.1**, some water treatment technologies cannot be selected simultaneously. For instance, if the electrocoagulation is selected in stage 3, conventional coagulation followed by flocculation should not be selected at the same time. It would be expected that the optimal solution to the problem includes only one of those alternatives. The numerical performance of the model can be improved by explicitly adding logical relationships, which reflects the physical knowledge of the system, and reduces the search space for the optimal solution. Follow the logical relationships included in the model in terms of Boolean variables and their reformulation in the form of algebraic equations depending only on binary variables. See Raman and Grossmann[43] for a detailed description of how to systematically go from the logic to the algebraic equations.

In the second stage of the superstructure, the following logical relationship is used to decide between the existence of the hydrocyclone or a bypass:

$$Y_{hy} \veebar Y_{by,1} \quad \rightarrow \quad y_{hy} + y_{by,1} = 1 \tag{2.1.16}$$

In the third stage, if the coagulation process is chosen, then the flocculation should be also selected to compose the WPS. However, only one option between coagulation and electrocoagulation processes can be selected in the superstructure. This choice can be ensured by the following logical relationships:

$$(Y_{co} \Rightarrow Y_{flo}) \veebar Y_{ec} \rightarrow \begin{cases} y_{co} + y_{ec} = 1 \\ y_{co} - y_{flo} \le 0 \end{cases} \tag{2.1.17}$$

In the fourth stage, the following three logic propositions must be defined. At most one of the technologies can be selected from sedimentation, granular filtration and DAF. If coagulation is selected, then the removal factor for the technologies in the fourth stage is adjusted according to the flocs present in the outlet stream of the third stage.

$$Y_{sd} \veebar Y_{gf} \veebar Y_{df} \quad \rightarrow \quad y_{sd} + y_{gf} + y_{df} = 1 \tag{2.1.18}$$

$$Y_{co} \Leftrightarrow (Y_{sd,m1} \veebar Y_{gf,m1} \veebar Y_{df,m1}) \quad \rightarrow \quad y_{co} = y_{sd,m1} + y_{gf,m1} + y_{df,m1} \tag{2.1.19}$$

$$Y_{ec} \Leftrightarrow (Y_{sd,m2} \veebar Y_{gf,m2} \veebar Y_{df,m2}) \quad \rightarrow \quad y_{ec} = y_{sd,m2} + y_{gf,m2} + y_{df,m2} \tag{2.1.20}$$

In the fifth stage, the softening technology and bypass are inclusive alternatives.

$$Y_{sof} \vee Y_{by,2} \quad \rightarrow \quad y_{sof} + y_{by,2} \ge 1 \tag{2.1.21}$$

In the last stage of the superstructure, the selection should be made between ultrafiltration, cartridge filtration or bypass. This decision is guaranteed by the following logical relationship.

$$Y_{uf} \veebar Y_{cf} \veebar Y_{by,3} \quad \rightarrow \quad y_{uf} + y_{cf} + y_{by,3} = 1 \tag{2.1.22}$$

Objective function

The total annualized cost (TAC) is composed of the capital investment of all equipment and operational expenses. The TAC of the WPS is given by **Eq. (2.23)**.

$$tac = \sum_{t \in T} (FAC \cdot C_t^{capital} + C_t^{operational}) \tag{2.1.23}$$

In which FAC is the annualization factor as defined by Smith[98]:

$$FAC = \frac{I \cdot (1+I)^W}{(1+I)^W - 1} \tag{2.1.24}$$

In which I is the fractional interest rate per year and W is the horizon time.

Correlations for the capital cost of some units ($c_t^{capital}$) has been extracted from the cost curves of the Environment Protection Agency (EPA) for water treatment plants[99], revised and updated by McGivney and Kawamura[100]. These cost correlations account for the purchase cost, material, labor, pipes and valves, secondary equipment and electrical equipment and instrumentation. The capital costs of the hydrocyclone and electrocoagulation tank are calculated using the equations obtained from Turton et al.[101]. **Table 2.1.2** shows the correlations used for the estimation of capital costs. All cost correlations have been updated for the relevant year by the CEPCI index (Chemical Engineering Plant Cost Index).

Table 2.1.2 Cost Correlations for Estimation of Capital Investment of Pretreatment Systems **

Description (*t*)	**Capital cost (US$) ****	**Variable**	**Units**
Hydrocyclone (*hy*)	$4590 \cdot v + 15495$	Volume	m^3
Rapid mixer (*co*)	$1103 \cdot v + 28829$	Volume	m^3
Flocculation (*flo*)	$-v^2 + 1202 \cdot v + 30201$	Volume	m^3
Electrocoagulation tank (*ec*)	$3884 \cdot v + 10204$	Volume	m^3
Sedimentation (*sd*)	$1363 \cdot a + 76934$	Area	m^2
Granular filtration (*gf*)	$-28 \cdot a^2 + 1795 \cdot a + 268110$	Area	m^2
DAF (*df*)	$-0.38 \cdot a^2 + 2891 \cdot a + 125479$	Area	m^2
Ultrafiltration (*uf*)	$10.9 \sum_{c \in C} f_j^{in} + 45357$	Inlet flow	$kg \cdot h^{-1}$
Cartridge filtration (*cf*)	$310^{-6} \left(\sum_{c \in C} f_j^{in} \right)^2 - 0.0359 \sum_{c \in C} f_j^{in} + 1697$	Inlet flow	$kg \cdot h^{-1}$
Filter press (*pf*)	$-0.95 \cdot a^2 + 1088.4 \cdot a + 107858$	Area	m^2

** Cost correlations have been updated to 2015 (CEPCI = 556.8)

The operational expenses ($c_t^{operational}$) include the cost of the chemicals added to the coagulation process ($C_{coagulant}$), operation cost of the electrocoagulation systethe m ($C_{electrodes}$), the cost of chemicals added in softening process ($C_{chemical}$), and cost of the freshwater needed in some the cases ($C_{freshwater}$).

$$c_t^{operational} = C_{coagulant} \sum_{c \in C} \left(\frac{f_t}{\rho} \right) \cdot WH \qquad \forall t \in \{co\} \tag{2.1.25}$$

$$c_t^{operational} = C_{electrodes} \sum_{c \in C} \left(\frac{f_t}{\rho} \right) \cdot WH \qquad \forall t \in \{ec\} \tag{2.1.26}$$

$$c_t^{operational} = \sum_{j \in chemicals} \sum_{c \in C} x_j \cdot \left(\frac{f_t}{\rho} \right) \cdot C_j \cdot WH \qquad \forall t \in \{sof\} \tag{2.1.27}$$

$$c_t^{operational} = C_{freshwater} \cdot \left(\frac{f_{freshwater}}{\rho} \right) \cdot WH \tag{2.1.28}$$

In which *WH* is the number of working hours for the equipment in one year (8760 h). The chemical coagulation cost is considered to be equal to 3.5 US$·m^{-3}. The electrocoagulation cost that includes electrode deterioration and energy consumption, is equal to 0.30 US$·m^{-3}.[102] The cost of surface water from lakes and rivers strongly depends on the availability and the location. Typical freshwater costs are in a range of 1.76–3.52 US$·m^{-3}.[103] The chemicals additives used in softening process are lime ($Ca(OH)_2$) and soda (Na_2CO_3). The cost of these chemicals, obtained from the Independent Chemical Information Services (ICIS)[104], are 0.074 US$·kg^{-1} and 0.165 US$·kg^{-1}, respectively.

The mathematical model was implemented in GAMS software[105] (version 24.7.1). The solver BARON[49] was used to optimize the problem. Note that, as BARON is a deterministic global optimization solver, global optimal solutions can be expected by the proposed approach. The model has been solved on a computer with a 3 GHz Intel Core Dual Processor and 4 GB RAM running Windows 7. The CPU time did not exceed some seconds to find the optimal solution and, in general, the model has been solved in less than one second. It should be highlighted that most of the constraints in this model are linear. The non-linearities are only in the objective function, **Eq. (2.1.3)** and **Eq. (2.1.11)**. The resulting problem has 569 continuous variables, 19 binary variables and 618 equations (these numbers can slightly change if some constraints are added or removed from the model, which depends on of the wastewater-desired destination).

2.1.4 Case Studies

Three cases studies are performed to evaluate the capabilities of the proposed model for the optimal WPS design, applied to the treatment of flowback water from shale gas production. As aforementioned in the introduction chapter, flowback water is usually reused on-field, allowing its reuse in the hydraulic fracturing process of new wells. In some cases, however, the

wastewater cannot be directly reused because either there are no more wells to drill (at least in a short period of time and the shale plays operate in a regimen of gas production only), or because a simple pretreatment cannot ensure the physicochemical characteristics needed for the on-site reuse.

In this work, three case studies are carried out to cover different situations. The main difference between them relies on the wastewater destination according to the target: membrane or thermal-based technology to remove TDS or reuse in fracturing operations. The best water pretreatment alternatives are evaluated for each of these desired destinations, considering four different water compositions for each one. As commented in the introduction chapter, the flowback water composition can be extremely variable. In fact, it is dependent on several factors such as the characteristics of the shale rock formation, and the composition of the fracturing fluid used in the drilling process. Hence, four different wastewater compositions, shown in **Table 2.1.1**, are analyzed to cover a wide range of water composition possibilities. Therefore, twelve different scenarios are initially considered to assess the applicability of the proposed mathematical model for optimizing the WPS design. However, due to reverse osmosis limitations (a maximum of around 40000 $mg \cdot L^{-1}$ in TDS) in the second case study only one scenario is possible, which reduces the number of scenarios considered to nine. **Figure 2.1.2** displays a graphical representation of the case studies.

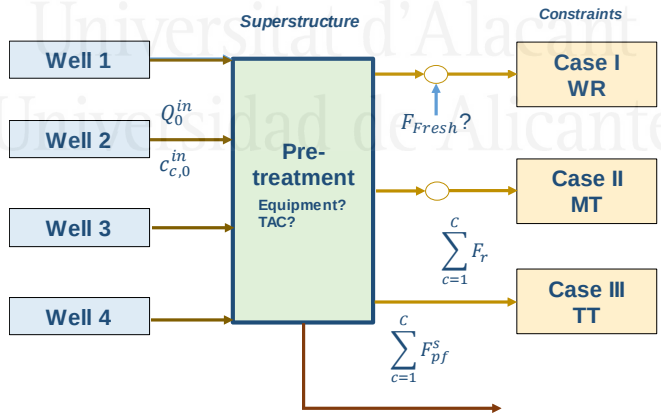

Figure 2.1.2 Graphical representation of the different case studies.

The specifications for each component for the desired composition in each case study are shown in **Table 2.1.3**. Note that, although some of the currently

fracturing fluids tolerate high concentration of salts, we limit the value of TDS in order to analyze the worst scenario.

Table 2.1.3. Constraints on outlet water concentration for the case studies

Case Studies	Limit concentration of component (c), kg·m^{-3}						
	TDS	**TSS**	**Ca**	**Mg**	**Ba**	**Fe**	**Oil**
Case I	50	0.05	2.5	2.5	2.5	0.035	0.025
Case II	35	0.05	0.052	0.016	30.5	0.050	0.010
Case III	-	-	0.026	0.008	15.25	-	0.010

In all cases studies, the WPS is designed to have a treatment capacity of 25 m^3·h^{-1} of shale gas flowback water. The interest rate per year (I) of 10% over a period (H) of 10 years is considered to estimate the annualized capital cost factor (FAC). The main results obtained for the different case studies, which are presented in the following sections, are summarized in **Table 2.1.4**.

Table 2.1.4 Optimal results obtained for the different pretreatment scenarios

Scenario	TAC (kUS$ year^{-1})	$C_{total}^{capital}$ (kUS$ year^{-1})	$C_t^{operational}$ (kUS$ year^{-1})	F_r (kg·h^{-1})	F^{slud} (kg·h^{-1})	$F_{freshwater}$ (kg·h^{-1})	CPU time (s)
1	139.35	40.88	98.57	25219	274	76780	3.22
2	382.97	41.31	341.66	25323	177	2334	3.19
3	95.31	38.17	57.13	25411	89	31120	7.06
4	95.11	38.15	56.96	25491	9	0	0.44
5	121.84	41.96	79.87	25485	15	0	1.11
6, 7, 8	These scenarios cannot be applied due to the constraint in the TDS concentration						
9	1,838.66	42.26	1796.40	24758	741	0	3.50
10	808.38	42.10	766.28	25202	298	0	49.70
11	485.14	51.13	434.01	25305	195	0	0.75
12	122.23	41.98	80.25	25485	15	0	1.20

Case I: Pretreatment of flowback water aiming its reuse

Firstly, water reuse for drilling and fracking new wells is considered the wastewater-desired destination. This target has a special interest in shale gas operations, due to its benefits that include a reduction of freshwater

consumption and, consequently, environmental impacts and transportation costs.

In this case, the optimal WPS configuration obtained by the proposed model is very similar to the water compositions of the four wells. Thus, the water initially passes through the strainer filter to remove the largest particles. Afterward, electrocoagulation is used to remove solids, organics compounds, and some inorganics ions present in the flowback water. After that, the particles formed by electrocoagulation are eliminated by sedimentation. Finally, in the first and second scenario part of the flow passes through the softening process for the further reduction of scale-forming ions. Nevertheless, the softening process is not needed for the last two scenarios. The TAC for the different scenarios is 139.4 kUS$·year^{-1}, 383.0 kUS$·year^{-1}, 95.3 kUS$·year^{-1} and 95.1 kUS$·year^{-1}, respectively.

The softening process cost contribution on the TAC is very large when the presence of scaling ions are high and only a small amount of external freshwater is necessary to satisfy the requirements to reuse the water in further hydraulic fracturing operations. (**Figure 2.1.3 (a)**). For instance, the inlet scaling ions concentration in the scenario 1 is higher than in scenario 2. However, the outlet treated water from Well 1 (scenario 1) must be mixed with 76,780 kg·h^{-1} of fresh water to satisfy the requirements diluting the concentration of the other contaminants.

In scenario 4 (Well 4), the feed water composition is a representative example for the case where the concentration of each component is quite low. In this case, the softening process is not necessary to achieve the acceptable limits on composition to reuse the water in other wells.

From this case study, it can be concluded that the TAC is strongly dependent on the inlet concentration, being the pretreatment more expensive when a high concentration of TDS and scaling ions are present in the inlet stream.

Case II: Pretreatment of flowback water aiming to remove TDS by membrane technologies

The pretreatment of shale gas flowback water for the membrane-based desalination as the desired destination is more restrictive than the Case I (see **Table 2.1.3**). Note that, the flowback water only can be treated by membrane technologies when the inlet composition of TDS is lower than 40000 mg·L^{-1}. Consequently, only the composition of well 4 (scenario 8) can be analyzed in this case.

The water pretreatment sequences obtained are very similar as in the previous case. The TAC of this process increases to 122 kUS$·year^{-1}. The process costs are increased as a response to the lower limit concentration of scaling forming ions allowed for the wastewater post-treatment through membrane technologies. **Figure 2.1.3 (b)** shows the cost analysis results obtained for this case study.

Case III: Pretreatment of flowback water aiming to remove TDS by thermal technologies

In Case III, lower concentrations of calcium, barium, magnesium, and oil (**Table 2.1.3**) are imposed as composition restrictions to allow for thermal-based desalination technologies. These concentration limits should be considered to avoid particle precipitation caused by the temperature changes in thermal desalination processes (MSF, MEE-MVR, MD, etc.). In this case, except scenario 11, the same optimal WPS configurations of Case I and II are again obtained for the pretreatment of the three wells (scenarios 9, 10 and 12). The only difference between them is the operational expenses associated with the softening process, which is higher in this case due to the tight concentration constraints. In scenario 11, DAF is selected instead of sedimentation.

In all scenarios, no freshwater is needed for decreasing the TDS contents, due to the ability of the thermal technologies to treat flowback water with elevated salinities. The TAC in scenarios 9, 10, 11 and 12 are 1,839 kUS$·year^{-1}, 808 kUS$·year^{-1}, 485 kUS$·year^{-1} and 122 kUS$·year^{-1}, respectively. **Figure 2.1.3 (c)** display the cost analysis results obtained for this case study.

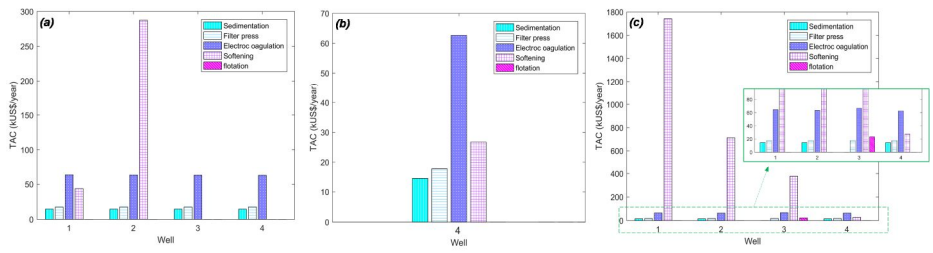

Figure 2.1.3 Effect of the inlet water composition on the total annualized cost (TAC): (a) Case I - Scenarios 1–4; (b) Case II - Scenarios 5–8; and, (c) Case III - Scenarios 9–12.

2.1.5 Conclusions

Selection of the best alternatives for treatment of shale gas water, allowing its reuse or recycle, is crucial to minimize freshwater usage, and consequently, related environmental impacts. However, the great variation in feed water compositions, concentration constraints for different wastewater-desired destinations, and regulation, make it difficult to choose the optimal WPS configuration.

A new mathematical programming model is introduced to optimize the WPS design, considering different alternatives for the pretreatment of shale gas flowback water. The mathematical model is formulated using GDP and optimized under GAMS as an MINLP problem, by the minimization of the total annualized cost of the system. For this purpose, a multistage superstructure is proposed composed by several stages with distinct water pretreatment technologies. The selection of the equipment in each superstructure stage was carried out on a stage-by-stage heuristic basis, in order to guarantee the workability of each upcoming stage. Hence, the superstructure for the optimal system design allows identifying the most cost-effective process to reduce specific contaminants, according to the feed water composition and wastewater-desired destination (i.e., water reuse or water recycling).

Since each wastewater-desired destination requires specific target composition constraints, three case studies are performed to assess the applicability of the proposed approach. Thus, four distinct feed water compositions covering a large range of flowback water concentrations are evaluated for three different target conditions: reuse; post-treatment by membrane-based technologies; and, post-treatment by thermal-based technologies.

The optimal WPS configurations obtained for the water treatment is very similar, or even equal, for the different case studies. The main differences between them are due to removing scaling forming ions and diluting the outlet flow to the required TDS concentration. However, the total annualized cost for these scenarios is as higher as more restrictive is the target water destination.

Note that the optimal WPS configurations obtained aiming wastewater reuse to fracture other wells (Case I) correspond to the lowest total annualized costs. This is again a consequence of the weaker restrictions imposed on the concentration limits for the water reuse in other wells.

Nomenclature

Parameters

$C_{chemical}$	Cost of chemical added in coagulation, US$·kg^{-1}
$C_{electrodes}$	Cost of the electrodes needed in electrocoagulation, US$·kg^{-1}
$C_{freshwater}$	Cost of freshwater, US$·m^{-3}
DT	Detention time, h
$F^{feed,water}$	Fresh water mass flowrate, kg·h^{-1}
FAC	Annualized capital cost factor
I	Fractional interest rate per year
LR	Loading rate, m·h^{-1}
WH	Working time in one year, h
W	Horizon time, year
μ	Viscosity, kg· (m·s)$^{-1}$
a	Removal factor
ϱ	Density, kg·m^{-3}
τ	Dynamic viscosity, kg· (m·s)$^{-1}$

Binary variables

y	Binary variable

Variables

a	Area, m^2
$c^{capital}$	Capital cost, kUS$·year^{-1}
$c^{operational}$	Operational cost, kUS$·year^{-1}
d_h	Diameter of hydrocyclone, m
f	Mass flowrate, kg·h^{-1}
tac	Total annualized cost, kUS$·year^{-1}
v	Volume, m^3

Subscripts

b	Bypass
c	component
cf	Cartridge filter
co	Coagulation
df	Dissolved air flotation
ec	Electrocoagulation
flo	Flocculation
gf	Granular filter

hy	Hydrocyclone
pf	Press filter
r	Post-treatment alternatives
sd	Sedimentation
sf	Strainer filter
t	Number of pretreatment technologies
uf	Ultrafiltration
WR	Water reuse
MT	Membrane treatment
TT	Thermal technology

Superscript

in	Inlet
out	Outlet
slud	Sludge

Acronyms

CEPCI	Chemical Engineering Plant Cost Index
DAF	Dissolved Air Flotation
EPA	Environment Protection Agency
GAMS	General Algebraic Modelling System
GDP	Generalized Disjunctive Programming
LCA	Life Cycle Assessment
MD	Membrane Distillation
MEE–MVR	Multiple-Effect Evaporation with/without Mechanical Vapor Recompression
MINLP	Mixed–Integer Linear Programing
MSF	Multistage Flash
NORM	Normally Occurring Radioactive Materials
PSE	Process Systems Engineering
RO	Reverse Osmosis
TAC	Total Annual Cost
TDS	Total Dissolved Solids
TOC	Total Organic Carbon
TSS	Total Suspended Solids
WPS	Water Pretreatment System
ZLD	Zero Liquid Discharge

I&EC research
Industrial & Engineering Chemistry Research

Article

Cite This: Ind. Eng. Chem. Res. 2018, 57, 13131−13143

pubs.acs.org/IECR

Chapter 2.2

Holistic Planning Model for Sustainable Water Management in the Shale Gas Industry

Alba Carrero-Parreño,[†] Juan A. Reyes-Labarta,[*,†,‡] Raquel Salcedo-Díaz,[†,‡] Rubén Ruiz-Femenia,[†,‡] Viviani C. Onishi,[†] José A. Caballero,[†,‡] and Ignacio E. Grossmann[§]

†Institute of Chemical Process Engineering, University of Alicante, Apartado de Correos 99, Alicante 03080, Spain

‡Department of Chemical Engineering, University of Alicante, Apartado de Correos 99, Alicante 03080, Spain

§Department of Chemical Engineering, Carnegie Mellon University, Pittsburgh, Pennsylvania 15213, United States

Received: May 11, 2018
Revised: August 3, 2018
Accepted: September 4, 2018
Published: September 4, 2018

DOI: 10.1021/acs.iecr.8b02055

Abstract

To address water planning decisions in shale gas operations, we present a novel water management optimization model that explicitly takes into account the effect of high concentration of total dissolved solids (TDS), and temporal variation in the impaired water. The model comprises different water management strategies: a) direct wastewater reuse, which is possible because of the new additives tolerant to high TDS concentrations but at the expense of increasing the costs; b) wastewater treatment, separately taking into account pretreatments, softening and desalination technologies; and c) the use of Class II disposal sites. The objective is to maximize the "sustainability profit" by determining the flowback destination (reuse, degree of treatment, or disposal), the

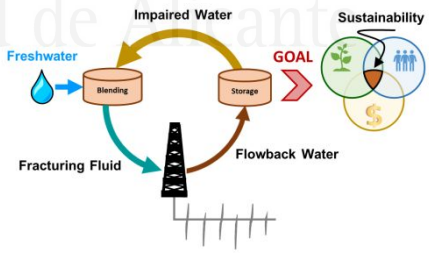

fracturing schedule, fracturing fluid composition, and the number of water storage tanks needed for each period of time. Because of the rigorous determination of TDS in all water streams, the model is a nonconvex MINLP model that is tackled in two steps: first, an MILP model is solved based on McCormick relaxations; next, the binary variables that determine the fracturing schedule are fixed, and a smaller MINLP is solved. Finally, several case studies based on Marcellus Shale Play are optimized to illustrate the effectiveness of the proposed formulation. The model identifies direct reuse as the best water management option to improve both economic and environmental criteria.

Annexes

Unpublished papers

Annex 1

Optimization of Multistage Membrane Distillation System for Treating Shale Gas Produced Water

Abstract

Thermal membrane distillation (MD) is an emerging technology to desalinate high-salinity wastewaters, including shale gas produced water to reduce the corresponding water footprint of fracturing operations. In this work, we introduce a rigorous optimization model with energy recovery for the synthesis of multistage direct contact membrane distillation (DCMD) system. The mathematical model (implemented in GAMS environment) is formulated via generalized disjunctive programming (GDP) and mixed-integer nonlinear programming (MINLP). To maximize the total amount of water recovered, the outflow brine is fixed close to salt saturation conditions (300 $g{\cdot}kg^{-1}$) approaching zero liquid discharge (ZLD). A sensitivity analysis is performed to evaluate the system's behavior under different uncertainty sources such as the heat source availability and inlet salinity conditions. The results emphasize the applicability of this promising technology, especially with low steam cost or waste heat, and reveal variable costs and system configurations depending on inlet conditions. For a produced water salinity ranging from 150 $g{\cdot}kg^{-1}$ to 250 $g{\cdot}kg^{-1}$ based on Marcellus play, an optimal treating cost are between 11.5 and 4.4 US$ per cubic meter is obtained when using low-cost steam. This cost can decrease to 2.8 US$ per cubic meter when waste heat from shale gas operations is used.

A.1.1 Introduction

Selecting a suitable water treatment technology in shale gas industry is complex and dynamic because it depends on a large number of interrelated parameters such as location, water quality and quantity, costs, and treatment technology capabilities. As mentioned in the introduction chapter, multi-effect

evaporation with mechanical vapor recompression (MEE-MVR) and membrane distillation (MD) are the most competitive treatments in the shale gas industry. In the execution of the project, optimization models for both treatments determining the optimal working conditions and configuration design minimizing the total annualized cost of the process are provided. To reduce the shale gas wastewater volume as much as possible by producing concentrated saline water close to Zero Liquid Discharge (ZLD) - outlet flowrate water at near saturated conditions – maximizing at the same time the total water recovered at the minimum cost. This approach represents an environmental breakthrough in freshwater preservation. Additionally, improving the process cost-effectiveness through the reduction of brine discharges allows lessening the environmental impacts associated with energy consumption and waste disposal.

MEE-MVR works are not included in this thesis, however, a comprehensive description of this technology can be found in Onishi et al.[38,39,106]. A counter-current flow multiple-effect evaporation with mechanical vapor recompression superstructure is proposed. The system also includes flashing tanks that are used to recover condensate vapor, enhancing process energy efficiency. Additionally, a preheated is placed at the beginning of the system taking into advantage the sensible heat from the condensed vapor. The first work[38] determines the best configurations depending on the inlet contamination and the optimal operations conditions, being an MEE-SVR process the optimal system at salinities between 10–100 $g{\cdot}kg^{-1}$. Between the salinities of 100 to 150 $g{\cdot}kg^{-1}$, the MEE-MVR system (with thermal integration) becomes the most economical process. Finally, from salinities higher than 150 $g{\cdot}kg^{-1}$, the SEE-MVR system is the optimal solution. Then, a rigorous design is performed highlighting that the desalination system can be placed on site.[39] Finally, due to the great uncertainty in well data from shale plays, a robust design of MEE-MVR under uncertainty in salinity and flowrates are studied. The methodology applied represents a useful tool to support decision-makers towards the selection of more robust design.[106]

Membrane Distillation is a promising thermal technology because the separation occurs across a hydrophobic semipermeable membrane below the normal boiling point of the inlet stream.[107,108] This option is especially advantageous in remote

unconventional hydrocarbon extraction sites where electrical energy supply is not available and many waste heating sources are present, such as geothermal heat energy process facilities, or flaring.[33,109–112] Furthermore, MD is also very

attractive for this application due to its mobility, modularity, and compactness, contrasting with conventional thermal desalination processes which involve a higher physical footprint.[113] Besides that, even though fouling is reduced in MD compared to the before mentioned membrane technology (RO), it can reduce its effectiveness.[14,114] Therefore, a pretreatment step to remove foulants, such as scaling materials and flocs, is required to maintain the productivity of the process, especially in high recovery conditions.[110,115,116] Additionally, pretreatment can remove components that promote membrane wetting by alcohols or surfactants present in shale gas water, which could cause the reduction of the feed liquid surface tension.[107]

Membrane distillation can operate in four configurations: direct contact (DCMD), vacuum (VMD), air gap (AGMD) and sweeping gas (SGMD). The main difference between these configurations is the method applied to generate the driving force. In this work, DCMD is the configuration selected since it is recognized as the most suitable for purification of feed streams with non-volatile solutes and for small-scale desalination.[117] The driving force in DCMD is the temperature gradient across the membrane, that is, the temperature difference between the inlet warm feed stream and ambient temperature of the permeate stream, which causes a difference of vapor pressures.[118] In VMD, the cold permeate is replaced with vacuum. Higher flux can be obtained if sufficient vacuum pressure is applied due to the pressure difference increase. The other two configurations offer high thermal energy efficiency, but AGMD presents low flux through the membrane and in SGMD low permeate recovery is obtained if there are not sufficient flows of sweeping gas.[107]

As mentioned before, several works have been dedicated to water desalination since the beginning of the 21st century.[107] However, there is little literature focused on the optimization of membrane distillation systems for flowback and produced water. Regarding membrane distillation optimization for the treatment of shale gas wastewater, El-Halwagi et al.[33] have developed an optimization approach for treating flowback water by using direct contact membrane distillation (DCMD). Multi-period formulation of the time-based variation in the flowrate and concentration was made. However, they consider that waste energy is always available, hence there is no calculation of the energy cost or heat integration within the process streams. Moreover, in their optimization model, they do not consider process configuration design. Lokare et al.[111] also evaluate the synergies and potential of DCMD technology for the treatment of shale gas water utilizing waste heat available from natural gas

extraction. They simulate DCMD in ASPEN Plus and calibrate the model using laboratory-scale experiment. Then, the model is used to design and determine the operating parameters for a full-scale DCMD system. In a later work[119], the same authors highlighted the applicability of DCMD for treating shale gas water by evaluating the economic feasibility. They revealed a cost of treating produced water of 5.7 US$ per cubic meter and 0.7 US$ per cubic meter when the waste energy source is available fixing the inlet salinity to 10% weight to volume fraction and the outlet salinity equal to 30%. Recently, Deshmukh et al.[109] highlighted the advantages of MD for small-scale desalination applications and emphasized the benefits for desalinating shale gas water. However, they remark that the viability of MD as an energy-efficient treatment remains uncertain. Moreover, they mention the necessity of comparison techniques to obtain more reliable cost and process optimization.

In this work, a multistage membrane distillation superstructure (comprising all potential membrane configurations in series and interconnections) is proposed, including the following novelties: (i) development of an optimization model for membrane distillation system (MDS) to attain close to ZLD conditions for the treatment of shale gas produced water; (ii) optimization and design of full-scale membrane distillation systems coupled with heat recovery to determine the optimal system configuration and optimal working conditions; (iii) application of the proposed model to real inlet flowrate and variable high-salinity to evaluate if the projected technology can be applied to desalinate produced water coming from different shale gas basins; and, (iv) analysis of the economic viability of MD in shale gas operations.

A.1.2 Problem Statement

The given parameters are the defined wastewater feed stream (inlet mass flowrate, salinity, and temperature); the corresponding membrane characteristics (permeability and thickness); and, the cost of the membrane, pumps, heat exchangers and the utilities used (low-pressure steam and cooling water). The objective function considers the equipment's annualized capital cost of expenditure and the operating costs related to membrane labor, replacement, and energy demand.

The multistage superstructure proposed for treating produced water is shown in **Figure A.1.1** The superstructure comprises n possible membrane modules in series and allows the possibility of various recycle connections. For instance, part of the concentrate obtained in stage two could be recycled in the same stage or could be sent to the first stage. There is only the possibility of

recirculating the concentrated water to previous stages. On the other hand, if a membrane stage of the superstructure is not selected, the concentrated stream circulates through a bypass to the next stage.

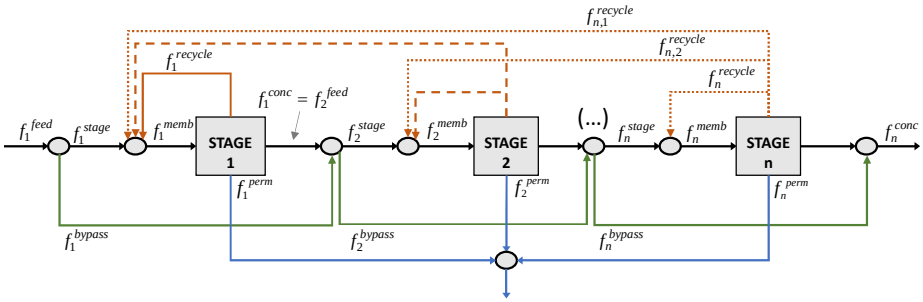

Figure A.1.1 Multistage Membrane Distillation superstructure for treating produced water from shale gas production.

Figure A.1.2 shows the scheme of a DCMD module including heat recovery.[120] Each membrane module is composed of the following equipment: shell and tube heat exchanger, heater and cooler; polytetrafluoroethylene membranes with polypropylene support; centrifugal pumps and storage tanks. The feed flowrate is heated before entering the membrane cell to induce the separation of salts and water. As mentioned before, the driving force in DCMD is the temperature gradient across the membrane, that is, the temperature difference between the inlet warm feed stream and ambient temperature of the permeate stream, which causes a difference of vapor pressures. To reduce the operational energy cost, a heat exchanger is used to preheat the inlet water with the hot permeate stream. Additionally, an external cooler is installed to cold down the recirculated permeate stream to generate a temperature difference across the membrane. To attain the specified outlet conditions, the concentrated stream leaving the membrane can also be recycled. Indeed, concentrate recycling is required for high recovery ratios.[121] The recirculated water of both sides of the membranes is stored in tanks installed in the feed and permeate loop, respectively. Finally, pumps are placed at the beginning of each stage and on the feed and permeate loop of each module to drive the recirculated water.

Throughout the work, we refer to heat exchangers when there is heat exchange between two streams within the system. Note that preheaters and coolers are also considered as heat exchangers but using external utilities.

Apart from the selection of the number of stages, the following decision variables are also calculated for each stage: membrane area; area and

heating/cooling utility needed in the preheater and cooler; heat exchanger area; outlet concentration; recycle ratio; and operating temperatures.

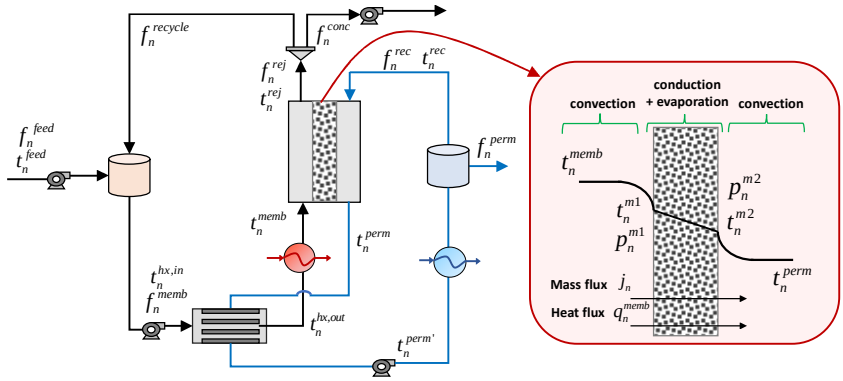

Figure A.1.2 Direct Contact Membrane Distillation module with heat recovery.

To simplify the mathematical formulation of the model, we have considered the following assumptions:

I. Steady state operation.
II. Heat losses in pipes, pumps, heater, and cooler are neglected.
III. Pressure drops in all thermal and mechanical equipment are negligible.
IV. Vaporization takes place on the surface of the membrane.
V. Flux decrease due to membrane fouling is negligible.
VI. Water with zero salinity goes through the membrane pores (permeate).
VII. Pumps and preheaters are made of nickel (to avoid corrosion).
IX. Capital costs of mixers, splitters, pumps, tanks, and pipes are negligible.

The mathematical model, which includes equality and inequality constraints, logic propositions, data restriction and an objective function for the optimal multistage MDS, is developed in the following section.

A.1.3 Mathematical Programming Model

The mathematical model for the optimal design of the multistage MDS is explained below. The problem is formulated via Generalized Disjunctive Programming (GDP)[64] and solved as a mixed-integer nonlinear programming (MINLP). The optimization problem is modeled using total flows and salt composition as variables, which involves bilinear terms - the multiplication of

two variables - in the salt water mass balances. These terms are one of the sources of the non-convexity; however, this representation is advantageous because the bounds of the variables can be easily determined. Note that throughout the mathematical model description, lower case letters are used for variables and capital letters for parameters.

The following data are assumed to be known:

F^{feed}	Inlet mass flowrate, kg·s^{-1}
T^{feed}	Inlet temperature,ºC
X^{feed}	Inlet salinity, g·kg^{-1}
X^{zld}	Outlet salinity, g·kg^{-1}
E	Membrane thickness, mm
B	Membrane permeability, kg (m^2·Pa·h)$^{-1}$
U^{preh}	Overall heat transfer coefficient of the preheater, kW·(m^2·ºC)$^{-1}$
U^{cooler}	Overall heat transfer coefficient of the cooler, kW·(m^2·ºC)$^{-1}$
T^{steam}	Steam low-pressure temperature,ºC
$T^{refrig,in}$	Cooling water inlet temperature,ºC
$T^{refrig,out}$	Cooling water outlet temperature,ºC
ΔT^{min}	Minimum temperature difference

Set definition

The following set is defined to develop the MINLP model.

$$N = \{n / n \text{ is a stage of membrane in series}\}$$

Membrane distillation model

Mass and salt balances around each membrane distillation are given by **Eq. (A.1.1-A.1.2)**,

$$f_n^{memb} + f_n^{rec} = f_n^{rec} + f_n^{perm} + f_n^{rej} \qquad \forall n \in N \tag{A.1.1}$$

$$f_n^{memb} \cdot x_n^{memb} = f_n^{rej} \cdot x_n^{rej} \qquad \forall n \in N \tag{A.1.2}$$

where, f_n^{memb}, f_n^{rec}, f_n^{perm} and f_n^{rej} represent the inlet mass flowrate, the recirculated flowrate, the permeate flowrate and the reject flowrate in the membrane module, respectively. x_n^{memb} and x_n^{rej} are the inlet and reject concentration in the membrane.

The energy balance across the membrane can be evaluated as follows,

$$h_n^s(t_n^{memb}, x_n^{memb}) \cdot f_n^{memb} - h_n^s(t_n^{rej}, x_n^{rej}) \cdot f_n^{rej} = a_n^{memb} \cdot q_n^{memb} \qquad \forall n \in N \tag{A.1.3}$$

$$h_n^p(t_n^{perm})\cdot\left(f_n^{rec}+f_n^{perm}\right)-h_n^p(t_n^{rec})\cdot f_n^{rec}=a_n^{memb}\cdot q_n^{memb}\quad\forall n\in N \tag{A.1.4}$$

where, a_n^{memb} and q_n^{memb} represent the membrane area and the heat transfer flux through the membrane. h_n^s and h_n^p are the specific enthalpies of saline water and permeate calculated at the specified conditions, correspondingly. Their values are calculated by the following rigorous correlations,

$$h_n^s=-15970+4.105\cdot t_n+8924\cdot x_n-3.709\cdot t_n\cdot x_n+84.77\cdot x_n^2\quad\forall n\in N \tag{A.1.5}$$

$$h_n^p=-15970+4.1178\cdot t_n\quad\forall n\in N \tag{A.1.6}$$

Where t_n and x_n are the corresponding temperature and composition.

These correlations are generated using the maxmin approach -maximize the minimum distance between two sample points- considering temperature ranging from 0ºC to 100ºC, and brine salinity between 0 to 400 g·kg^{-1}. Aspen HYSYS® simulator has been used to obtain the specific enthalpies by using the thermodynamic package NRTL electrolytes. It is important to highlight that these rigorous correlations are crucial to simulate the real behavior of the MDS since the specific enthalpies in saline streams are significantly dependent on temperature and composition. **Figure A.1.3** shows the surface plot of enthalpy as a function of salinity and temperature and the relative error obtained for each point.

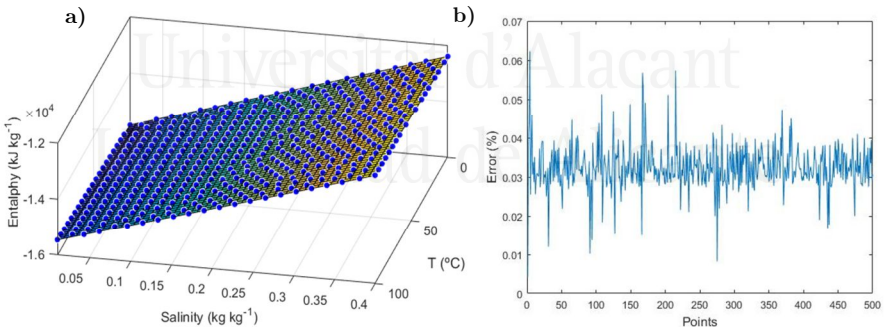

Figure A.1.3 (a) Surface plot of enthalpy as a function of salinity and temperature and (b) relative error.

The membrane area is given by **Eq. (A.1.7)**.

$$a_n^{memb}\cdot j_n=f_n^{perm}\qquad\forall n\in N \tag{A.1.7}$$

Where j_n is the permeate flux throughout the membrane calculated as proposed by Elsayed et al.[122],

$$j_n = B \cdot (p_n^{m1} \cdot \gamma_n (1-\omega_n) - p_n^{m2}) \qquad \forall n \in N \tag{A.1.8}$$

in which, B is the membrane permeability, ω_n is the salt molar fraction in the feed side, γ_n represents the activity coefficient of the water in the feed side, and p_n^{m1} and p_n^{m2} are the vapor pressures at both sides of the membrane surface. The salt molar fraction of the feed water is given by **Eq. (A.1.9).**

$$\omega_n \cdot (x_n^{memb} / 58.4 + (1 - x_n^{memb} / 18) = x_n^{memb} / 58.4 \qquad \forall n \in N \tag{A.1.9}$$

The activity coefficient is estimated as a function of the salt molar concentration by the following equation as proposed by Lawson and Loyd[123],

$$\gamma_n = 1 - 0.5 \cdot \omega_n - (10 \cdot \omega_n)^2 \qquad \forall n \in N \tag{A.1.10}$$

Vapor pressure is estimated with the correlation described in **Eq. (A.1.11),** which has been obtained using Antoine's equation for the range of the working temperatures (20ºC - 90ºC).

$$p_n = 16.56 \cdot (t_n)^2 - 935.90 \cdot t_n + 16960 \qquad \forall n \in N \tag{A.1.11}$$

The heat transfer across each membrane, q_n^{memb}, is calculated by standard heat transfer models accounting the corresponding four contributions:

- Convection from the feed bulk to the membrane interface as expressed by **Eq. (3.12).**

$$q_n^{m1} = ht_n^{m1} \cdot (t_n^{memb} - t_n^{m1}) \qquad \forall n \in N \tag{A.1.12}$$

In which, ht_n^{m1} is the convective heat transfer coefficient given by the correlation described by **Eq. (A.1.13)** as a function of temperature and brine salinity. The produced water properties needed to calculate rigorously the convective heat transfer coefficient (density, viscosity, heat capacity and thermal conductivity) have been obtained from OLI's software[124] using the thermodynamic package for electrolytes. The physical properties correlations have been generated by considering temperature ranging from 40ºC to 90ºC, and brine salinity between 40 to 300 g·kg^{-1}.

$$ht_n^{m1} = 2.61 - 4.96 \cdot x_n^{memb} + 0.03 \cdot t_n^{memb} \qquad \forall n \in N \tag{A.1.13}$$

- Conduction and water evaporation inside the membrane are given by **Eq. (A.1.14)**. Note that the first term of the right-hand side of the equation refers to heat transfer by conduction and the second term by the water evaporation.

$$q_n^{memb} = ht_n^{cond} \cdot (t_n^{m1} - t_n^{m2}) + hv_n \cdot j_n \qquad \forall n \in N \tag{A.1.14}$$

hv_n is the water latent heat of vaporization. The conduction heat transfer coefficient, ht_n^{cond} , is defined by **Eq. (A.1.15)**.

$$ht_n^{cond} \cdot E = k_n \qquad \forall n \in N \tag{A.1.15}$$

In which, E is the thickness of the membrane and k_n is its thermal conductivity given by the following correlation proposed by Elsayed et al.[122], where t_n is the average temperature between t_n^{memb} and t_n^{perm} :

$$k_n = 1.7 \cdot 10^{-7} \cdot t_n - 4 \cdot 10^{-5} \qquad \forall n \in N \tag{A.1.16}$$

- Convection from the membrane interface to the permeate bulk is calculated by **Eq. (A.1.17)**.

$$q_n^{m2} = ht_n^{m2} \cdot (t_n^{m2} - t_n^{perm}) \qquad \forall n \in N \tag{A.1.17}$$

In which, ht_n^{m2} is the convective heat transfer coefficient at the permeate side given by the correlation defined in **Eq. (A.1.18)**. The same procedure detailed before for the calculation of the convective heat transfer coefficient at the feed side is used. In this case, the water salinity in the permeate side is equal to zero (salt-free), and the temperature range is considered to vary from 20 to 90ºC.

$$h_n^{m2} = 0.004 \cdot t_n^{perm} + 2.8 \qquad \forall n \in N \tag{A.1.18}$$

At steady state, the overall heat transfer flux must be balanced [118,125]:

$$q_n^{m1} = q_n^{memb} = q_n^{m2} \qquad \forall n \in N \tag{A.1.19}$$

Recycle splitter mass balance

The possibility of various recycle connections is defined by the following equation:

$$f_n^{rej} = f_n^{recycle} + \sum_{\substack{n' \in N \\ n > n'}} f_{n,n'}^{recycle} + f_n^{conc} \qquad \forall n \in N \tag{A.1.20}$$

Where $f_n^{recycle}$, $f_{n,n'}^{recycle}$ and f_n^{conc} represent the direct recycle, the interstate recycles and the concentrate stream, respectively. The concentration, temperature and, consequently, the specific enthalpy of these streams are the same as for the reject stream.

Inlet mixer balances

The membrane inlet conditions are defined by the following mass, salt and energy balances around the inlet mixer placed before each membrane module.

$$f_n^{stage} + f_n^{recycle} + \sum_{\substack{n' \in N \\ n>n'}} f_{n,n'}^{recycle} = f_n^{memb} \qquad \forall n \in N \tag{A.1.21}$$

$$f_n^{stage} x_n^{feed} + f_n^{recycle} \cdot x_n^{rej} + \sum_{\substack{n' \in N \\ n>n'}} f_{n,n'}^{recycle} \cdot x_{n'}^{rej} = f_n^{memb} \cdot x_n^{memb} \quad \forall n \in N \tag{A.1.22}$$

$$h_n^s(t_n^{feed}, x_n^{feed}) \cdot f_n^{stage} + h_n^s(t_n^{rej}, x_n^{rej}) \cdot f_n^{recycle} + \\ + \sum_{\substack{n' \in N \\ n>n'}} h_{n'}^s(t_{n'}^{rej}, x_{n'}^{rej}) \cdot f_{n,n'}^{recycle} = h_n^s(t_n^{hx,in}, x_n^{memb}) \cdot f_n^{memb} \qquad \forall n \in N \tag{A.1.23}$$

Outlet salinity constraint

The following design specification is included to reach close to ZLD conditions.

$$x_n^{rej} \geq X^{zld} \qquad n = |N| \tag{A.1.24}$$

Constraints on each membrane module n

To avoid inconsistent performance of the membrane modules and solutions without physical meaning, the following constraints that ensure suitable working conditions (i.e. outlet flow should not be higher than inlet flow) should be introduced in the model:

$$f_n^{rej} \leq f_n^{memb} \quad \forall n \in N \tag{A.1.25}$$

$$f_n^{conc} \leq f_n^{rej} \quad \forall n \in N \tag{A.1.26}$$

$$t_n^{m1} \leq t_n^{memb} \quad \forall n \in N \tag{A.1.27}$$

$$t_n^{m2} \leq t_n^{m1} \quad \forall n \in N \tag{A.1.28}$$

$$t_n^{perm} \leq t_n^{m2} \quad \forall n \in N \tag{A.1.29}$$

Design equations for the preheater, cooler and heat exchanger

The energy required in the preheater is given by **Eq. (A.1.30)**,

$$q_n^{preh} = f_n^{memb} \cdot \left(h_n^s(t_n^{memb}, x_n^{memb}) - h_n^s(t_n^{hx,out}, x_n^{memb}) \right) \qquad \forall n \in N \tag{A.1.30}$$

Where t_n^{memb} and $t_n^{hx,out}$ are the inlet membrane temperature and the outlet heat exchanger temperature, respectively.

The heat transfer area is defined by the following equation:

$$a_n^{preh} \cdot U^{preh} \cdot lmtd_n^{preh} = q_n^{preh} \qquad \forall n \in N \tag{A.1.31}$$

where U^{preh} is the overall heat transfer coefficient and $lmtd_n^{preh}$ is the log mean temperature difference that is reformulated using Chen's approximation[126] to overcome the numerical difficulties created by the logarithm, in which, the temperature differences, θ, are given by **Eqs. (A.1.32-A.1.34).**

$$lmtd_n^{preh} = (0.5 \cdot (\theta_n^1 \cdot \theta_n^2)(\theta_n^1 + \theta_n^2))^{1/3} \qquad \forall n \in N \tag{A.1.32}$$

$$\theta_n^1 = T^{steam} - t_n^{memb} \qquad \forall n \in N \tag{A.1.33}$$

$$\theta_n^2 = T^{steam} - t_n^{hx,out} \qquad \forall n \in N \tag{A.1.34}$$

The temperature difference between the fluids flowing in shell and tubes sides must be greater than the design minimum difference temperature to allow effective heat transfer,

$$\Delta T^{min} \le T^{steam} - t_n^{memb} \qquad \forall n \in N \tag{A.1.35}$$

$$\Delta T^{min} \le T^{steam} - t_n^{hx,out} \qquad \forall n \in N \tag{A.1.36}$$

The same procedure, which is detailed in **Appendix A**, is applied to design the heat exchanger and cooler.

GDP in membrane stages

To determine the number of distillation stages present in the desalination system, the disjunction showed in **Eq. (A.1.37)** is introduced to formulate the decision of the existence of a stage. If the stage exists, the concentrate stream of the previous stage, $f_{n-1}^{conc} = f_n^{feed}$, is equal to the inlet flowrate through stage n, f_n^{stage} (see **Figure A.1.1**). Otherwise, f_n^{stage} is equal to zero and $f_n^{feed} = f_n^{bypass}$. In this equation, the Boolean variable: Y_n^{stage} will be «True» if the stage n exists and «False», otherwise.

$$\begin{bmatrix} Y_n^{stage} \\ F_n^{stage,LO} \le f_n^{stage} \le F_n^{stage,UP} \\ f_n^{bypass} = 0 \end{bmatrix} \veebar \begin{bmatrix} \neg Y_n^{stage} \\ F_n^{bypass,LO} \le f_n^{bypass} \le F_n^{bypass,UP} \\ f_n^{stage} = 0 \end{bmatrix} \forall n \in N \tag{A.1.37}$$

$$Y_n^{stage} \in \{True, False\}$$

The previous disjunction can be reformulated into an MINLP model, by using the hull reformulation[63] as follows:

$$
\begin{aligned}
&f_n^{stage} \le F_n^{stage,UP} \cdot \mathrm{y}_n^{stage} \\
&f_n^{stage} \ge F_n^{stage,LO} \cdot \mathrm{y}_n^{stage} \\
&f_n^{bypass} \le F_n^{bypass,UP} \cdot (1-\mathrm{y}_n^{stage}) \\
&f_n^{bypass} \ge F_n^{stage,LO} \cdot (1-\mathrm{y}_n^{stage}) \\
&y_n^{stage} \in \{1,0\}
\end{aligned}
\tag{A.1.38}
$$

Logical relationships

The following logical relationships (**Eqs. A.1.39-A.1.40**) are included in the model, in terms of Boolean variables and their corresponding re-formulation to algebraic equations using binary variables. See Raman and Grossmann[43] for a detailed description of how to systematically transform logic propositions into algebraic equations. **Eq. A.1.39** specifies that a membranes stage or a bypass must exist.

$$Y_n^{stage} \veebar Y_n^{bypass} \quad \rightarrow \quad y_n^{stage} + y_n^{bypass} = 1 \qquad \forall n \in N \tag{A.1.39}$$

If a bypass exists in stage n, then the bypass should also exist in all subsequent stages to avoid the non-existence of intermediate stages.

$$Y_n^{bypass} \Rightarrow Y_{n+1}^{bypass} \quad \rightarrow \quad y_n^{bypass} \le y_{n+1}^{bypass} \qquad n < |N| \tag{A.1.40}$$

Objective function

The objective function to be minimized corresponds to the total annualized cost (TAC) of the multistage MDS. The TAC comprises the contributions related to the annualized capital investment (CAPEX) of the equipment (including membrane modules and heat exchangers), and the annual operational expenses (OPEX) associated with the cost of membranes replacement, pumping, heating, and cooling:

$$tac = capex \cdot F + opex \tag{A.1.41}$$

In which, F is the annualization factor as defined by Smith[98]:

$$F \cdot \left((1+I)^W - 1\right)^{-1} = I \cdot (1+I)^W \tag{A.1.42}$$

where I is the interest rate per year and W is the time horizon.

The capital expenditure includes the membrane cost (C^{memb}) and the capital cost of the heat exchangers, which are calculated by the correlation proposed by Turton et al.[101] All capital costs have been updated for the relevant year by the CEPCI index (Chemical Engineering Plant Cost Index).

$$capex = C^{memb} \cdot a_n^{memb} + FBM \cdot \left[114.79 \cdot (a_n^{preh} + a_n^{hx} + a_n^{preh}) + 407914)\right] \tag{A.1.43}$$

In **Eq. (A.1.43)**, *FBM* corresponds to a correction factor which correlates the operating pressure with the construction material.

As aforementioned, the operational expenses (*OPEX*) include membrane replacement cost (C^{replac}), considered to be equal to 15% of the capital cost per year; pumping cost (C^{pumps}); heating cost (C^{steam}); and cooling cost (C^{water}).

$$opex = \sum_{n \in N} C^{memb} \cdot a_n^{memb} \cdot C^{replac} + (C^{steam} \cdot f_n^{steam} + C^{pumps} \cdot f_n^{pumps} + C^{water} \cdot q_n^{cooler}) \cdot WH \quad \text{(A.1.44)}$$

In **Eq. (A.1.44)**, WH is the working hours per year; f_n^{steam} is calculated from the total energy required and the water heat of vaporization, and f_n^{pumps} includes the process flows which need pumping.

A.1.4 Case Studies

Several case studies, based on data from Marcellus shale formation, have been performed to evaluate the capabilities of the proposed mathematical model to optimize MDS applied to close to ZLD desalination of shale gas water. The U.S. Environmental Protection Agency[16] reported that produced water generated per well in the U.S ranges from $1.71 \cdot 10^{-2}$ kg·s^{-1} to $4.82 \cdot 10^{-2}$ kg·s^{-1} while Marcellus shale salinity average sampling data for 19 sites is 200 g·kg^{-1}. The present work considers that the MDS has the capacity to treat the produced water generated by 3 wellpads of 12 wells each.[127] Therefore, the input mass flowrate is equal to 2 kg·s^{-1} (7.22 m^3·h^{-1}), based on the maximum capacity per well (i.e $4.82 \cdot 10^{-2}$ kg·s^{-1} including 15% extra capacity). Although the base case study considers Marcellus shale salinity of 200 g·kg^{-1}, the produced water from different wells can have significant salinity differences depending on the shale gas formation. For this reason, sensitivity studies of the system behavior have been performed under different salt concentrations ranging from 150 to 250 g·kg^{-1}.

The MDS outlet concentrate salinity has been fixed to 300 g·kg^{-1} (i.e. close to salt saturation condition of ~350 g·kg^{-1}) to maximize the water recovery. The membrane permeability used in this study is 5.6 10^{-3} kg·(m^2·Pa·h)$^{-1}$, determined in a laboratory-scale study by Lokare et al.[111], using a polytetrafluoroethylene membrane with polypropylene support. **Table A.1.1** summarizes all the input data used in the case studies.

Additionally, in order to ensure that the system works within its operational limits, the following variables have been fixed or constrained: 1) the membrane inlet temperature is restricted between 40-90ºC; 2) minimum temperature difference between the shell and tubes in the heat exchanger is equal to 10ºC; 3) cooler outlet temperature is fixed to 30ºC to allow sufficient difference of vapor pressure at both sides of the membrane (i.e. membrane driving force) and 4) the use of water as refrigerant fluid (i.e. other refrigerant fluids have been discarded due to their higher comparative price).[101]

The MINLP problem for the base case has 6 binary variables, 265 continuous variables and 311 constraints. The model has been solved on a computer with a 3 GHz Intel Core Dual Processor and 4 GB RAM running Windows 10.

Table A.1.1 Input data.

Source	**Feed water**	
[128]	Mass flowrate	7.22 $m^3 \cdot h^{-1}$ (2 $kg \cdot s^{-1}$)
[38]	Temperature	20ºC
Source	**Membrane parameters**	
[129]	Thickness	0.65 mm
[111]	Permeability	5.6 10^{-3} kg $(m^2 \cdot Pa \cdot h)^{-1}$
Source	**Output parameters**	
[38]	Outlet Salinity	300 $g \cdot kg^{-1}$
Source	**Cost Data**	
[101]	Cooling water cost	11.2 US$ $(kW \cdot year)^{-1}$
[129]	Steam cost	0.007 US$·$kg^{-1}$
[129]	Membrane cost	90 US$ m^{-2}
[130]	Pumping cost	0.056 US$ m^{-3}
	Factor of annualized capital cost	0.13 (5% - 10 year)
	Factor of annualized membrane capital cost	0.28 (5% - 4 year)

Multistage membrane distillation design

The resulting optimal MDS configuration for the base case, using Marcellus real shale salinity of 200 $g \cdot kg^{-1}$, consists of three MD stages with a total required membrane area of 603 m^2 (225, 221 and 157 m^2, respectively). Additionally, a recycle ratio (total recycle flowrate with respect to the feed flowrate) of 9 allows reaching the outlet salinity specification (i.e. 300 $g \cdot kg^{-1}$). The optimum configuration and the main process variables (i.e. areas, flows, temperatures, utilities, etc.) are shown in **Figure A.1.4.**

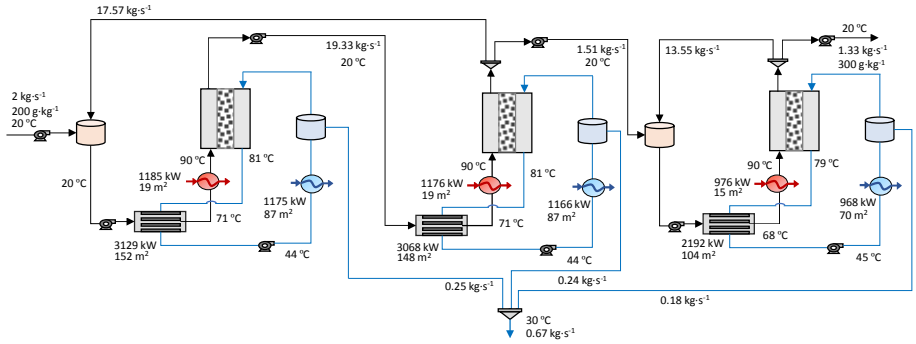

Figure A.1.4 Optimal solution of the multistage membrane distillation system (MDS) with heat integration obtained for the base case study.

The accuracy of the optimal solution obtained is verified using the commercial software Aspen HYSYS® (version 8.8) assuming steady-state conditions and using the thermodynamic package NRTL-electrolytes. To simulate the MDS, the variables have been classified as process variables and design variables, being the design variables the input data needed to simulate the system (i.e. outlet temperature of heaters, coolers and heat exchangers, reject temperature and outlet salt concentration). A logical unit balance operation is used to simulate the energy and mass balances through the membrane. In **Appendix B, Figure B.1** shows the MDS diagram in Aspen HYSYS® and **Table B.1** the values of the process variables obtained from the mathematical model, from the simulation and the difference between them. For all variables, the differences found comparing both values are below 1%.

The optimal MDS solution achieves a total annualized cost (TAC) of 523 kUS$·year^{-1}, including 88 kUS$·year^{-1} related to capital expenditure and 435 kUS$·year^{-1} in operational expenses. **Figure A.1.5** shows the fractional contribution of various cost elements for the optimal solution. As can be observed, TAC mayor contributor is the heating energy required by the system (~62%), followed by the pumping costs (~12%). Since high recycle ratios are needed to reach the outlet specified salinity and these streams must be reheated before entering the membrane stage again, the amount of thermal and pumping energy required increases dramatically.

Optimal recycle configuration includes direct recycle in stage three while an interstate recycles between the second and first stages is established, obtaining the lowest overall recycle ratios.

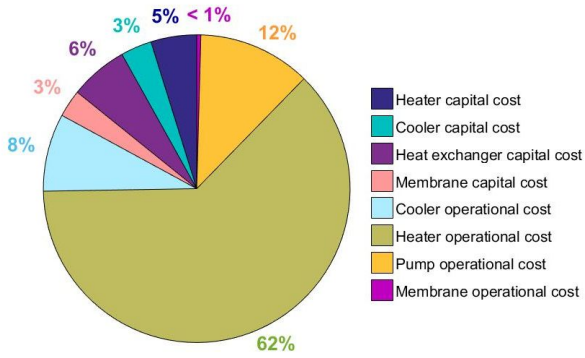

Figure A.1.5 Fractional contribution of various cost elements for the optimal solution of the base case study.

To analyze the effect of the system configuration (i.e. the recycle connections and the number of MD stages) on the cost of the MDS, several cases have been solved by varying these design variables.

Firstly, to study the influence of the recycle connections, the system has been solved predetermining different recycle configurations. The results for the CAPEX, OPEX and the heating cost, which is the maximum contribution to OPEX, are detailed in **Table A.1.2**.

Table A.1.2 Optimal costs (kUS$·year^{-1}) of MDS under different recycle connections.

Recycle ratio configuration description	CAPEX	OPEX	Heating cost
Direct recycle in each stage	88	452	310
Interstate recycle from stage three to stage one	87	466	343
Interstate recycle from stage three to stage two and direct recycle in stage one	88	440	321

If only direct recycle is allowed, the total cost increases 17 kUS$·year^{-1} with respect to the base case optimal solution. Considering interstate recycle from stage three to stage one, the operating cost increases 31 kUS$·year^{-1} compared with the optimal solution. The solution of the last recycling possibility, interstate recycle from stage three to stage two and direct recycle in stage one, is only 5 kUS$·year^{-1} higher than the optimal solution. In all these three cases, higher recycle ratios than the obtained for the optimal solution are needed, and consequently, the resulting operating costs are higher.

As said before, the influence of the number of membrane distillation stages is also analyzed to find out the process cost differences compared to the optimal

solution. The results, shown in **Figure A.1.6**, highlight that defining fewer stages than those calculated for the optimal solution is less attractive since a higher TAC is obtained. Although in these configurations (1 or 2 stages) the capital expenditure decreases, the operating costs rise to a larger extent, thus causing the increase of the TAC. When fewer membrane stages are used, higher recycle ratios are needed, consequently, the heating and pumping costs increase. For instance, when considering only one stage, although the capital cost is lower (58 kUS$·year^{-1}) due to the fewer installed equipment, the operational cost is 15% higher than that in the optimal solution (500 kUS$·year^{-1}). On the contrary, the operational savings attained by adding more than three membranes do not compensate the capital cost increment (e.g., the capital cost is 132 kUS$·year^{-1} and the operational cost equal to 413.57 kUS$·year^{-1} considering six membranes in series).

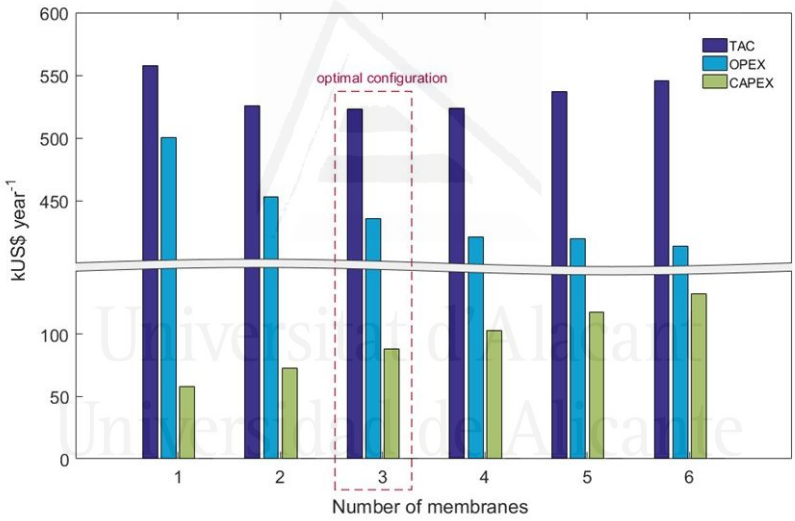

Figure A.1.6 Effect of the number of membrane stages in series on the process cost.

Parametric study of the effect of steam cost

As aforementioned, the TAC is significantly affected by steam cost. Some works in literature have considered the use of inexpensive heat sources such as the waste heat of process facilities or flaring [33,122,131–133]. That consideration is very attractive for membrane distillation where the separation occurs below the normal water boiling point.

Taking into account that the steam cost varies significantly depending on the location of the plant and country, in this section we study the impact of the

steam cost on the system configuration and total process cost. We analyze the base case, which considers low-cost steam equal to US$ 0.007 kg^{-1} [129], and the extreme situations, considering a high-cost steam equal to US$ 0.028 kg^{-1} [101] and free heating source. In the latter case, the heating cost is removed from the objective function since the energy is provided from the waste heat of shale gas production.

Figure A.1.7 shows the capital and operation and maintenance (O&M) costs for the optimal solution of the three considered situations for the steam cost (inlet salinity in maintained constant at 200 $g \cdot kg^{-1}$). The TAC of treating produced water is equal to 1546 $kUS\$ \cdot year^{-1}$ considering high energy costs; 523 kUS$ $year^{-1}$ for the base case (low heating cost); and 174 $kUS\$ \cdot year^{-1}$ when energy is provided from waste heat of shale gas production. The operational expenses take the value of 1345 $kUS\$ \cdot year^{-1}$, 435 $kUS\$ \cdot year^{-1}$ and 65 $kUS\$ \cdot year^{-1}$, respectively, which means that operational cost savings up to 95% could be obtained depending on the heating source. Although clearly the cost savings are affected by the heating cost reduction, they also arise from the differences in the system configuration. As can be seen in **Figure A.1.7**, the capital expenses also decrease as the heating cost is lower, being the system configuration equal to four, three and two stages, respectively. This is due to the trade-off between the amount of water recycled and the number of membrane stages. The higher the number of membrane stages, the lower recycle ratios are needed. Therefore, when the heating cost is low, it is more cost-effective to preheat high recycle ratios than increase the number of membranes stages.

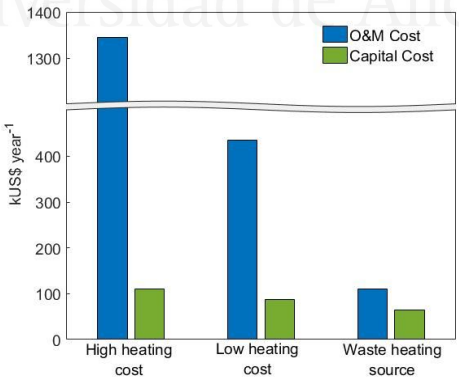

Figure A.1.7 Effect of steam cost on the total process cost for the optimal solution of the base case study.

Parametric study of the effect of produced water salinity

The composition of the produced water is another uncertain parameter for designing MDS. It depends on the exploitation site and it varies also over the well lifetime. In this section, the analysis of the optimal system configuration and economic performance of the system under different inlet salinities, ranging from 150 to 250 g·kg^{-1}, is evaluated. Note that the outflow brine salinity remains up to 300 g·kg^{-1} to achieve close to ZLD conditions and therefore, the maximum water recovery.

Figure A.1.8 shows the effect of the produced water salinity on treated water cost and desalinated water cost. In this figure, it is possible to observe that the treated water cost decreases when the inlet salinity increases, changing from 11.54 to 4.42 US$ per cubic meter of inlet water. This reduction in process costs occurs since, as the concentrations of the inlet and outlet streams are more similar, less energy is needed to achieve the outflow stream near saturation conditions. Note that equipment size and the number of membrane modules are also reduced for treating feed water with higher TDS contents. For instance, the total membrane area for the MDS configuration, for the extreme salt concentrations (i.e., inlet concentration of 150 g·kg^{-1} and 250 g·kg^{-1}), decreases from 925 m^2 to 295 m^2, correspondingly. Also, in the case of inlet salinity equal to 150 g·kg^{-1}, an optimal solution of four MD stages is obtained, while only two MD stages are required to achieve the desired outlet condition with the highest inlet salinity (250 g·kg^{-1}).

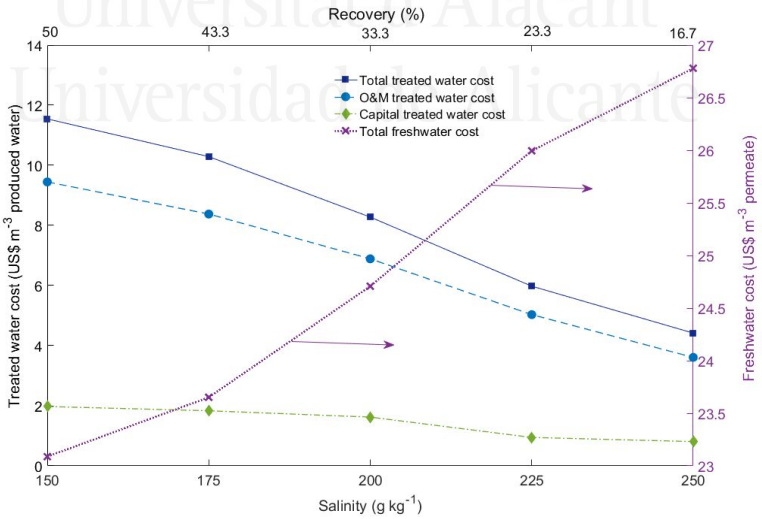

Figure A.1.8 Comparative effect of produced water salinity and water recovery on water treatment cost and freshwater cost of the multistage membrane distillation system.

It is worth mentioning that, the recovered water production rate is reduced when considering higher feed water salinities. The water recovered when the inlet salinity is significantly high (250 $g \cdot kg^{-1}$), decreases 67% comparing with the water recovered when the inlet salinity is equal to 150 $g \cdot kg^{-1}$, thus increasing the amount of brine to be disposed. Hence, although the cost per cubic meter of inlet water decreases, the same cost expressed in terms of cost per cubic meter of permeate increases, changing from just over 23 US$ per cubic meter of water generated in the process to nearly 27 US$ per cubic meter.

Membrane distillation feasibility for treating shale gas produced water

Previous sections highlighted the applicability of MDS to desalinate produced water to reach conditions close to ZLD. Nevertheless, the results indicate that the source of uncertainties such as the available heat source and inlet salinity conditions impact significantly the economic feasibility and configuration of MDS.

Without a low-cost steam source or waste heat available, the heating costs associated to obtain high permeate flux are significantly high. Whereas the steam source is usually known before deciding the selection of MDS as desalination technology, the reliability of the MDS design relies on the accuracy of the predicted value for the inlet salinity. On the one hand, if the MDS is designed for the worst case of the inlet salinity (lowest forecast value), the system will always satisfy the imposed specific salinity outlet conditions. However, this design would be at the expense of a high initial capital investment that might not be worthwhile if the real value (once the uncertainty is revealed) of the inlet salinity is significantly higher than the worst-case value. On the other hand, a design of the MDS considering the mean forecast value requires a lower capital expenditure than the previous situation. Nevertheless, the specific outlet salinity may not be attained if the feed concentration is below the mean value.

A comparison between the proposed MDS and the results obtained using MEE-MVR[36] has been carried out. As the MEE-MVR was designed for a higher flow rate, the treated cost has been updated using the equation of the effect of the capacity on the equipment defined by Turton et al.[101] **Table A.1.3** summarizes the treated cost obtained with both technologies considering three different inlet water salinity and inlet flow equal to 2 $kg \cdot s^{-1}$.

Table A.1.3 Treated water cost to desalinate shale gas water using MEE-MVR or MDS* (US$ per cubic meter shale gas water).

Shale gas water salinity ($g \cdot kg^{-1}$)	MEE-MVR**	MDS	
		Low heating cost	Waste heating source
70	9.9	15.4	5.5
150	9.4	12.4	4.1
200	7.8	8.2	2.7

* Results obtained by specifying brine salinity levels near to salt saturation concentration (i.e., 300 g kg^{-1}) and inlet flow equal to 2 $kg \cdot s^{-1}$.
** Updated cost using the equation of the effect of the capacity on the equipment defined by Turton et al.[101]

Clearly, if only heating source at high cost is available, MEE-MVR should be selected since the cost is significantly lower. If low heating cost is accessible, the decision is not trivial. Although the treated cost using MD is higher than the obtained with MEE-MVR, it must be emphasized that the difference is smaller as the salinity is higher. Additionally, as mentioned in the introduction section, it should consider that nowadays flowback water is reused to fracture other wells. Then, the water treated for discharge will be produced water (inlet salinity higher than 150 $g \cdot kg^{-1}$). Another important point that can influence the decision is that MEE-MVR requires a continuous electrical supply such as a power grid, which could be limited or unavailable in remote shale gas extraction sites. Besides, specialized equipment is necessary such as electrical-driven compressors or flash tanks. On the contrary, the inherent modular nature of MD is advantageous for produced water treatment, since its compactness and mobility make it easy to install small desalination plants close to remote extraction sites. Moreover, MD can operate using low-grade industrial steam that can be easily obtained in shale gas operations from waste heat recovered from the process facilities or flaring. Additionally, the treating cost of MD using waste heat is approximately half of the cost obtained using MEE-MVR (see **Table A.1.3**).

A.1.5 Conclusions

The present work highlights the potential for designing and deploying membrane distillation systems to treat shale gas produced water with high salt concentration. For this purpose, a multistage membrane distillation system (MDS) superstructure with energy recovery is modeled using the GDP framework as a MINLP problem in the GAMS modelling language. Then, this model is optimized to minimize the total annualized cost (TAC) of the system subject to the zero-liquid discharge (ZLD) condition (i.e., a concentrate stream

close to salt saturation conditions), which guarantees the maximum water recovery. It is worth noting that improving the cost-effectiveness of the process by reducing brine discharges decreases the water footprint associated with the shale gas production.

As a result, an optimal full-scale membrane distillation is designed to desalinate wastewater from shale gas operations by establishing the number of membrane modules in series, the size of heat exchangers, and the system operating conditions. Note also, the high complexity of the model, since the mass flowrates and temperatures of the streams are decision variables, and many of the equations that define the problem are non-convex and non-linear.

The results obtained emphasize the applicability of this promising technology, especially when a low-cost energy source or waste heat is available. The treatment cost varies significantly depending on the energy cost since it represents more than 50% of the total annualized cost. For example, the cost per cubic meter of treated water is 23.0 US$ per cubic meter for high energy costs; 8.3 US$ per cubic meter for low energy costs; and 2.8 US$ per cubic meter when energy is provided from waste heat of shale gas production.

Additionally, due to the uncertain salinity forecast of produced water, the reliability of the model has been checked by a sensitivity analysis carried out by varying the TDS concentration from 150 to 250 $g \cdot kg^{-1}$. The results reveal that the optimal configuration and the treatment cost depend significantly on the inlet salinity. Both the number of membrane stages and the total cost decrease as the inlet salinity increases. For the lowest value of salinity used in the analysis (i.e., 150 $g \cdot kg^{-1}$), a cost of 11.5 US$ per cubic meter is obtained with a system configuration composed of four membrane stages. On the contrary, for the highest salinity value (i.e., 250 $g \cdot kg^{-1}$) both the cost and the number of membranes in the system decrease to 4.4 US$ per cubic meter and two stages, respectively. Although the solutions considering higher feed water salinities are more cost effective, they have an important drawback for the water footprint of the shale gas exploitation activity. That is the low permeate flux of the MD process, which implies that only a small fraction of the huge amount of wastewater for the gas production is recovered.

The proposed model does not intend to provide exact realistic costs for the MD desalination process but a systematic tool to guide the decision-maker towards the most cost-effective MDS design for this particular application. Additionally, although MDS can be economically advantageous in remote areas where waste heat or low-grade thermal energy is available, more

laboratory analysis and pilot scale tests are still necessary to make this technology commercially attractive for shale gas wastewater desalination processes.

Nomenclature

Parameters

B	Membrane permeability, kg·(m^2·Pa·h)$^{-1}$
E	Membrane thickness, mm
F	Annualized capital cost factor
I	Fractional interest rate per year
W	Horizon time, year
U	Overall heat transfer coefficient, kW·(m^2·ºC)$^{-1}$
WH	Working hours in one year, h
ϑ	Temperature difference, ºC

Binary variables

y	Binary variable

Variables

a	Area, m^2
$capex$	Capital cost, kUS$·year^{-1}
h	Specific entalphy, kJ·kg^{-1}
f	Mass flowrate, kg·s^{-1}
ht	Heat transfer coefficient, W·m^{-2} ·K^{-1}
hv	Latent heat of vaporization of water, kJ·kg^{-1}
j	Vapor flux through the membrane, kg·m^{-2}·h^{-1}
$lmtd$	Logarithmic mean temperature difference
$opex$	Operational cost, kUS$ year^{-1}
p	Pressure, Pa
q	Heat flow, kW
t	Temperature, ºC
x	Salt mass fraction
γ	Activity coefficient of the water
ω	Salt molar fraction

Superscript

conc	Concentrate
cond	Conduction
hx	Heat exchanger
LO	Lower bound
m1	Membrane feed side
m2	Membrane permeate side
memb	Membrane

perm	Permeate
rec	Recirculated
refrig	Refrigerant
rej	Reject
UP	Upper bound
Subscripts	
n	Membrane stage
Acronyms	
CWT	Centralized Water Treatment
DCMD	Direct Contact Membrane Distillation
GAMS	General Algebraic Modelling System
GDP	Generalized Disjunctive Programming
MD	Membrane Distillation
MDS	Membrane Distillation System
MEE-MVR	Multiple-Effect Evaporation with Mechanical Vapor Recompression
MINLP	Mixed–Integer Nonlinear Programming
TAC	Total annualized cost
RO	Reverse Osmosis
TDS	Total Dissolved Solids
ZLD	Zero Liquid Discharge

Annex 2

Economic and Environmental Strategic Water Management in the Shale Gas Industry: An Assessment from the Viewpoint of Cooperative Game Theory

.

Abstract

In this work, we study possible cooperative strategies among shale gas companies that allow increasing benefits and reduce costs and environmental impacts of water management in shale gas production. If different companies are working in the same shale zone and their shale pads are relatively close, they might adopt a cooperative strategy, which can offer economic and environmental advantages. The objective is to compute a distribution of whatever quantifiable unit among the different companies to achieve a stable agreement on cooperation among them. To do this, a Mixed-Integer Linear Programming (MILP) model has been developed to address shale gas water management. To allocate the cost, profit and/or environmental impact among stakeholders, the Core and Shapley value are applied. Finally, the impact of cooperation among companies is shown by two examples involving three and eight players, respectively. The results shown that adopting cooperative strategies in the shale water management, companies are allowed to improve their benefits and to enhance the sustainability of their operations

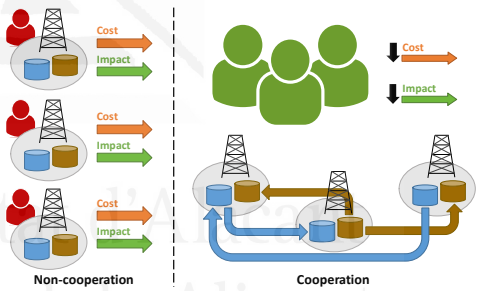

A.2.1 Introduction

All shale gas water management works, mentioned in **Chapter 2.2**, consider that all wellpads are exploited by a single company, but in practice, nearby wellpads could be exploited by different ones. However, none of those works has addressed from cooperative game theory the benefits that might be obtained if companies (i.e., wellpads, players, stakeholders) cooperate.[134] Gao and You[135] proposed the optimal design of non-cooperative shale gas supply chain considering economics and life cycle greenhouse emissions following the Stackelberg game. In this game, the players are a leader and a follower, and they compete on quantity. However, their work was focused on gas production and processing. Additionally, although some works have study game theory in the management of water resources[136–139] and others have shown that game theory can help resolve conflicts over water acquisition[140,141], none of them were focused in shale gas industry.

This work studies possible cooperative strategies among companies that allow reducing both costs and environmental impacts of water management in shale gas production. If different companies are working in the same shale zone and their shale pads are relatively close to each other it is eventually possible to develop cooperation activities like sharing freshwater transportation and storage costs. Water recycled among different wellpads (owned by different companies) reduces the total demand for freshwater and the storage capacity in some wellpads and, consequently, the transportation costs. Cooperation also allows building and sharing onsite water treatment facilities. In addition, the fracturing schedule can be adapted among different wellpads to maximize revenue and water reuse. Therefore, the objective of the proposed work is to compute the optimal operating conditions and to perform a distribution of the total cost among the different companies in order to achieve a stable agreement on cooperation among them. Operating conditions include the time, place and amount of freshwater acquired by each company, the number and size of water storage tanks, the drilling and fracturing schedule of each wellpad, the schedule of water reuse, and the characteristics of on-site treatment facilities.

The rest of this chapter is structured as follows: the next section gives a general description of the cooperative game theory and its applications. Then, the problem statement is described. Different case studies are proposed in order to show the benefits of cooperative games in shale gas water management and, finally, the conclusions are drawn.

A.2.2 Cooperative game theory: Overview

The cooperative game theory predicts rational strategic behaviours of individuals in cooperating situations, i.e., it studies the interaction among coalitions of players. Generally, a cooperative game is defined by a set of players $N = \{1,2,...,|N|\}$ and any subset of cooperation players $S \subseteq N$ is called "coalition". When all players cooperate in a unique coalition, it is called the "grand coalition" $S \equiv N = \{1,2,...,|N|\}$. The main question is: given the sets of feasible payoffs for each coalition, what payoffs will be given to each player? There are a lot of solution concepts in cooperative game theory to allocate whatever quantifiable unit of the grand coalition among the players. Note that, the function that assigns the quantifiable unit to each coalition is called "characteristic function". This quantifiable unit can be interpreted according to stakeholder interest. In this work, we deal with profit, environmental and cost games. In a profit game, players favour a higher outcome for themselves, whereas in environmental and cost games, they prefer lower amounts. To allocate whatever outcome, we applied the Core solution concept, which is formed by all the imputations for which there is no a sub-coalition that can obtain better results than the grand coalition, and the Shapley value, which yields for a unique allocation of a quantifiable unit that captures an average marginal contribution of each player.

Allocations properties

Players would be willing to form the grand coalition given fair allocation of the quantifiable unit among the players, otherwise, the outcome will be ineffective, and the players will not want to cooperate. In case of profit allocation, the following properties should achieve it:

- *Efficiency* guarantees that the total profit of the grand coalition, $v(N)$, must be equal to the sum of the cost share of each player N:

$$v(N) = \sum_{i \in N} \pi_i \tag{A.2.1}$$

- *Individual rationality* describes that the profit of the player that acts alone, $v(\{i\})$, must be lower or equal than the profit of that player cooperating, π_i :

$$v(\{i\}) \leq \pi_i \quad i \in N \tag{A.2.2}$$

- *Coalitional rationality* indicates that any coalition S cannot improve the allocation profit from the grand coalition:

$$\upsilon(S) \leq \sum_{i \in S} \pi_i \qquad S \subset N, S \neq \varnothing \tag{A.2.3}$$

Note that, in environmental and cost games, the characteristic function in individual and coalitional rationality (**Eqs. A.2.2 – A.2.3**) will be higher than or equal to the corresponding outcome.

The Core

The Core is a central concept in game theory[142] formed by all the imputations for which there is no a sub-coalition that can obtain better results than the grand coalition. The Core is then formed by the set of imputations that are efficient and stable. An imputation is efficient if the total profit is distributed among all the partners and it is stable if the principles of individual rationality (i.e., a single player has higher (or at least equal) profits while cooperating than when acting alone) and coalitional rationality (i.e., the imputation to each sub-coalition in the grand coalition must be higher or equal than when they act without the rest of the partners) are met. Therefore, the Core combines the three properties abovementioned and is defined as follows:

$$C(N,c) := \left\{ \pi \in \mathbb{R}^{|N|} \left| \overbrace{\sum_{i \in N} \pi_i = \upsilon(N)}^{efficiency} \text{ and } \overbrace{\sum_{i \in S} \pi_i \leq \upsilon(S)}^{rationality} \text{ for all } S \subset N, S \neq \varnothing \right. \right\} \tag{A.2.4}$$

The Shapley Value

The Shapley Value, given by **Eq. 5.5**, yields for a unique allocation of a quantifiable unit that captures an average marginal contribution of each player. The solution among the players follows three axioms (see Shapley (1953) for a detailed description)[143].

$$\Phi_i(c) = \sum_{S \subseteq N \setminus \{i\}} \frac{|S|!(|N|-|S|-1)!}{|N|!} \left[c(S \cup \{i\}) - c(S) \right] \tag{A.2.5}$$

The Shapley value is usually viewed as a good answer in cooperative game theory due to it based on those who contribute more to the groups that include them should be receive more. However, the uniqueness of Shapley value does not permit any flexibility, which can be a disadvantage in any case.[144]

Row generation algorithm

The number of coalitions rises exponentially ($2^{|N|}$) with an increasing number of players. In a <three-player games the number of coalitions is equal to eight

(including the empty set). However, for example, the number of coalitions increases to 256 in eight-player games. Therefore, it is not feasible (or at least practical) to solve an optimization problem for each sub-coalition. Due to that fact, a row generation algorithm was suggested to tackle the problem.[145] In this work, a game of eight-player games to allocate water-related cost is studied. Thus, the nomenclature used is concerning the cost allocation. The algorithm is detailed in the following steps.

1. Set $\mathcal{S}$; e.g., $\mathcal{S} = \{\{1\},\{2\},\ldots,\{|\ N\ |\}\}$. Compute the individual costs $c(S)$ for those coalitions $S \in \mathcal{S}$ and the total cost $c(N)$ for the coalition N.
2. Solve the **master problem** (LP)

$$\begin{cases} \min & w \\ s.t., & \sum_{i \in N} \pi_i = c(N) \\ & \sum_{i \in S} \pi_i - w \le c(S) \qquad S \in \mathcal{S} \\ & \pi_i \in \mathbb{R} \qquad i \in N \end{cases}$$

3. If $w > 0$, STOP (the instance has an empty core).
4. Otherwise, find a coalition $S' \notin (\mathcal{S})\left(S' \neq \varnothing\right)$ for which allocation is not in the core $\sum_{i \in S'} \pi_i > c(S')$, i.e., find the most violated core constraint fixing the cost allocation provided by the previous master problem π_i^*.

Sub-problem (MILP)

$$\begin{cases} \max & \mu \\ s.t., & \text{Assigmment constraints} \\ & \text{Shale gas water recovered} \\ & \text{Water demand} \\ & \text{Mass balance in storage tanks} \\ & \text{Mass balance in onsite treatment and CWT plant} \\ & \text{Treatment and storage capacity constraints} \\ & \sum_{i \in S} \pi_i^* x_i + c(S') = \mu, \quad S' := \{i \in N \mid x_i = 1\} \\ & \mu \in \mathbb{R};\ y_{t,p}^{on}, y_{t,p,w}^{hf}, y_{t,p,w}^{fb}, x_i \in \{0,1\} \quad p \in S \subseteq N \end{cases}$$

5. If no such coalition S' can be found, then STOP the algorithm because the found allocation is in the core.
6. Otherwise, compute the total cost $c(S')$ for this coalition, add the constraint $\sum_{i \in S'} \pi_i - w \le c(S')$ to the master problem (i.e., update $\mathcal{S} = \mathcal{S} \cup \{S'\}$), go to STEP 2.

The main idea of the algorithm is to avoid testing the constraints for all possible coalitions to find an element in the Core, i.e. avoid solving the water management mathematical model for all possible coalitions. First, a master problem is solved using some subcoalitions (i.e. coalitions formed by individual players). The solution of the master problem provides a possible imputation. Then, fixing the imputation obtained in the last master problem, we solve an extended water management problem that searches for a coalition that violates most of the stability constraints. If such a coalition exists, the master problem is then updated, and the procedure is repeated until we get an imputation inside the Core.

A.2.3 Problem Statement

In this chapter, we use the shale gas water management superstructure and a simplified version of mathematical model defined in **Chapter 2.2**[146]. The main difference is that, in this work, we do not consider the flowback and produced water contamination. Besides, the onsite treatment is leased by company; hence as each company belongs one wellpad. The onsite treatment cannot be transported from one wellpad to another one. We also consider that each wellpad is drilled by one different company with their own fracturing crew. Additionally, companies are working in the same shale zone, i.e. shale pads are relatively close.

Briefly, given a set of wells grouped in a set of wellpads that must be fractured, the model determines optimal coordinated operation conditions, such as the fracturing schedule, the storage capacity, the flowback destination (reuse, treatment and disposal), the water recycled among different wellpads, the location and the number of onsite water treatment facilities required. A detailed description of the general superstructure of shale gas water management operations and the assumptions done are given in the **Appendix D - Section 1**.

The mathematical model, outlined in **Eq. (A.2.6)** and detailed in the **Appendix D - Section 2**, comprises: assignment constraint, logic constraints, shale gas and flowback water production, well water demands, mass balances in storage tanks, onsite and offsite treatments, treatment and storage capacity constraints and objectives function. Depending on the objective function regarded, the mathematical model will identify the best water management strategy maximizing the profit or minimizing the environmental impacts or water-related costs (depending on the interests of companies) considering any number of players. The gross profit to be

maximized includes revenue from shale gas and expenses for wellpad construction and preparation, shale gas production and water-related costs (i.e., wastewater disposal cost, freshwater withdrawal, friction reducer cost, onsite and offsite treatment cost, wastewater and freshwater transportation cost and storage tank cost). The cost objective function to minimize includes the aforementioned water-related cost. The life cycle impact assessment minimizes environmental impacts associated with water withdrawal, treatment and transportation. They are evaluated according to the principles of Life Cycle Assessment (LCA) using the ReCiPe indicator (**Appendix D - Section 3**).

$$\max \begin{Bmatrix} profit(f^{w}_{t,p,w}, f^{gas}_{t,p,w}, y^{on}_{t,p}, y^{hf}_{t,p,w}, y^{fb}_{t,p,w}), -LCIA(f^{w}_{t,p,w}, y^{on}_{t,p}, y^{hf}_{t,p,w}, y^{fb}_{t,p,w}), \\ cost(f^{w}_{t,p,w}, y^{on}_{t,p}, y^{hf}_{t,p,w}, y^{fb}_{t,p,w}) \end{Bmatrix}$$

$$\begin{aligned} s.t., \quad & \text{Assigmment constraints} \\ & \text{Shale gas water recovered} \\ & \text{Water demand} \\ & \text{Mass balance in storage tanks} \\ & \text{Mass balance in onsite treatment and CWT plant} \\ & \text{Treatment and storage capacity constraints} \\ & f^{w}_{t,p,w}, f^{gas}_{t,p,w} \in \mathbb{R} \\ & y^{on}_{t,p}, y^{hf}_{t,p,w}, y^{fb}_{t,p,w} \in \{0,1\} \\ & p \in S \subseteq N \end{aligned} \tag{A.2.6}$$

In **Eq. (A.2.6)**, f represents the continuous variables representing flowrates and y are the binary variables that involve discrete decisions. The problem is implemented in GAMS 25.0.1.[105] and solved using Gurobi 7.5.2.[56]

A.2.4 Case studies and discussion

Benefits of cooperation

We explore the benefits from non-cooperation to full cooperation among players in a motivation example composed of three-player games (i.e., companies, wellpad). Throughout this work, we suppose that each wellpad is drilled by one different company with their own fracturing crew. Additionally, we consider that companies are working in the same shale zone; hence, their shale pads are relatively close. Life-cycle impact assessment (LCIA) database and data of the problem based on Marcellus play –cost coefficients and model parameters– are given in the **Appendix C**, **Table C.1** and **Table C.2**, respectively. The time period is discretized in two years at one week per time period since most of the shale gas water is extracted during the first month

after the well is drilled. However, this time period might be extended until the exploitation ends (10 – 20 years) with the renewal of the contract. The optimization model also includes one interruptible freshwater source, one centralized water treatment facility (CWT), one class II disposal well and three wellpads. Wellpads one, two and three are composed of five, four and six wells, respectively. Each wellpad belongs and is operated by different companies.

Water management solution in shale gas operations exhibits different performance of economic and environmental indicators: the gross profit and LCIA, respectively. After applying the epsilon-constraint method Pareto frontier[147] to this multi-objective problem, we obtain the Pareto set of solutions, as shown in **Figure A.2.1**, which indicates the existing trade-off between both objectives. Reductions of the LCIA can only be achieved by compromising the gross profit. **Figure A.2.1** also displays the also displays the following cases: **Point A**: cooperative solution when companies minimize the LCIA; **Point B**: no cooperative solution when companies minimize the LCIA; **Point C**: the fracturing schedule is fixed in advance and each company maximizes its revenue cooperating in water management costs; **Point D**: cooperative solution when companies maximize the gross profit and **Point E**: no cooperative solution when companies maximize the gross profit.

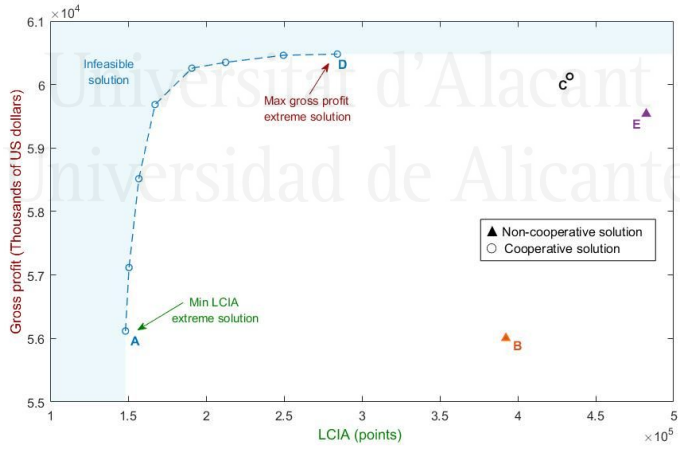

Figure A.2.1 Pareto set of solutions (blue circles) for the bi-objective problem that maximizes the gross profit and minimizes life-cycle impact assessment (LCIA) for a cooperative shale gas water management. Cooperative solutions are displayed by circles (○) and non-cooperative solutions by triangles (▲). Extreme solution A and solution B corresponds with the case where shale companies minimize LCIA, whereas in the extreme solution D and solution E companies are focus on maximizing gross profit. Solution C has the fracturing schedule fixed in advance. Each company maximize its shale gas revenue cooperating in shale gas water management costs.

Comparing **points A&B** and **points D&E**, the benefits of cooperation are clearly presented. On the one hand, regarding the solution of the minimization of LCIA when companies work cooperating or independently –points A&B–, a reduction of 62% in the environmental impact is achieved when all players work together. Cooperation strategy is an environmental breakthrough in freshwater preservation, increasing the total freshwater reused and, consequently, decreasing the total water withdrawal 38153 m3. Additionally, reusing wastewater for fracturing operations reduces water transportation impacts since companies are working in the same area. On the other hand, taking into consideration the economic objective (points D&E), besides the profit increment of $942K when companies cooperate, a reduction of 41% in environmental impacts are achieved. Note that, as shown in **Figure A.2.2**, shale gas revenue is higher when a company works independently ($87.2M in case E) that cooperating ($86.8M in case D). However, important saving in water-related cost is achieved by changing the schedule to maximize the cooperation between the partners. Fracturing schedules obtained for points A&D are shown in **Figure 5.3 (a)-(b)**.

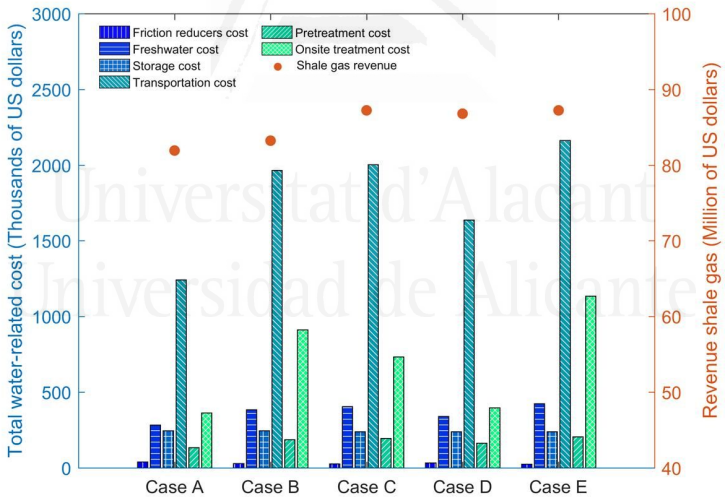

Figure A.2.2 Disaggregated water-related cost contribution (left axis) and total shale gas revenue (right axis) for cases A, B, C, D & E of shale water management strategies of three companies (i.e., wellpads, players). Case A (cooperation) and Case B (non-cooperation) corresponds with the case where shale companies minimize LCIA, whereas Case D (cooperation) and Case E (non-cooperation) companies are focus on maximizing gross profit. In Case C (cooperation) has the fracturing schedule fixed in advance.

We also analyze the situation in which each company does not want to change the fracturing schedule that maximizes its revenue (**Figure A.2.3** (c)). However, they are willing to cooperate in order to minimize LCIA impacts and water-related costs. In this case, water-related cost decreases, increasing the gross profit \$590K with respect non-cooperative solution. However, setting the schedule limits the possibilities of cooperation being the water-related cost 22% higher than in the cooperative solution.

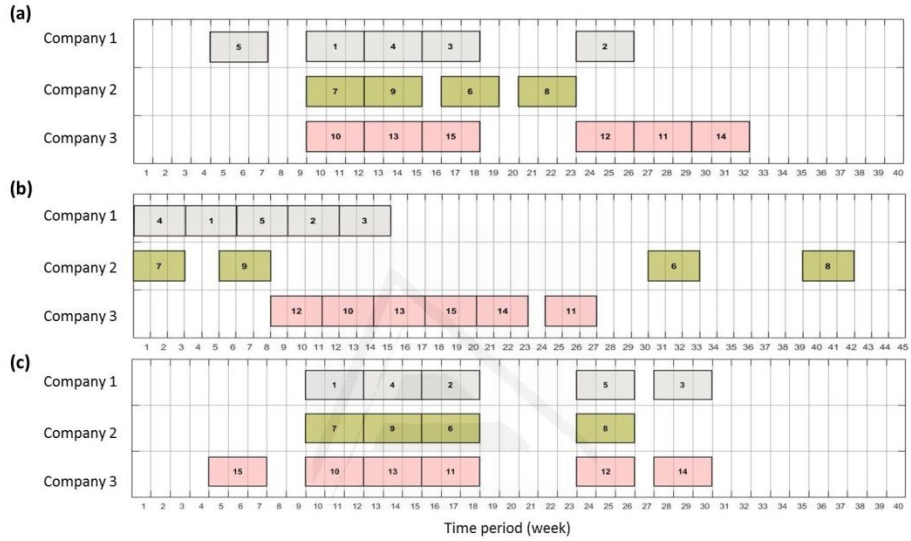

Figure A.2.3 Fracturing schedule obtained (a) maximizing revenues, (b) minimizing environmental impacts, and (c) established in advance for each company that maximized its revenue according to shale gas price forecast.

A further analysis of the optimal shale gas water management strategy of points B, C &E is showed in **Figure A.2.4**. In the cooperative game (Case D), the best strategic solution is to install an onsite treatment in wellpad 1. The optimal schedule obtained tries to maximize the total water reused between companies (80932 m^3). Note that company 3 only uses 18638 m^3 of freshwater for its fracturing operations. This is because wellpad 3 is the furthest away from the freshwater source. As transportation is the highest individual cost (**Figure A.2.2**), this strategy leads to significant saving compared with the other two cases (Cases C&E) where it is not possible to reuse the same amount of water. In the non-cooperative game (Case E), the water that each company can use in drilling operations is the water generated for the fractured wells belonging to its company. Therefore, the total withdrawal of water increases to 160752 m^3 reducing at the same time the reused water. Additionally, each company must lease an onsite treatment to

manage the wastewater when there are no more wells to fracture (at the end of the total time horizon), which increases the total cost due to the extra money spent on transportation and installation of each onsite treatment. The cooperative game that sets the schedule in advance (Case C) does not allow the maximization of reused water (being equal to 51631 m^3), which increases the total water treated. This implies the necessity of installing an extra onsite treatment in wellpad 2 –compared with the cooperative solution–, which increases the water treatment cost (**Figure A.2.2**).

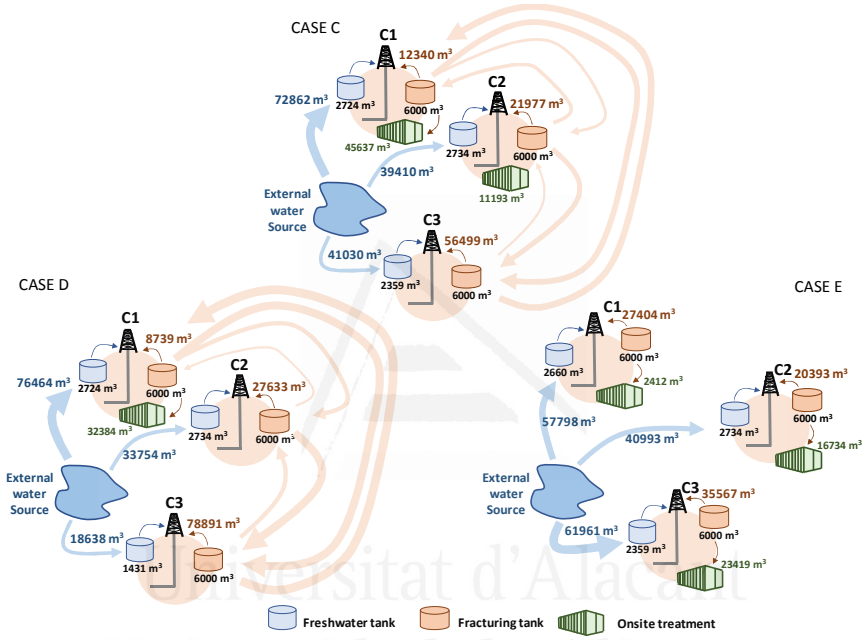

Figure A.2.4 Optimal solution of: (a) cooperative with a fixed fracturing schedule (Case C), (b) cooperative (Case D), and (c) non-cooperative (Case E) for shale water management strategies of three companies (i.e., wellpads, players).

Life Cycle Assessment (LCA) methodology in a three-player games

Regarding further analysis of environmental impacts, the results show that the total emissions from the water management vary greatly among the five cases (see **Figure A.2.5**).

On the one hand, in the cases focused on minimizing the environmental impacts, the LCIA is around 49.6% lower when the three companies cooperate (Case A) than the case when the companies non-cooperate (Case B). On the other hand, in the cases focused on maximizing the profit, the LCIA is around 31.7% lower when the three companies cooperate (Case D) than in the case when the companies non-cooperate (Case E). In case when the schedule is

fixed in advance, maximizing the revenues of each company independently (Case C), it has an environmental impact 27.9% higher than Case D, but it is around 5.4% lower than Case E.

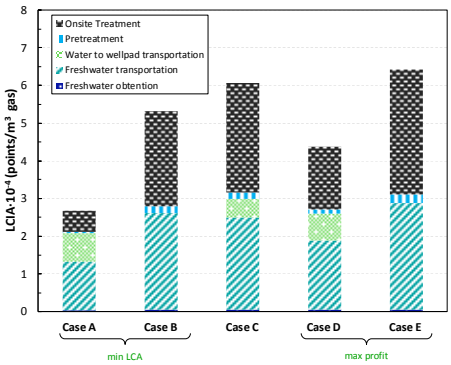

Figure A.2.5 Environmental impact of the different life cycle stages using ReCiPe Endpoint (H,A) in points.m^{-3} gas.

Additionally, the three main impact categories (ecosystem quality, human health and resource depletion) and the eighteen subcategories have been analyzed in **Figure A.2.6**. Human health and resource depletion are the most affected categories due to the use of fossil fuels in transportation and the use of electricity in the wastewater treatment. For the same reasons, climate change and fossil depletion are the most affected subcategories. As can be seen again, there is a substantial difference in environmental impacts between the cooperative cases and the non-cooperative ones.

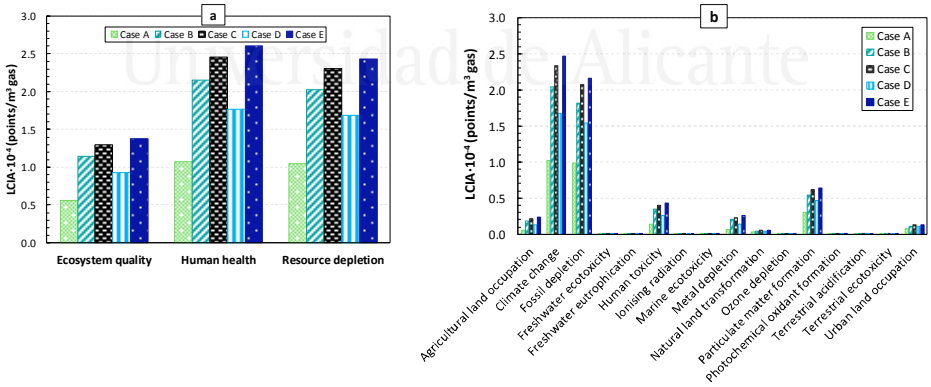

Figure A.2.6 Comparison between case studies A, B, C, D and E using ReCiPe Endpoint (H,A). a) Comparison between the main impact categories. b) Comparison between subcategories.

As climate is the contribution with the highest impact in the ReCiPe endpoint, its corresponding midpoint indicator, the Global Warming Potential (GWP), is selected to be analyzed. The GWP obtained for each case study (from A to E), in kT CO2-eq, is equal to 1.2, 2.5, 2.9, 2.1 and 3.1, respectively, considering that the extraction of shale gas per well is around 37.5 Mm^3 gas, and there are 15 wells grouped in 3 wellpads, the total amount of shale gas considered is 562.5 Mm^3 gas. On the one hand, in the cases focused on minimizing the LCIA, GWP decreases around 52% when cooperation is carried out (Case A) compared non-cooperation case (Case B). On the other hand, in the cases focused on maximizing the profit, GWP decreases around 32% comparing cooperative with non-cooperative game. It should be noted that water-related cost follows the same tendency that the environmental impact, basically because transportation and electricity are the most influential factors.

Profit and environmental impact allocation in a three-player games

Clearly, full cooperation between companies brings potential economic and environmental benefits, but the question then arises as how to fairly allocate the profit or environmental impact (depending on players' interest) among the players of the grand coalition. As mentioned in section 5.2, the Core and shapely value are two prominent solution concepts to allocate profit (and environmental impact) in cooperative game theory.

According to the Core solution concept, first, we compute the characteristic function, which assigns a profit value (maximizing the gross profit in the shale gas water management model) or environmental impact value (minimizing the LCIA) to each possible coalition. **Table A.2.1** displays the characteristic values obtained, where υ is the characteristic function when the gross profit is maximized and μ when the LCIA is minimized, respectively. Note that in a three-player game the number of possible coalitions is equal to eight, including the empty set.

Table A.2.1 Characteristic function for the three-player games focus in (a) the maximization of gross profit (k$) and (b) minimization of LCIA (points).

a) $\upsilon(\{1\})$	$\upsilon(\{2\})$	$\upsilon(\{3\})$	$\upsilon(\{1,2\})$	$\upsilon(\{1,3\})$	$\upsilon(\{2,3\})$	$\upsilon(\{1,2,3\})$
21314	15079	23145	36666	45142	38623	60480

b) $\mu(\{1\})$	$\mu(\{2\})$	$\mu(\{3\})$	$\mu(\{1,2\})$	$\mu(\{1,3\})$	$\mu(\{2,3\})$	$\mu(\{1,2,3\})$
118054	115689	158639	95558	118943	142664	148319

As abovementioned, the Core combines the properties of efficiency, and individual and coalitional rationality. Therefore, to determine the profit allocation (π_1, π_2, π_3) among players, the constraint satisfaction problem described in **Eq. A.2.7** must be solved. Note that if the interest of stakeholders is to minimize LCIA, the environmental impact allocation in individual and coalitional rationality will be lower than or equal to the characteristic function.

$$
\begin{aligned}
&\min \quad z = 1 \\
&s.t., \quad \pi_1 + \pi_2 + \pi_3 = \upsilon(\{1,2,3\}) = 60480 \\
&\qquad \pi_1 \geq \upsilon(\{1\}) = 21307 \\
&\qquad \pi_2 \geq \upsilon(\{2\}) = 15073 \\
&\qquad \pi_3 \geq \upsilon(\{3\}) = 23138 \\
&\qquad \pi_1 + \pi_2 \geq \upsilon(\{1,2\}) = 36666 \\
&\qquad \pi_1 + \pi_3 \geq \upsilon(\{1,3\}) = 45142 \\
&\qquad \pi_2 + \pi_3 \geq \upsilon(\{2,3\}) = 38623 \\
&\qquad \pi_1, \pi_2, \pi_3 \in \mathbb{R}
\end{aligned}
\tag{A.2.7}
$$

where υ is the optimal profit of each coalition and π_1, π_2 and π_3 define the portion of the profit that is allocated to each player.

The Core contains an infinite number of stable imputations, i.e. any sub-coalition could not arise to reach a better result than in the grand coalition. It is important to highlight that the non-empty Core of three player is guaranteed in advance if the following sub-additive property is satisfied: $\upsilon(\{1,2\})+\upsilon(\{1,3\})+\upsilon(\{2,3\}) \leq 2\upsilon(N)$ $\upsilon(\{1,2\})+\upsilon(\{1,3\})+\upsilon(\{2,3\}) \leq 2\upsilon(N)$. The non-empty Core guarantee that no conflicts are captured by the characteristic function satisfying all players simultaneously.

The geometrical interpretation of the Core of three-player games is easily illustrated graphically in a ternary plot. **Figure A.2.7** displays the geometrical interpretation of the Core and Shapley value to allocate environmental impact for three-player games**.**

Each individual and coalitional rationality divides the space into two regions being one region feasible with the Core allocation. (the direction of the arrows points out into the feasible region). The compact convex polyhedron formed by intersection of all half-spaces is the Core. In case of profit allocation, the feasible region that defines the Core is a small area which is difficult to observe in the geometrical interpretation. That is, the unique payoff division got with the Shapley value and the extreme points of the convex polyhedron that define the feasible Core region are very close.

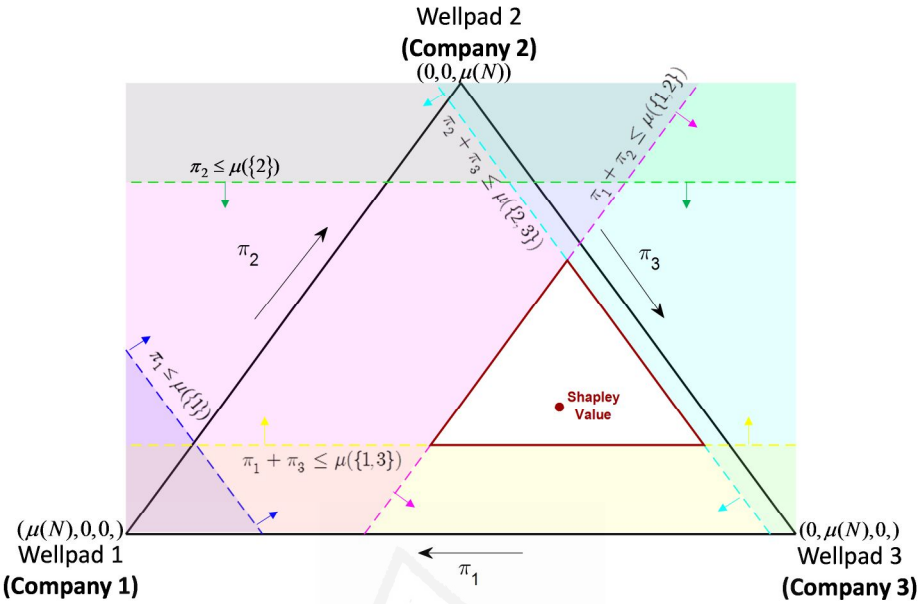

Figure A.2.7 Geometrical interpretation of the Core and Shapley value to allocate environmental impacts for a three player games.

Table A.2.2 shows the marginal benefit of each player considering both the profit allocation (obtained by using the Shapley value and the extreme allocation profit of the polyhedron that shapes the Core), and in **Table A.2.3** the environmental impacts allocation among each company based on both allocation concepts.

Table A.2.2. Marginal benefit (k$) of each player estimating the profit allocation based on Shapley value and the Core concept,

Solution concept		Player 1	Player 2	Player 3
Shapley Value		344	201	407
The Core - extreme points in the polyhedron of three companies game*	a	541	255	156
	b	285	0	667
	c	541	0	411
	d	30	255	667

**a,b,c,d are the extreme points of the polyhedron. Note that this polyhedron is not displayed in any figure because it is difficult to observe its geometrical interpretation due to the proximity of points.

Table A.2.3 Environmental impact reduction (%) in the cooperative game case compared to the non-cooperative case for each player, estimating the environmental impact allocation based on the Shapley value and the Core solution concept.

Solution concept		**Player 1**	**Player 2**	**Player 3**
Shapley Value		73.5	63.7	52.6
Extreme points in the polyhedron of three companies game**	a'	70.0	22.3	66.7
	b'	95.2	74.6	28.6
	c'	43.9	74.6	66.7

** a',b',c' are the extreme points of the polyhedron displayed in Figure 5.7.

Water cost allocation and environmental analysis in an eight-player game

A further analysis of cooperative game theory in the shale gas industry is performed by analyzing a larger case study composed of eight players (i.e., wellpads). In this case, we focus on the minimization of water-related cost, minimizing at the same time environmental impacts related to transportation and water withdrawal. A total of 30 wells are allocated among the eight wellpads. Besides, three different natural sources are considered in this example.

The analysis of possible strategies and cost allocation of an eight-player game is not trivial. In this case, the number of possible coalitions increases to 256. Hence, computing the characteristic function of all possible coalitions to formulate the constraint satisfaction problem and calculate the Shapley value will require extensive time and efforts. Thus, the problem is tackled applying the row generation algorithm following the steps detailed in section 2. First, we compute the optimal individual cost (shown in **Figure A.2.8,** non-cooperative solution) and the grand coalition cost, which is equal to \$2911.3K. Then, we start the iteration process to allocate the cost among the players without computing the cost for each coalition. The iteration process to allocate the costs is detailed in **Table A.2.4,** displaying in the last row the cost allocated to each stakeholder.

As can be seen in **Figure A.2.8,** each player obtains significant savings cooperating. Moreover, the sum of total water management cost when eight companies work separately (non-cooperative game theory) is equal to \$5398.5K, which is 46% higher than the optimal cost obtained when all companies cooperate (\$2911.3K).

Table A.2.4 Iteration process of row generation algorithm for eight-player games.

Iteration	Master Problem								Subproblem
	π_1^*	π_2^*	π_3^*	π_4^*	π_5^*	π_6^*	π_7^*	π_8^*	
1	-1865	522	1040	784	619	820	435	555	{2,3,4,5,6,7,8}
2	622	-1965	1040	784	619	820	435	555	{1,3,4,5,6,7,8}
3	622	289	1040	784	-1635	820	435	555	{1,2,3,4,6,7,8}
4	622	522	1040	784	619	820	435	-1932	{1,2,3,4,5,6,7}
5	375	289	-542	784	619	820	435	129	{1,2,4,5,6,7}
6	375	289	577	-335	619	820	435	129	{3,5,6,7}
7	375	289	577	451	414	239	435	129	{1,2,4,7}
8	375	289	577	451	414	428	247	129	{1,2,4,6,7}
9	375	289	577	451	453	389	247	129	{2,3,5,7}
10	**375**	**289**	**577**	**472**	**453**	**389**	**226**	**129**	**No coalition found**

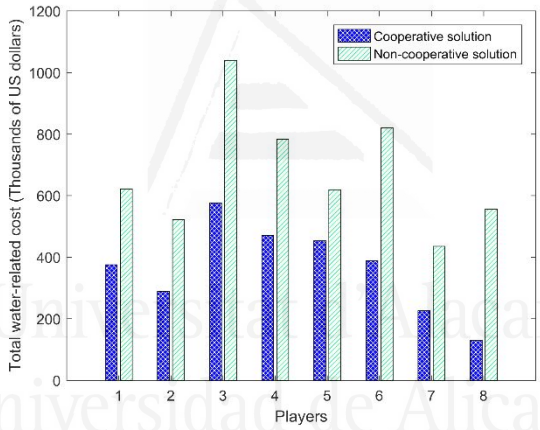

Figure A.2.8 Optimal water-related cost of each player in eight-player games (cooperating and in the absence of cooperation).

A further analysis of the solution can be seen in **Figure A.2.9**. It shows the optimal strategic solution of the cooperative game theory for eight companies (i.e., wellpads, players). As can be seen, companies 1 and 4 drill the wells using flowback water coming from the same and neighboring wellpads, while companies 7 and 8 only use freshwater from source 1 for fracturing operations. Company 6 withdrawal water from the freshwater source 3, while companies 2, 3 and 4 from the freshwater source 2. Additionally, only the installation of one onsite treatment in wellpad 5 is required. Besides, the total water withdrawal cooperating (241764 m^3) decreases by around 27% with respect to the non-cooperative solution (329608 m^3).

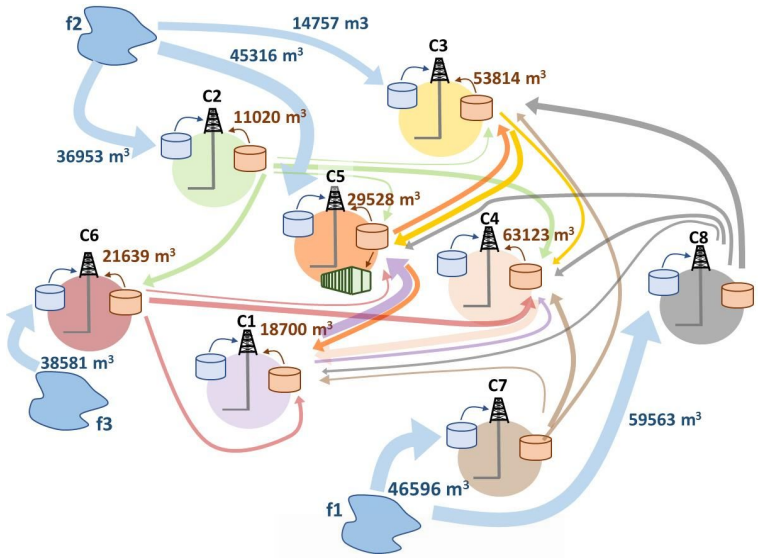

Figure A.2.9 Optimal shale water management solution of the cooperative game theory of eight companies (i.e., wellpads, players).

Regarding Life Cycle Assessment (LCA) for this case study, **Figure A.2.10** shows that the environmental impact when the eight companies cooperate is around 58.0% lower than the environmental impact when the companies non-cooperate. Mainly, this is due to the reduction of water sent to onsite treatment and consequently, the increment of water reuse for fracturing purposes.

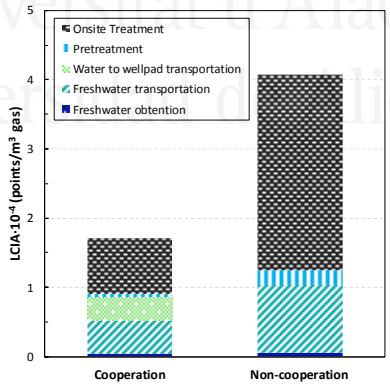

Figure A.2.10 Comparison of the total environmental impact using ReCiPe Endpoint (H,A) when companies cooperate and in the absence of cooperation.

Additionally to the total environmental impact, the three main impact categories (ecosystem quality, human health and resource depletion) and the eighteen subcategories have also been analyzed in **Figure A.2.11.** Note that

the most affected categories are human health and resource depletion, driven again, as we observed in three-player games, by the amount of fossil fuel in water transport and by the use of electricity in the wastewater treatment. For the same reasons, climate change and fossil depletion are the most affected subcategories.

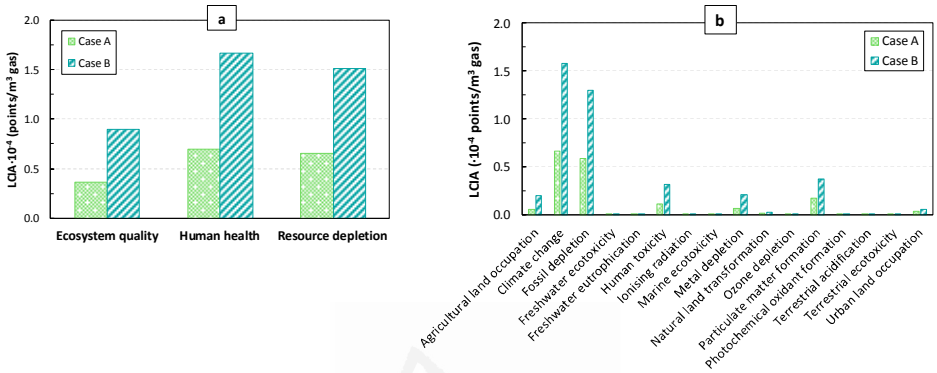

Figure 5.11 Comparison between the two case studies using ReCiPe Endpoint (H,A). a) Comparison between the main impact categories. b) Comparison between subcategories.

In this case study, considering again that the extraction of shale gas per well is around 37.5 Mm^3 gas, and taking into account that this case study is composed by 30 wells grouped in 8 wellpads, the amount of shale gas is 1125 Mm^3 gas. The total emissions (expressed in kT CO_2-eq) obtained is 1.6 in cooperative game and 3.9 in non-cooperation game. Therefore, GWP decreases around 59% when cooperation is carried out.

A.2.5 Conclusions

This study highlights the importance of cooperation in shale gas industry to reduce the costs but also to contribute to to reduce the costs and environmental impact. The objective of the work is how to distribute cost, profit or environmental impact in shale gas water management among stakeholders when all companies work together. To do this, we use two important solution concepts in cooperative game theory, the Core and Shapley value. The environmental impacts are evaluated according to the principles of LCA using the ReCiPe method.

First, a motivation example formed by three-player games shows the existing trade-off between maximizing profit and minimizing environmental impacts in a cooperative and non-cooperative game. Additionally, both profit and environmental impact allocation are performed. Then, a larger example composed of an eight-player game focused on minimizing water-related cost is

analyzed. In this case, allocation cost is achieved using a row generation algorithm.

The results obtained with both examples reveals savings of 30-50% when all companies work together instead of working independently. The major economics saving is due to the increase of water reused, reducing at the same time water withdrawal and transportation. As regards environmental concerns, this water management alternative helps in reducing the water footprint and emissions.

Chapter 3

Conclusions and Future Works

This work is focused on water management optimization in shale gas operations for enhancing overall shale gas process efficiency and sustainability.

The first objective (**Chapter 2.1** and **Annex A.1**) involves the development of economic efficient of wastewater treatments for water reuse and adequate disposal to the environment. The second part (**Chapters 2.2** and **Annex A.2**) deals with water management and cooperative strategies. The objective is to systematically obtain in a superstructure-based design a cost-effective and sustainable solution. In this chapter, we summarize the most relevant findings of the four main chapters of the thesis. Then we enumerate the main contributions, followed by a discussion of future works.

3.1 Conclusions summary

The MINLP mathematical model presented in **Chapter 2.1** for the wastewater pretreatment determines the selection of the best water pretreatment alternatives depending on its final destination, its reuse or later desalination treatments. The multistage superstructure proposed is composed of several stages with distinct water pretreatment technologies. The selection of the equipment at each superstructure stage was carried out on a stage-by-stage heuristic basis, in order to guarantee the workability of each upcoming stage. Since each wastewater-desired destination requires specific target composition constraints, three case studies are performed to assess the applicability of the proposed approach. Thus, four distinct feed water compositions covering a large range of flowback water concentrations are evaluated for three different target conditions: reuse; post-treatment by membrane-based technologies; and, post-treatment by thermal-based technologies. The optimal water pretreatment system configurations obtained is very similar, or even equal, for the different case studies: strainer filter, electrocoagulation, sedimentation and softening. The main differences between them are due to the need of removing scaling forming ions and diluting the outlet flow to the required TDS concentration.

In **Annex A.1**, the multistage membrane distillation superstructure highlights the potential for designing and deploying membrane distillation systems to treat shale gas produced water with high salt concentration. The mathematical model is focused on minimizing the cost of the system subject to the zero-liquid discharge (ZLD) condition (i.e., a concentrate stream close to salt saturation conditions), which guarantees the maximum water recovery. Note that improving the cost-effectiveness of the process by reducing brine discharges decreases the water footprint associated with the shale gas production.

The results obtained emphasize the applicability of this promising technology, especially when a low-cost energy source or waste heat is available. The treatment cost varies significantly depending on the energy cost since it represents more than 50% of the total annualized cost. For example, the cost per cubic meter of treated water for the base case (e.i., inlet salinity 200 $g \cdot kg^{-1}$) is 23.0 US$ per cubic meter for high energy costs; 8.3 US$ per cubic meter for low energy costs; and 2.8 US$ per cubic meter when energy is provided from waste heat of shale gas production. Additionally, due to the uncertain salinity forecast of produced water, the reliability of the model has been checked by a sensitivity analysis carried out by varying the TDS concentration from 150 to 250 $g \cdot kg^{-1}$. The results reveal that the optimal configuration and the treatment cost depend significantly on the inlet salinity. Both the number of membrane stages and the total cost decrease as the inlet salinity increases. For the lowest value of salinity used in the analysis (i.e., 150 $g \cdot kg^{-1}$), a cost of 11.5 US$ per cubic meter is obtained with a system configuration composed of four membrane stages. On the contrary, for the highest salinity value (i.e., 250 $g \cdot kg^{-1}$) both the cost and the number of membranes in the system decrease to 4.4 US$ per cubic meter and two stages, respectively. Although the solutions considering higher feed water salinities are more cost effective, they have an important drawback for the water footprint of the shale gas exploitation activity. That is the low permeate flux of the MD process, which implies that only a small fraction of the huge amount of wastewater for the gas production is recovered. Additionally, although MDS can be economically advantageous in remote areas where waste heat or low-grade thermal energy is available, more laboratory analysis and pilot scale tests are still necessary to make this technology commercially attractive for shale gas wastewater desalination processes.

Both models proposed in **Chapter 2.2** and **Annex A.2** are not intended to provide exact realistic costs for the pretreatment and membrane distillation

desalination process but a systematic tool to guide the decision-maker towards the most cost-effective system designs for this particular application.

Chapter 2 proposes an MINLP mathematical model accounting for economic, environmental and social objectives in shale gas production, considering the TDS concentration of flowback and impaired water. The sustainability profit, a new weighted sum objective expressed in monetary value, helps the decision-makers towards more economic and sustainable decisions.

The model is applied to different case studies based on Marcellus Play. Different assumptions are analyzed in each case study to gain a clear understanding of the nature of the problem. The results reveal that reusing flowback water is compulsory to obtain a compromise solution among the three pillars of sustainability: economic, environmental and social criteria. Furthermore, the solution unveils that the level of TDS in reused water is not an obstacle to use it as fracturing fluid in shale gas operations, although the concentration increases over the time, and consequently the cost of the friction reducers. Regarding the wastewater management alternatives, it has been also shown that onsite desalination is the most cost-effective once water demand for fracturing new wells would be less than the volume of water produced by active wells. Finally, it should be noted that transportation is the highest water-related contribution to both economic and environmental impacts.

Finally, the study carried out in **Annex A.2** highlights the importance of cooperation in the shale gas industry to reduce the costs but also to contribute to saving the environment. The objective of the work is how to distribute cost, profit or environmental impacts in shale gas water management among stakeholders when all companies work together. Two important solution concepts in cooperative game theory, the Core solution concept and Shapley value are used.

First, a motivation example formed by three-player games shows the existing trade-off between maximizing profit and minimizing environmental impacts in a cooperative and non-cooperative game. Additionally, both profit and environmental impact allocation are performed using the Core and Shapley value solution concept. Then, a higher example composed by eight-player games focused on minimizing water-related cost is analyzed. In this case, allocation cost is achieved using the row generation algorithm. The results obtained with both examples reveals savings of around 30-50% when all companies work together instead of working independently. The major economic saving is due to the increase of the amount of water reused, reducing at the same time water withdrawal and transportation.

3.2 Research contributions

The main contributions of the present work are listed below:

- Collection of the main water pretreatment technologies used in shale gas industry within a more comprehensive multistage superstructure.
- Systematic mathematical modelling approaches for synthesizing the optimal set of alternatives for water pretreatment system (WPS), applied to shale gas production.
- Detailed cost analysis embracing all water pretreatment alternatives.
- Global optimization of WPS design, considering a large range of feed water compositions and specific composition constraints for each wastewater-desired destination.
- Development of an optimization model for membrane distillation system (MDS) to attain close to ZLD conditions for the treatment of shale gas produced water.
- Optimization and design of full-scale membrane distillation systems coupled with heat recovery to determine the optimal system configuration and optimal working conditions.
- Application of the MDS model to real inlet flowrate and variable high-salinity to evaluate if the projected technology can be applied to desalinate produced water coming from different shale gas basins.
- Development of a rigorous MINLP shale gas water planning model including the estimation of friction reducers expenses as a function of TDS concentration, including rigorous handling at storage solution by determining the required number of tanks installed and uninstalled over the time period.
- Application of cooperative game theory to shale gas water management.
- Environmental, cost and profit allocation among the stakeholders using the Core and Shapley value solution concepts.

3.3 Future Research

The models are flexible to be used in several situations (U.S., Europe, China...). However, the major drawback of the models is the quality of the information (i.e., it is expected that the forecast in the U.S. produces better results than those in other countries). Several fluctuation factors as wastewater flowrate forecast, natural water availability and natural gas price are presented in the optimization. These factors can significantly affect the fracturing schedule and consequently, the final benefits. Therefore, the next

step would consist of taking these uncertainties into consideration formulating a stochastic programming problem to obtain a better estimation of the expectedprofit related to shale gas operations.

As it is explained throughout the thesis, shale gas operations present important potential adverse impact on the environement. In this work, a brief environmental analysis is done focus in the water management section; however, a large size problem including shale gas treatment and management could be another interesting step. Moreover, multiobjective optimization framework under uncertainty could be addressed to find the trade-off between environmental impacts and profit using different environmental indicators.

3.4 Conclusiones

Este trabajo se centra en la optimización de la gestión del agua en las operaciones de gas de esquisto para mejorar la eficiencia y la sostenibilidad del proceso global.

El primer objetivo (**Capítulo 2.1** y **Anexo A.1**) implica el desarrollo económico y eficiente de tratamientos para las aguas residuales generadas debido a la extracción del gas de esquisto. La segunda parte (**Capítulos 2.2** y **Anexo A.2**) trata sobre la gestión del agua y las estrategias de cooperación. El objetivo es obtener un diseño rentable y sostenible basado en superestructura. En este apartado, resumimos los hallazgos más relevantes.

El modelo matemático (MINLP) presentado en el **Capítulo 2.1** para el pretratamiento de aguas residuales determina la selección de las mejores alternativas según su destino final, su reutilización o los tratamientos de desalinización posteriores. La superestructura propuesta está compuesta de varias etapas con distintas tecnologías de pretratamiento de agua. La selección del equipo en cada etapa se lleva a cabo de forma heurística etapa por etapa, con el fin de garantizar la viabilidad de cada próxima etapa. Dado que cada destino final requiere restricciones específicas de la composición de entrada, se realizan tres casos de estudio para evaluar la aplicabilidad del enfoque propuesto. Por lo tanto, cuatro distintas composiciones de agua de entrada que cubren un amplio rango de concentraciones de agua de retorno se evalúan para tres destinos diferentes: reutilización; postratamiento mediante tecnologías basadas en membrana; y, postratamiento mediante tecnologías de base térmica. Las configuraciones óptimas del sistema de pretratamiento obtenidas son muy similares, o incluso iguales, para los diferentes casos de estudio: filtro, electrocoagulación, sedimentación y ablandamiento. Las principales diferencias entre ellos se deben a la necesidad de eliminar las incrustaciones formando iones y diluyendo el flujo de salida a la concentración de TDS requerida.

En el **Anexo A.1**, la superestructura de destilación de membrana de múltiples etapas destaca el potencial para diseñar sistemas de destilación de membrana para tratar el agua producida debido a las extracciones de gas de esquisto. El modelo matemático se enfoca en minimizar el coste del sistema sujeto a la condición de descarga de líquido cero (ZLD) (es decir, la corriente de concentrado cerca de las condiciones de saturación de sal), que garantiza a

la vez la máxima recuperación de agua. Mejorando la rentabilidad del proceso al reducir las descargas de salmuera disminuye la huella hídrica asociada con la producción de gas de esquisto.

Los resultados obtenidos enfatizan la aplicabilidad de esta prometedora tecnología, especialmente cuando se dispone de una fuente de energía de bajo coste o calor residual. El coste del tratamiento varía significativamente según el coste de la energía, ya que representa más del 50% del coste total anualizado. Por ejemplo, el coste por metro cúbico de agua tratada para el caso base (ejemplo, salinidad de entrada 200 $g \cdot kg^{-1}$) es de 23.0 US$ por metro cúbico para costes altos de energía; 8.3 US$ por metro cúbico para costes de energía bajos; y 2.8 US$ por metro cúbico cuando la energía proviene del calor residual de la producción de gas de esquisto. Además, debido al pronóstico incierto de la salinidad del agua producida, la confiabilidad del modelo se verificó mediante un análisis de sensibilidad realizado variando la concentración de TDS de 150 a 250 $g \cdot kg^{-1}$. Los resultados revelan que la configuración óptima y el coste del tratamiento dependen significativamente de la salinidad de entrada. Tanto el número de etapas de membrana como el coste total disminuyen a medida que aumenta la salinidad de entrada. Para el valor más bajo de salinidad utilizado en el análisis (es decir, 150 $g \cdot kg^{-1}$), se obtiene un coste de 11.5 US$ por metro cúbico con una configuración de sistema compuesta por cuatro etapas de membrana. Por el contrario, para el valor de salinidad más alto (es decir, 250 $g \cdot kg^{-1}$), tanto el coste como el número de membranas en el sistema disminuyen a 4.4 US$ por metro cúbico y dos etapas, respectivamente. Aunque la destilación por membranas puede ser rentable en áreas remotas donde se dispone de calor residual aún son necesarios más análisis de laboratorio y pruebas a escala piloto para hacer que esta tecnología sea comercialmente atractiva para los procesos de desalinización de aguas residuales de gas de esquisto.

Los dos modelos propuestos en el **Capítulo 2.2** y el **Anexo A.2** no pretenden proporcionar costes exactos para el proceso de pretratamiento y desalinización por destilación, sino una herramienta sistemática para guiar al responsable de la toma de decisiones un diseño más rentable para esta aplicación en particular.

El **Capítulo 2** propone un modelo matemático (MINLP) que tiene en cuenta criterios económicos, ambientales y sociales en la producción de gas de esquisto, considerando la concentración de sales en el flujo de retorno. Este beneficio sostenible es un nuevo objetivo de suma ponderada expresado en

valor monetario, y ayuda a los responsables de la toma de decisiones hacia decisiones económicas y sostenibles.

El modelo se aplica a diferentes casos de estudio basados en Marcellus Play para obtener una comprensión clara de la naturaleza del problema. Los resultados revelan que la reutilización del agua de retorno es obligatorio para obtener una solución de compromiso entre los tres pilares de la sostenibilidad: criterios económicos, ambientales y sociales. Además, la solución revela que el nivel de sales en el agua reutilizada no es un obstáculo para usarlo como fluido de fracturamiento en las operaciones de gas de esquisto, aunque la concentración aumente con el tiempo y, en consecuencia, el coste de los aditivos. Con respecto a las alternativas de gestión de aguas residuales, también se ha demostrado que la desalinización in situ, ya que la demanda de agua para fracturar nuevos pozos sería menor que el volumen de agua producida por los pozos activos. Finalmente, cabe señalar que el transporte es la mayor contribución tanto para los impactos económicos como ambientales.

Finalmente, el estudio realizado en el **Anexo A.2** destaca la importancia de la cooperación en la industria del gas de esquisto para reducir los costes, pero también para contribuir a reducir los impactos ambientales. El objetivo del trabajo es cómo distribuir los costes, las ganancias o los impactos ambientales en la gestión del agua de gas de esquisto entre las partes interesadas cuando todas las empresas trabajan juntas. Se utilizan dos conceptos importantes en la teoría de juegos cooperativos, el concepto de Core y el valor de Shapley.

Primero, un ejemplo de motivación formado por tres jugadores muestra el compromiso existente entre maximizar el beneficio y minimizar los impactos ambientales en un juego cooperativo y no cooperativo. Además, tanto la asignación de beneficios como el impacto ambiental se realizan utilizando el concepto de Core y el valor de Shapley. Luego, se analiza un ejemplo más grande compuesto por ocho jugadores enfocados en minimizar el coste relacionado con el agua. En este caso, el coste de asignación se logra utilizando un algoritmo de generación de filas. Los resultados obtenidos con ambos ejemplos revelan ahorros de alrededor del 30-50% cuando todas las empresas trabajan juntas en lugar de trabajar de forma independiente. El mayor ahorro económico se debe al aumento de la cantidad de agua reutilizada, que reduce al mismo tiempo la extracción de agua y el transporte.

Chapter 4

Scientific Contributions

This chapter summarizes all the scientific contributions of the candidate, including the publications that constitute this thesis.

4.1 Journal Articles

Onishi, V.C., **Carrero-Parreño, A.**; Reyes-Labarta, J.A.; Fraga, E.S.; Caballero, J.A.; Desalination of shale gas produced water: A rigorous design approach for zero-liquid discharge evaporation systems. *Journal of Cleaner Production*. **2017**. 140: p. 1399-1414.

Onishi, V.C.; **Carrero-Parreño, A.**; Reyes-Labarta, J.A.; Ruiz-Femenia, R.; Salcedo-Díaz, R.; Fraga, E.S.; Caballero, J.A.; Shale gas flowback water desalination: Single vs multiple-effect evaporation with vapor recompression cycle and thermal integration. *Desalination*. **2017**. 404: p. 230-248.

Carrero-Parreño, A.; Onishi, V.C.; Salcedo-Diaz, R.; Ruiz-Femenia, R.; Fraga, E.S.; Caballero, J.A.; Reyes-Labarta, J.A.; Optimal Pretreatment System of Flowback Water from Shale Gas Production. *Industrial & Engineering Chemistry Research*. **2017**. 56: p. 4386-4398.

Onishi, V.C., Ruiz-Femenia, R.; Salcedo-Diaz, R.; **Carrero-Parreño, A.**; Reyes-Labarta, J.A.; Fraga, E.S.; Caballero, J.A.; Process optimization for zero-liquid discharge desalination of shale gas flowback water under uncertainty. *Journal of Cleaner Production*, **2017**. 164: p. 1219-1238.

Carrero-Parreño, A.; Reyes-Labarta, J.A.; Salcedo-Diaz, R.; Ruiz-Femenia, R.; Onishi, V.C.; Caballero, J.A.; Grossman, I.E.; A holistic planning model for sustainable water management in the shale gas industry. *Industrial & Engineering Chemistry Research*. **2018.** 57, p. 13131-13143

Carrero-Parreño, A.; Onishi, V.C.; Ruiz-Femenia, R.; Salcedo-Diaz, R.; Caballero, J.A.; Reyes-Labarta, J.A.; Optimization of multistage membrane

distillation system for treating shale gas produced water. *Desalination*. **Under review (July 14, 2018).**

Carrero-Parreño, A.; Quirante, N.; Ruiz-Femenia, R.; Reyes-Labarta, J.; Salcedo-Díaz, R.; Caballero, J.A.; Economic and Environmental Strategic Water Management in the Shale Gas Industry: An Assessment from the Viewpoint of Cooperative Game Theory. *ACS Sustainable Chemistry & Engineering*. **Submitted.**

4.2 Book Chapters

Carrero-Parreño, A.; Onishi, V.C.; Ruiz-Femenia, R.; Salcedo-Diaz, R.; Caballero, J.A.; Reyes-Labarta, J.A.; Multistage Membrane Distillation for the Treatment of Shale Gas Flowback Water: Multi-Objective Optimization under Uncertainty, in *Computer Aided Chemical Engineering 40*, A. Espuña, M. Graells, and L. Puigjaner, Editors. **2017**, Elsevier. p. 571-576.

Salcedo-Diaz, R., Ruiz-Femenia, R.; **Carrero-Parreño, A**.; Onishi, V.C.; Reyes-Labarta, J.A.; Caballero, J.A.; Combining Forward and Reverse Osmosis for Shale Gas Wastewater Treatment to Minimize Cost and Freshwater Consumption, in *Computer Aided Chemical Engineering 40*, A. Espuña, M. Graells, and L. Puigjaner, Editors. **2017**, Elsevier. p. 2275-2730.

Onishi, V.C., Ruiz-Femenia, R.; Salcedo-Diaz, R.; **Carrero-Parreño, A**.; Reyes-Labarta, J.A.; Caballero, J.A.; Multi-Objective Optimization of Renewable Energy-Driven Desalination Systems, in *Computer Aided Chemical Engineering 40*, A. Espuña, M. Graells, and L. Puigjaner, Editors. **2017**, Elsevier. p. 499-504.

Onishi, V.C., Ruiz-Femenia, R.; Salcedo-Diaz, R.; **Carrero-Parreño, A**.; Reyes-Labarta, J.A.; Caballero, J.A.; Optimal Shale Gas Flowback Water Desalination under Correlated Data Uncertainty, in *Computer Aided Chemical Engineering 40*, A. Espuña, M. Graells, and L. Puigjaner, Editors. **2017**, Elsevier. p. 943-948.

Carrero-Parreño, A.; Ruiz-Femenia, R.; Caballero, J.A.; Reyes-Labarta, J.A.; Grossmann, I.E.; Sustainable Optimal Strategic Planning for Shale Water Management, in *Computer Aided Chemical Engineering 43*, A. Friedl, et al., Editors. **2018**, Elsevier. p. 657-662.

4.3 Conferences

Carrero-Parreño, A.; Onishi, V.C.; Ruiz-Femenia, R.; Salcedo Díaz, R.; Caballero, J. A. ; Reyes-Labarta, J. A. Shale gas flowback water desalination: multistage membrane distillation considering different configurations and heat integration. *3rd International Conference on Desalination using Membrane Technology* - MEMDES 2017 (Gran Canaria. April, 2017).

Onishi, V.C., Ruiz-Femenia, R.; Salcedo-Diaz, R.; **Carrero-Parreño, A**.; Reyes-Labarta, J.A.; Caballero, J.A.; Optimal shale gas flowback water desalination under correlated data uncertainty. *10th World Congress of Chemical Engineering – ESCAPE 27 joint event.* (Barcelona. October, 2017).

Onishi, V.C., Ruiz-Femenia, R.; Salcedo-Diaz, R.; **Carrero-Parreño, A**.; Reyes-Labarta, J.A.; Caballero, J.A.; Multi-Objective Optimization of Renewable Energy-Driven Desalination Systems. *10th World Congress of Chemical Engineering – ESCAPE 27* joint event. (Barcelona. October, 2017).

Carrero-Parreño, A.; Onishi, V.C.; Ruiz-Femenia, R.; Salcedo-Diaz, R.; Caballero, J.A.; Reyes-Labarta, J.A.; Multistage Membrane Distillation for the Treatment of Shale Gas Flowback Water: Multi-Objective Optimization under Uncertainty. *10th World Congress of Chemical Engineering – ESCAPE 27* joint event. (Barcelona. October, 2017).

Salcedo-Diaz, R., Ruiz-Femenia, R.; **Carrero-Parreño, A**.; Onishi, V.C.; Reyes-Labarta, J.A.; Caballero, J.A.; Combining Forward and Reverse Osmosis for Shale Gas Wastewater Treatment to Minimize Cost and Freshwater Consumption. *10th World Congress of Chemical Engineering – ESCAPE 27* joint event. (Barcelona. October, 2017).

Caballero, J.A; Onishi, V.C.; Reyes-Labarta, J.A.; **Carrero-Parreño, A**.; Ruiz-Femenia, R.; Salcedo-Diaz, R.; Optimal Shale Gas Water Management: A Perspective from the Cooperative Games Theory. *2018 AIChE Annual Meeting.* (Pittsburgh. November, 2018).

Caballero, J.A; **Carrero-Parreño, A**.; Onishi, V.C.; Reyes-Labarta, J.A.; Salcedo-Diaz, R.; Ruiz-Femenia, R.; Grossmann, I.E.; Sustainable Optimal Strategic Planning for Shale Water Management. *2018 AIChE Annual Meeting.* (Pittsburgh. November, 2018).

4.4 Research Stay

Place: Center of Advanced Decision-making at Carnegie Mellon University, Pittsburgh, United States

Advisor: Prof. Ignacio E. Grossmann

Duration: 6 months (from June 19 to December 16, 2017).

This research stay was supported by the University of Alicante grant for an international predoctoral mobility (BOUA January, 21 2017)

4.5 Award

Second Prize of the EURECHA Student Contest Problem 2017.
Organized by: European Committee for the Use of Computers in Chemical Engineering Education (EURECHA).
Presented project: Carbon CO_2 Reuse in Direct DME Synthesis from Syngas.
Authors: **Carrero A**, Medrano JD, Quirante N.
Presentation of the work in CAPE-Forum Conference. Athens, Greece. 06-08, September, 2017.

Appendices

Appendix A. Design equations for heat exchanger and cooler in the chapter 2.1.

Heat Exchanger design equations

Energy balance

$$\begin{aligned}&\left(f_n^{rec}+f_n^{perm}\right)\cdot\left(h_n^p(t_n^{perm})-h_n^p(t_n^{perm'})\right)=\\&=f_n^{memb}\cdot\left(h_n^s(t_n^{hx,out},x_n^{memb})-h_n^s(t_n^{hx,in},x_n^{memb})\right)\qquad\forall n\in N\end{aligned}\tag{A.1}$$

Heat exchanger area calculation

$$a_n^{hx}\cdot U^{hx}\cdot lmtd_n^{hx}=q_n^{hx}\qquad\forall n\in N\tag{A.2}$$

Chen's approximation for the calculation of logarithmic mean temperature difference

$$lmtd_n^{hx}=(0.5\cdot(\theta_n^3\cdot\theta_n^4)(\theta_n^3+\theta_n^4))^{1/3}\qquad\forall n\in N\tag{A.3}$$

$$\theta_n^3=t^{perm}-t_n^{hx,out}\qquad\forall n\in N\tag{A.4}$$

$$\theta_n^4=t_n^{perm'}-t_n^{hx,in}\qquad\forall n\in N\tag{A.5}$$

Design temperature constraints

$$\Delta T^{min}\le t^{perm}-t_n^{hx,out}\qquad\forall n\in N\tag{A.6}$$

$$\Delta T^{min}\le t_n^{perm'}-t_n^{hx,in}\qquad\forall n\in N\tag{A.7}$$

Cooler design equations

Energy balance

$$q_n^{cooler}=f_n^{rec}\cdot\left(h_n^p(t_n^{perm'})-h_n^p(t_n^{rec})\right)\qquad\forall n\in N\tag{A.8}$$

Area calculation

$$a_n^{cooler}\cdot U^{cooler}\cdot lmtd_n^{cooler}=q_n^{cooler}\qquad\forall n\in N\tag{A.9}$$

Chen's approximation for the calculation of logarithmic mean temperature difference

$$lmtd_n^{cooler}=(0.5\cdot(\theta_n^5\cdot\theta_n^6)(\theta_n^5+\theta_n^6))^{1/3}\qquad\forall n\in N\tag{A.10}$$

$$\theta_n^5=t_n^{perm'}-T^{refrig,out}\qquad\forall n\in N\tag{A.11}$$

$$\theta_n^6=t_n^{rec}-T^{refrig,in}\qquad\forall n\in N\tag{A.12}$$

Design temperature constraints

$$\Delta T^{min} \leq t_n^{perm'} - T^{refrig,out} \qquad \forall n \in N \tag{A.13}$$

$$\Delta T^{min} \leq t_n^{rec} - T^{refrig,in} \qquad \forall n \in N \tag{A.14}$$

Appendix B. Aspen Hysys® flow diagram and comparison between mathematical model and simulated results of membrane distillation system.

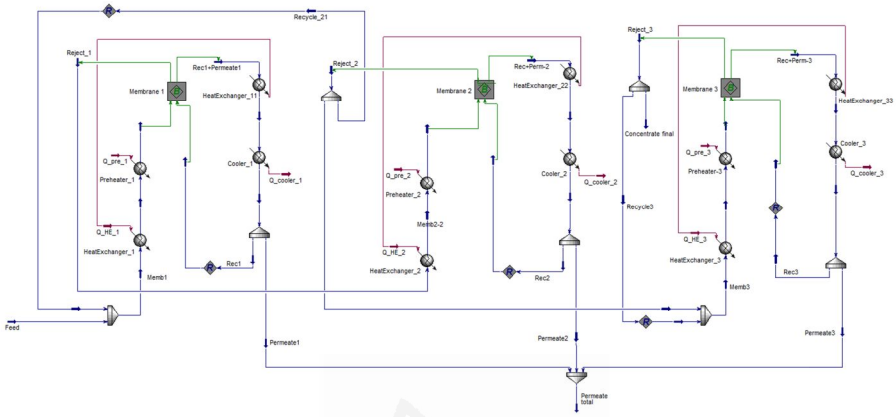

Figure B.1 Membrane distillation system process flow diagram in Aspen HYSYS® of the optimal solution for the base case.

Table B.1 Process variables for the optimal solution of the MDS model and values obtained from the simulation.

Process Variables	Stage	Model	Hysys	Relative error (%)
Heat flow preheater (kW)	1	1185	1191	-0.50
	2	1176	1183	-0.59
	3	976	986	-1.01
Heat flow heat exchanger (kW)	1	3130	3113	0.54
	2	3068	3053	0.49
	3	2192	2186	0.27
Heat flow cooler (kW)	1	1175	1181	-0.51
	2	1166	1173	-0.60
	3	968	977,90	-1.01
Permeate temperature (^{o}C)	1	80.78	80.69	0.11
	2	80.60	80.50	0.12
	3	78.44	78.52	-0.10
Final concentrate (kg·s^{-1})	-	1.33	1.33	0.00
Final permeate (kg·s^{-1})	-	0.66	0.66	0.00

Appendix C: Input data used in Chapter 2.2: cost coefficients, model parameters, eco-cost, and social coefficients.

The following tables provides the parameters used in the mathematical model of Chapter 2.2.

Table C.1. Costs coefficient

Parameter	Value	Units	Ref
Drilling cost	270,000	$	[148]
Production cost	0.014	$/m^3	[148]
Disposal cost	90 - 120	$/m^3	[149]
Truck cost	0.15	$/km/m^3	[149]
Storage cost	70	$/week/tank	*
Impoundment cost	3.86	$/m^3	[103]
Pretreatment cost	0.8 - 2	$/m^3	[150]
Desalination cost	6 - 15	$/m^3	[38,151]
Demobilize, mobilize and clean out cost	2,000	$/week	*
Centralized water treatment	42 - 84	$/m^3	[149]
Demobilize, mobilize and clean out cost	1,500	$	*
Friction reducer cost	0.18 - 0.30	$/m^3	*
Freshwater withdrawal cost	1.76 - 3.5	$/m^3	[103]
Moving crew cost	83,000	$	*

*Provided by a company

Table C.2. Model parameters

Parameter	Value	Units	Ref
CST_s	60	m^3	*
$C_{t,p,w}^{well}$	3,000 - 200,000	ppm	[16]
C^{con}	300	g kg^{-1}	[38]
$F_n^{on,UP}$	4,000	m^3 $week^{-1}$	*
$F_k^{cwt,UP}$	16,700	m^3 $week^{-1}$	*
N_s^{UP}	100	-	*
$N^{im,UP}$	3	-	*
$N_n^{on,UP}$	3	-	*
V^{im}	120	m^3	*
WD_w	4,800 - 18,600	m^3 $week^{-1}$	[16]
τ_w	1-5	weeks	[16]

*Provided by a shale gas company

Table C.3. Eco-cost coefficients [69]

Raw material (μ_r)	**Eco-cost**	**Interpretation**
Freshwater	0.19 € m^{-3}	water scarcity
Products (μ_g)	**Eco-cost**	**Interpretation**
Desalinated water to discharge	1 € m^{-3}	Water from drilling is treated and returned to natural resource
Desalinated water to reuse	1 € m^{-3}	Water from drilling is treated and used for new drilling operations
Disposal water	37 € m^{-3}	Disposal
Natural gas at extraction	0.05 € m^{-3}	Natural gas extraction
Transport (μ_g^T , μ_r^T)	**Eco-cost**	**Interpretation**
Transport	0.01 € m^{-3} km^{-1}	Truck plus container

Table C.4. Social coefficients

Parameter	Value	Units	Ref
N^{jobs}	145	-	[152]
S^{Gross}	857	\$ week^{-1}	[153]
S^{Net}	685	\$ week^{-1}	[153,154]
$C^{UNE,State}$	125	\$ week^{-1}	[71]
$C^{EMP,State}$	12.5	\$ week^{-1}	[71]
$C^{company}$	6.5	\$ week^{-1}	[71]

Appendix D:

D.1 Supply Chain Network Description

The superstructure addressed (see **Figure D.1**) comprises wellpads (i.e., companies, player) p, unconventional shale gas wells w, centralized water treatment technologies (CWT) k, natural freshwater sources f, and disposal wells d.

Natural freshwater needed for hydraulic fracturing is obtained from an uninterruptible freshwater source and is stored in freshwater tanks (FWT). After hydraulic fracturing, the water that comes out, called flowback water, is stored onsite in fracturing tanks (FT) before pretreatment (removing suspended solids, oil and grease, bacteria and certain ions) in mobile units, or else transported to CWT facility, to a neighboring wellpad or Class II disposal. It is assumed that each company has its own freshwater and fracturing tanks and its own pretreatment. After pretreatment, the flowback and produced water stored in fracturing tanks can be recycled as a fracturing fluid in the same wellpad, or it can be desalinated in portable onsite treatment.

Throughout the problem, the following assumptions are made: (1) A fixed time period is discretized into weeks as time intervals; (2) Water transportation is only executed by trucks; (3) The volume of water used to fracture a well is obtainable at the beginning of well drilling including water required in drilling, construction and completion (4) Each wellpad belong to a different shale gas company.

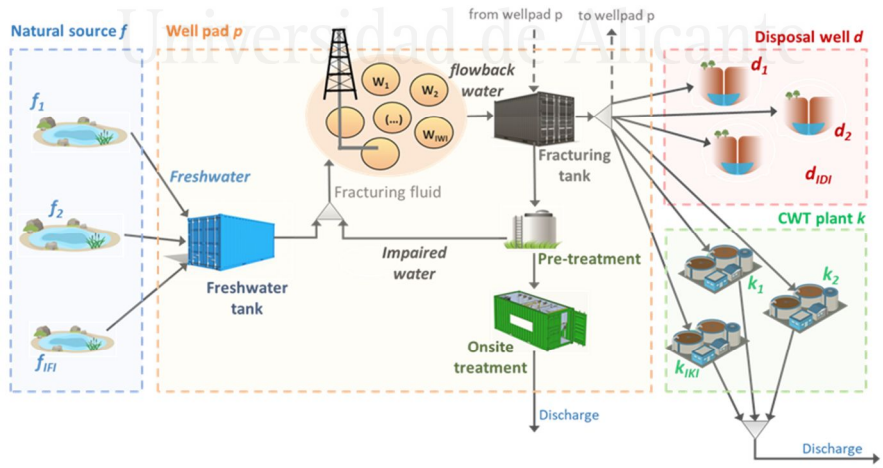

Figure D.1. Supply chain network of shale gas water management operations.

D.2 Mathematical Model Formulation

The shale gas water management mathematical model is a simplified version of the model proposed by Carrero-Parreño et al.[146] The main difference is that, in this work, we do not consider the flowback and produced water contamination. The equations that define this problem are detailed below:

Assignment constraint

Eq. (D1) guarantees that at the time period each well is going to fracture,

$$\sum_{t \in T} y^{hf}_{t,p,w} = 1 \qquad \forall w \in RPW_p, p \in P \tag{D1}$$

where indicates that the well w in wellpad p is stimulating in time period t.

Eq. (D2) ensures that there is no overlap in drilling operations between different wells,

$$\sum_{p \in P} \sum_{w \in RPW_p} \sum_{tt=t-\tau_w+1}^{t} y^{hf}_{tt,p,w} = 1 \qquad \forall t \in T \tag{D2}$$

where τ_w is a parameter that indicates the time required to fracture well w.

Shale water recovered

After fracturing a well, a portion of the freshwater injected returns to the wellhead,

$$y^{hf}_{t,p,w} = y^{fb}_{t+\tau_w,p,w} \qquad t \le T - \tau_w, \forall w \in RPW_p, p \in P \tag{D3}$$

where $y^{fb}_{t,p,w}$ represents the time period when the flowback water comes out. The binary variable $y^{fb}_{t,p,w}$ is treated as a continuous variable since its integrality is enforced by **Eq. (D3)**.

The wastewater from each wellpad is calculated with **Eq. (D4),**

$$f^{well}_{t,p,w} = \sum_{w \in RPW_p} \sum_{tt=0}^{tt \le t-1} F^{well}_{t-tt,p,w} \cdot y^{fb}_{tt+1,p,w} \qquad \forall t \in T, p \in P \tag{D4}$$

where $F^{well}_{t,p,w}$ are parameters that indicate flowback flowrate.

Eq. (D5) describes the mass balance of flowback water collected from the wells belonging to wellpad p,

$$f^{pad}_{t,p} = \sum_{w \in RPW_p} f^{well}_{t,p,w} \qquad \forall t \in T, p \in P \tag{D5}$$

Mass balance in storage tanks

The level of the fracturing tank in each time period ($st_{t-1,p,s}$) depends on water stored in the previous time period, the flowback water recovered after the hydraulic fracturing ($f_{t,p}^{pad}$), the water sent to another wellpad to be reused ($f_{t,pp,p}^{imp,pad}$), the water sent to CWT ($f_{t,p,k}^{cwt,in}$) or onsite ($f_{t,p}^{onpre,in}$) treatment and the water sent to disposal ($f_{t,p,d}^{dis}$). The mass balance in the storage tank is described in **Eq. (D6).**

$$st_{t-1,p,s} + f_{t,p}^{pad} + \sum_{\substack{pp\in P \\ pp\neq p}} f_{t,pp,p}^{imp,pad} = st_{t,p,s} + \sum_{\substack{pp\in P \\ pp\neq p}} f_{t,p,pp}^{imp,pad} + f_{t,p}^{onpre,in} + \sum_{k\in K} f_{t,p,k}^{cwt,in} + \sum_{d\in D} f_{t,p,d}^{dis} \qquad \forall t\in T, p\in P, s\in\{s1\} \tag{D6}$$

The fresh water is also stored in portable tanks. The mass balance is detailed in **Eq. (D7)**.

$$st_{t-1,p,s} + \sum_{f\in F} f_{t,p,f}^{source} = st_{t,p,s} + f_{t,p}^{fresh} \qquad \forall t\in T, p\in P, s\in\{s2\} \tag{D7}$$

The volume of the tank (V_S) is calculated by **Eq. (D8)**,

$$st_{t,p,s} + \theta_{t,p,s} \le v_s \qquad \forall t\in T, p\in P, s\in S \tag{D8}$$

where $\theta_{t,p,s}$ represents the inlet water in the storage tank divided by the number of days in a week. This variable is introduced due to as the time horizon is discretized into weeks, the storage tank should handle the inlet water that comes from one day.

The volume of the tank is bounded by the maximum storage capacity allowed in a wellpad per week.

$$v_s \le V_s^{UP} \qquad \forall s\in S \tag{D9}$$

Water demand

The water demand per wellpad ($f_{t,p}^{dem}$) can be provided by a mixture of impaired water ($f_{t,p}^{imp}$) or fresh ($f_{t,p}^{fresh}$),

$$f_{t,p}^{dem} = f_{t,p}^{fresh} + f_{t,p}^{imp} \qquad \forall t\in T, p\in P \tag{D10}$$

The amount of water demand per well is given by **Eq. (D11)**,

$$f_{t,p}^{dem} = \sum_{w\in RPW_p} f_{t,p,w}^{dem} \qquad \forall t\in T, p\in P \tag{D11}$$

Eq. (D12) indicates that the water when the well is going to be drilled, must be greater or equal than the well water demand (WD_w),

$$f_{t,p,w}^{dem} \geq WD_w \cdot \sum_{c \in C} y_{t,p,w,c}^{hf} \qquad \forall t \in T, w \in RPW_p, p \in P \tag{D12}$$

Onsite treatment

Onsite pretreatment mass balance is described in **Eq. (D13)**,

$$f_{t,p}^{pre,out} + f_{t,p}^{on,slud} = f_{t,p}^{pre,in} \qquad \forall t \in T, p \in P \tag{D13}$$

The recovery factor (α^{pre}) is used to model the relationship between inlet and outlet streams.

$$f_{t,p}^{pre,out} = \alpha^{pre} \cdot f_{t,p}^{pre,in} \qquad \forall t \in T, p \in P \tag{D14}$$

The outlet pretreated water can be used as a fracturing fluid ($f_{t,p}^{imp}$) or/and can be sent to onsite desalination treatment ($f_{t,p}^{on,in}$),

$$f_{t,p}^{pre,out} = f_{t,p}^{imp} + f_{t,p}^{on,in} \qquad \forall t \in T, p \in P \tag{D15}$$

Mass balance around onsite desalination technology is given by **Eq. (D16)**,

$$f_{t,p}^{on,out} + f_{t,p}^{on,brine} = f_{t,p}^{on,in} \qquad \forall t \in T, p \in P \tag{D16}$$

Again, the relation between inlet and outlet mass flowrate in onsite desalination unit is addressed by using the recovery factor (α^{on}),

$$f_{t,p}^{on,out} = \alpha^{on} \cdot f_{t,p}^{on,in} \qquad \forall t \in T, p \in P \qquad \forall t \in T, p \in P \tag{D17}$$

The following equation **Eq. (D18)** represents the maximum and minimum capacity of the desalination treatment.

$$F^{on,LO} \cdot y_{t,p}^{on} \leq f_{t,p}^{on,in} \leq F^{on,UP} \cdot y_{t,p}^{on} \qquad \forall t \in T, p \in P \tag{D18}$$

Centralized water treatment

Eq. (D19) shows the connection between inlet and outlet streams, and **Eq. (D20)** limits the inlet water of CWT k with the maximum capacity allowed.

$$f_{t,k}^{cwt,out} = \alpha_k^{off} \cdot \sum_{p \in P} f_{t,p,k}^{cwt,in} \qquad \forall t \in T, k \in K \tag{D19}$$

$$\sum_{p \in P} f_{t,p,k}^{cwt,in} \leq F_k^{cwt,UP} \qquad \forall t \in T, k \in K \tag{D20}$$

Objective function

Different objective functions have been considered depending on the scenario studied. In the first case, we solve a multi-objective optimization problem

considering two objective functions (**Eq. (D21)** and **Eq. (D22)**). Specifically, the gross profit to be maximized includes revenue from shale gas and expenses for wellpad construction and preparation, shale gas production and water-related costs. The life cycle impact assessment minimizes environmental impacts associated with water withdrawal, treatment and transportation. We obtain a set of solutions (i.e., the Pareto frontier) which present trade-off among the different objectives. For the calculation of the Pareto frontier, we use the epsilon-constraint method.

$$
\begin{aligned}
\max: GP = & \sum_{t\in T}\sum_{p\in P}\sum_{w\in RPW_p}\sum_{tt=0}^{tt\le t-1} F_{t-tt,p,w}^{gas}\cdot y_{tt+1,p,w}^{fb}\cdot \alpha_t^{gas} \\
& - \sum_{t\in T}\sum_{p\in P}[\sum_{d\in D}\alpha_d^{dis}\cdot f_{t,p,d}^{dis} \\
& + \sum_{w\in RPW_p}(\alpha^{drill}\cdot y_{t,p,w}^{hf}+\alpha^{prod}\cdot f_{t,p,w}^{gas}) \\
& + \sum_{f\in F}\alpha_f^{source}\cdot f_{t,p,f}^{source} \\
& + \alpha^{fr}\cdot f_{t,p}^{imp} \\
& + \alpha^{reuse}\cdot f_{t,p}^{imp}+\alpha^{treat}\cdot f_{t,p}^{on,in}+\alpha_p^{on}\cdot f_{t,p}^{on,in}+\beta_p^{on}\cdot y_p^{on} \\
& + \sum_{k\in K}\alpha_k^{cwt}\cdot f_{t,p,k}^{cwt,in} \\
& + (\sum_{f\in F} f_{t,p,f}^{source}\cdot D_{f,p}^{pad-source}+\sum_{k\in K} f_{t,k}^{cwt,in}\cdot D_{p,k}^{pad-cwt}+\sum_{pp\in P} f_{t,p,pp}^{pad,imp}\cdot D_{p,pp}^{pad-pad})\cdot\alpha_p^{trans}] \\
& + \alpha^{fwt}\cdot v_{fwt}+\alpha^{ft}\cdot v_{ft}+\beta^{ft}
\end{aligned}
\tag{D21}
$$

$$
\begin{aligned}
\min: LCIA = & \sum_{t\in T}\sum_{p\in P}[\sum_{f\in F}\sigma^{source}\cdot f_{t,p,f}^{source} \\
& + \sigma^{on}\cdot f_{t,p}^{on,in} \\
& + \sum_{k\in K}\alpha_k^{cwt}\cdot f_{t,p,k}^{cwt,in} \\
& + (\sum_{f\in F} f_{t,p,f}^{source}\cdot D_{f,p}^{pad-source}+\sum_{k\in K} f_{t,k}^{cwt,in}\cdot D_{p,k}^{pad-cwt}+\sum_{pp\in P} f_{t,p,pp}^{pad,imp}\cdot D_{p,pp}^{pad-pad})\cdot\sigma^{trans}]
\end{aligned}
\tag{D22}
$$

In the second case, the objective function to be minimized (see **Eq. (D23)**) only includes water-related cost, i.e., wastewater disposal cost, freshwater

withdrawal, friction reducer cost, onsite and offsite treatment cost, wastewater and freshwater transportation cost and storage tank cost.

$$
\begin{aligned}
TC = \sum_{t\in T}\sum_{p\in P}[\sum_{d\in D}\alpha_d^{dis}\cdot f_{t,p,d}^{dis} \\
+ \quad & \sum_{f\in F}\alpha_f^{source}\cdot f_{t,p,f}^{source} \\
+ \quad & \alpha^{fr}\cdot f_{t,p}^{imp} \\
+ \quad & \alpha^{reuse}\cdot f_{t,p}^{imp}+\alpha^{treat}\cdot f_{t,p}^{on,in}+\alpha_p^{on}\cdot f_{t,p}^{on,in}+\beta_p^{on}\cdot y_p^{on} \\
+ \quad & \sum_{k\in K}\alpha_k^{cwt}\cdot f_{t,p,k}^{cwt,in} \\
+ \quad & (\sum_{f\in F} f_{t,p,f}^{source}\cdot D_{f,p}^{pad-source}+\sum_{k\in K} f_{t,k}^{cwt,in}\cdot D_{p,k}^{pad-cwt}+\sum_{pp\in P} f_{t,p,pp}^{pad,imp}\cdot D_{p,pp}^{pad-pad})\cdot\alpha_p^{trans}] \\
+ \quad & \alpha^{fwt}\cdot v_{fwt}+\alpha^{ft}\cdot v_{ft}+\beta^{ft}
\end{aligned}
$$

(D23)

References

(1) U.S. Energy Information Administration (EIA). Annual Energy Outlook 2018 with Projections to 2050; DC, USA, **2018**.

(2) Schnoor, J. L. Shale Gas and Hydrofracturing. *Environ. Sci. Technol.* **2012**, 46 (9), 4686.

(3) Finkel, M.; Hays, J.; Law, A. The Shale Gas Boom and the Need for Rational Policy. *Am. J. Public Health* **2013**, 103 (7), 1161.

(4) Hughes, J. D. A Reality Check on the Shale Revolution. *Nature* **2013**, 494 (7437), 307.

(5) Weber, C. L.; Clavin, C. Life Cycle Carbon Footprint of Shale Gas: Review of Evidence and Implications. *Environ. Sci. Technol.* **2012**, 46 (11), 5688.

(6) Mauter, M. S.; Alvarez, P. J. J.; Burton, A.; Cafaro, D. C.; Chen, W.; Gregory, K. B.; Jiang, G.; Li, Q.; Pittock, J.; Reible, D.; Schnoor, J.L. Regional Variation in Water-Related Impacts of Shale Gas Development and Implications for Emerging International Plays. *Environ. Sci. Technol.* **2014**, 48 (15), 8298.

(7) Kuhn, M. and Umbach, F. Strategic Perspectives of Unconventional Gas: A game changer with implications for the EU's energy security. *Eur. Cent. Energy Resour. Secur.* (EUCERS). Dep. War Stud. King's Coll. London., **2011**. 1

(8) Michot, M. The Outlook for U.S. Gas Prices in 2020: Henry Hub Ar 3$ or 10$?; https://www.oxfordenergy.org/ (accessed September 18, 2018)

(9) U.S. Energy Information Administration (EIA). Technically Recoverable Shale Oil and Shale Gas Resources: An Assessment of 137 Shale Formations in 41 Countries Outside the United States; Washington, DC, USA, **2013**.

(10) U.S. Energy Information Administration. World Shale Resource Assessments. https://www.eia.gov/analysis/studies/worldshalegas/ (accessed Aug 24, 2018).

(11) Egan, M. U.S. energy independence looks "tantalizingly close" https://money.cnn.com/ (accessed Aug 22, 2018).

(12) Caulton, D. R.; Shepson, P. B.; Santoro, R. L.; Sparks, J. P.; Howarth, R. W.; Ingraffea, A. R.; Cambaliza, M. O. L.; Sweeney, C.; Karion, A.; Davis, K. J.; et al. Toward a Better Understanding and Quantification of Methane Emissions from Shale Gas Development. *Proc. Natl. Acad. Sci.* **2014**, 111 (17), 6237.

(13) Ellsworth, W. L. Injection-Induced Earthquakes. *Science.* **2013**, *341* (6142).

(14) Shaffer, D. L.; Arias Chavez, L. H.; Ben-sasson, M.; Romero-Vargas Castrillón, S.; Yip, N. Y.; Elimelech, M.; Sha, D. L.; Chavez, L. H. A.; Ben-sasson, M.; Castrillo, S. R. Desalination and Reuse of High-Salinity Shale Gas Produced Water: Drivers, Technologies, and Future Directions. *Environ. Sci. Technol.* **2013**, 47 (17), 9569.

(15) Takahashi, S.; Kovscek, A. R. Spontaneous Countercurrent Imbibition and Forced Displacement Characteristics of Low-Permeability, Siliceous Shale Rocks. *J. Pet. Sci. Eng.* **2010**, 71, 47.

(16) U.S. Environmental Protection Agency. Technical Development Document For Effluent Limitations Guidelines and Standars for the Oil and Gas Extraction Point Source Category; Washington, DC, **2016**.

(17) Estrada, J. M.; Bhamidimarri, R. A Review of the Issues and Treatment Options for Wastewater from Shale Gas Extraction by Hydraulic Fracturing. *Fuel* **2016**, 182, 292.

(18) Vidic, R. D.; Brantley, S. L.; Vandenbossche, J. M.; Yoxtheimer, D.; Abad, J. D. Impact of Shale Gas Development on Regional Water Quality. *Science* **2013**, 340 (6134).

(19) Barbot, E.; Vidic, N. S.; Gregory, K. B.; Vidic, R. D. Spatial and Temporal Correlation of Water Quality Parameters of Produced Waters from Devonian-Age Shale Following Hydraulic Fracturing. *Environ. Sci. Technol.* **2013**, 47 (6), 2562.

(20) Gregory, K. B.; Vidic, R. D.; Dzombak, D. A. Water Management Challenges Associated with the Production of Shale Gas by Hydraulic Fracturing. *Elements* **2011**, 7 (3), 181.

(21) Holditch, S. A. Getting the Gas Out of the Ground. *Chem. Eng. Prog.* **2012**.

(22) Beckman, B. A.; Ambulkar, A.; Umble, A.; Rosso, D.; Husband, J.; Cleary, J.; Sandino, J.; Goldblatt, M.; Horres, R.; Neufeld, R.; Mau, R.; Jeyayanagam, S. Considerations for Accepting Fracking Wastewater at Water Resource Recovery Facilities. **2012**, Water Environment Federation.

(23) Chen, H.; Carter, K. E. Water Usage for Natural Gas Production through Hydraulic Fracturing in the United States from 2008 to 2014. *J. Environ. Manage.* **2016**, 170, 152.

(24) Chen, G.; Wang, Z.; Nghiem, L. D.; Li, X. M.; Xie, M.; Zhao, B.; Zhang, M.; Song, J.; He, T. Treatment of Shale Gas Drilling Flowback Fluids (SGDFs) by Forward Osmosis: Membrane Fouling and Mitigation. *Desalination* **2015**, 366, 113.

(25) Balaba, R. S.; Smart, R. B. Total Arsenic and Selenium Analysis in Marcellus Shale, High-Salinity Water, and Hydrofracture Flowback Wastewater. Chemosphere 2012, 89 (11), 1437.

(26) Hayes, T.; Severin, B. F. Barnett and Appalachian Shale Water Management and Reuse Technologies; **2012**. G.T. Institute, Editor. 2009, Marcellus Shale Coalition: Des Plaines, IL.

(27) Olsson, O.; Weichgrebe, D.; Rosenwinkel, K.-H. Hydraulic Fracturing Wastewater in Germany: Composition, Treatment, Concerns. *Environ. Earth Sci.* **2013**, 70 (8), 3895.

(28) Almond, S.; Clancy, S. A.; Davies, R. J.; Worrall, F. The Flux of Radionuclides in Flowback Fluid from Shale Gas Exploitation. *Environ. Sci. Pollut. Res.* **2014**, 21 (21), 12316.

(29) Silva, J.; Gettings, R.; Kostedt, W. Produce Water Pretrearment for Water Recovery and Salt Production. RPSEA Final Report, **2014**.

(30) Ruyle, B.; Fragachan, F. E. Quantifiable Costs Savings by Using 100 % Raw Produced Water in Hydraulic Fracturing. *In SPE International; Ecuador*, **2015**.

(31) Mimouni, A.; Kuzmyak, N.; Oort, E. van; Sharma, M.; Katz, L. Compatibility of Hydraulic Fracturing Additives with High Salt Concentrations for Flowback Water Reuse. In *World Environmental and Water Resources Congress* **2015**; pp 496–509.

(32) Paktinat, J.; Neil, B. O.; Tulissi, M.; Service, T. W. Case Studies: Improved Performance of High Brine Friction Reducers in Fracturing Shale Reserviors. *SPE Int.* **2011**.

(33) El-Halwagi, M.; Elsayed, N.; Barrufet, M.; Eljack, F. Optimal Design of Thermal Membrane Distillation Systems for the Treatment of Shale Gas Flowback Water. *Int. J. Membr. Sci. Technol.* **2015**, 2 (2), 1.

(34) Michel, M. M.; Reczek, L.; Granops, M.; Rudnicki, P.; Piech, A. Pretreatment and Desalination of Flowback Water from the Hydraulic Fracturing. *Desalin. Water Treat.* **2015**, 57, 1.

(35) Malmali, M.; Fyfe, P.; Lincicome, D.; Sardari, K.; Wickramasinghe, S. R. Selecting Membranes for Treating Hydraulic Fracturing Produced Waters by Membrane Distillation. *Sep. Sci. Technol.* **2017**, 52 (2), 266.

(36) Coday, B. D.; Xu, P.; Beaudry, E. G.; Herron, J.; Lampi, K.; Hancock, N. T.; Cath, T. Y. The Sweet Spot of Forward Osmosis: Treatment of Produced Water, Drilling Wastewater, and Other Complex and Difficult Liquid Streams. *Desalination* **2014**, 333 (1), 23.

(37) Hayes, T. D.; Severin, B. F. Electrodialysis of Highly Concentrated Brines: Effects of Calcium. *Sep. Purif. Technol.* **2017**, 175, 443.

(38) Onishi, V. C.; Carrero-Parreño, A.; Reyes-Labarta, J. A.; Ruiz-Femenia, R.; Salcedo-Díaz, R.; Fraga, E. S.; Caballero, J. A. Shale Gas Flowback Water Desalination: Single vs Multiple-Effect Evaporation with Vapor Recompression Cycle and Thermal Integration. *Desalination* **2017**, 404.

(39) Onishi, V. C.; Carrero-Parreño, A.; Reyes-Labarta, J. A.; Fraga, E. S.; Caballero, J. A. Desalination of Shale Gas Produced Water: A Rigorous Design Approach for Zero-Liquid Discharge Evaporation Systems. *J. Clean. Prod.* **2017**, 140.

(40) Siirola, J. J.; Rudd, D. F. Computer-Aided Synthesis of Chemical Process Designs. From Reaction Path Data to the Process Task Network. *Ind. Eng. Chem. Fundam.* **1971**, 10 (3), 353.

(41) Balas, E. Disjunctive Programming; in *Annals of Discrete Mathematics* **1979**; pp 3–51.

(42) Raman, R.; Grossmann, I. E. Relation between MILP Modelling and Logical Inference for Chemical Process Synthesis. *Comput. Chem. Eng.* **1991**, 15 (2), 73.

(43) Raman, R.; Grossmann, I. E. Modelling and Computational Techniques for Logic Based Integer Programming. *Comput. Chem. Eng.* **1994**, 18 (7), 563.

(44) Nash, J. C. The (Dantzig) Simplex Method for Linear Programming. *Comput. Sci. Eng.* **2000**, 2 (1), 29.

(45) Adler, I.; Resende, M. G. C.; Veiga, G.; Karmarkar, N. An Implementation of Karmarkar's Algorithm for Linear Programming. *Math. Program.* **1989**, 44 (1–3), 297.

(46) Drud, A. CONOPT: A GRG Code for Large Sparse Dynamic Nonlinear Optimization Problems. *Math. Program.* **1985**, 31 (2), 153.

(47) Wächter, A.; Biegler, L. T. On the Implementation of an Interior-Point Filter Line-Search Algorithm for Large-Scale Nonlinear Programming. *Math. Program.* **2006**, 106 (1), 25.

(48) Gill, P. E.; Murray, W.; Saunders, M. A. SNOPT: An SQP Algorithm for Large-Scale Constrained Optimization. SIAM Rev. 2005, 47 (1), 99.

(49) Sahinidis, N. V. BARON: A General Purpose Global Optimization Software Package. *J. Glob. Optim.* **1996**, 8 (2), 201.

(50) Misener, R.; C. A. Floudas. ANTIGONE: Algorithms for CoNTinuous / Integer Global Optimization of Nonlinear Equations. *J. Glob. Optim.* **2013**, 57, 3.

(51) Vigerske, S.; Gleixner, A. SCIP: Global Optimization of Mixed-Integer Nonlinear Programs in a Branch-and-Cut Framework. Optim. Methods Softw. 2018, 33 (3), 563.

(52) Murtagh, B. A.; Saunders, M. A. Large-Scale Linearly Constrained Optimization. *Math. Program.* **1978**, 14 (1), 41.

(53) Han, S.-P. Superlinearly Convergent Variable Metric Algorithms for General Nonlinear Programming Problems. *Math. Program.* **1976**, 11 (1), 263.

(54) Bonnans, J. Frédéric; Gilbert, J. Charles; Lemaréchal, Claude; Sagastizábal, C. A. Numerical Optimization: Theoretical and Practical Aspects; Springer Berlin Heidelberg, 2006.

(55) IBM. CPLEX Optimization Studio CPLEX User's Manual; Armonk, NY, USA, **2013**.

(56) Gurobi Optimization, I. Gurobi Optimizer Reference Manual http://www.gurobi.com (accessed Mar 12, 2018).

(57) Inc, F. XPRESS Optimization Suite Release 8.1; California, USA, 2017.

(58) Dakin, R. J. A Tree-Search Algorithm for Mixed Integer Programming Problems. *Comput. J.* **1965**, 8 (3), 250.

(59) Duran, M. A.; Grossmann, I. E. An Outer-Approximation Algorithm for a Class of Mixed-Integer Nonlinear Programs. *Math. Program.* **1986**, 36, 307.

(60) Westerlund, T.; Pettersson, F. An Extended Cutting Plane Method for Solving Convex MINLP Problems. *Comput. Chem. Eng.* **1995**, 19, 131.

(61) Lee, S.; Grossmann, I. E. Logic-Based Modeling and Solution of Nonlinear Discrete/Continuous Optimization Problems. *Ann. Oper. Res.* **2005**, 139 (1), 267.

(62) Türkay, M.; Grossmann, I. E. Logic-Based MINLP Algorithms for the Optimal Synthesis of Process Networks. *Comput. Chem. Eng.* **1996**, 20 (8), 959.

(63) Vecchietti, A.; Lee, S.; Grossmann, I. E. Modeling of Discrete/Continuous Optimization Problems: Characterizaton and Formulations of Disjunctions and Their Relaxations. Comput. Chem. Eng. 2003, 27, 433.

(64) Trespalacios, F.; Grossmann, I. E. Review of Mixed-Integer Nonlinear and Generalized Disjunctive Programming Methods. *Chem. Ing. Tech.* **2014**, 86 (7), 991.

(65) Čuček, L.; Klemeš, J. J.; Kravanja, Z. A Review of Footprint Analysis Tools for Monitoring Impacts on Sustainability. *J. Clean. Prod.* **2012**, 34, 9.

(66) Rebitzer, G.; Ekvall, T.; Frischknecht, R.; Hunkeler, D.; Norris, G.; Rydberg, T.; Schmidt, W.-P.; Suh, S.; Weidema, B. P.; Pennington, D. W. Life Cycle Assessment. *Environ. Int.* **2004**, 30 (5), 701.

(67) ISO 14040:2006. Nvironmental Management – Life Cycle Assessment – Principles and Framework; Geneva, Switzerland, **2006**.

(68) ISO 14044:2006. Environmental Management – Life Cycle Assessment – Principles and Framework; Geneva, Switzerland, **2006**.

(69) Delft University of Technology. The Model of the Eco-costs/Value Ratio (EVR) http://www.ecocostsvalue.com (accessed Dec 1, 2017).

(70) Goedkoop M, Heijungs R, Huijbregts M, Schryver AD, Struijs J, V. Z. R. ReCiPe 2008. A Life Cycle Impact Assessment Method Which Comprises Harmonized Category Indicators at the Midpoint and the Endpoint Level. Report I: Characterisation., 1st ed.; Bilthoven, The Netherlands, The Netherlands, 2013.

(71) Zore, Ž.; Čuček, L.; Kravanja, Z. Syntheses of Sustainable Supply Networks with a New Composite Criterion – Sustainability Profit. *Comput. Chem. Eng.* **2017**, 102, 139.

(72) Cho, H.; Choi, Y.; Lee, S.; Sohn, J.; Koo, J. Membrane Distillation of High Salinity Wastewater from Shale Gas Extraction: Effect of Antiscalants. *Desalin. Water Treat.* **2016**, 57 (55), 26718.

(73) Beery, M.; Wozny, G.; Repke, J.-U. Sustainable Design of Different Seawater Reverse Osmosis Desalination Pretreatment Processes. *In Computer Aided Chemical Engineering* **2010**; Vol. 28, pp 1069–1074.

(74) Beery, M.; Hortop, A.; Wozny, G.; Knops, F.; Repke, J.-U. Carbon Footprint of Seawater Reverse Osmosis Desalination Pre-Treatment: Initial Results from a New Computational Tool. *Desalin. Water Treat.* **2011**, 31 (1–3), 164.

(75) Beery, M.; Wozny, G.; Repke, J. Computer-Aided Model-Based SWRO Pretreatment Process Design: A Multidisciplinary Approach. *IDA J.* **2012**, 18–25.

(76) Beery, M.; Lee, J. J.; Kim, J. H.; Repke, J.-U. Ripening of Granular Media Filters for Pretreatment of Seawater in Membrane Desalination. *Desalin. Water Treat.* **2010**, 15 (1–3), 29.

(77) Kraipech, W.; Chen, W.; Dyakowski, T.; Nowakowski, A. The Performance of the Empirical Models on Industrial Hydrocyclone Design. *Int. J. Miner. Process.* **2006**, 80 (2–4), 100.

(78) Emamjomeh, M. M.; Sivakumar, M. Review of Pollutants Removed by Electrocoagulation and Electrocoagulation/Flotation Processes. *J. Environ. Manage.* **2009**, 90 (5), 1663.

(79) Geraldino, H. C. L.; Simionato, J. I.; Freitas, T. K. F. de S.; Garcia, J. C.; Carvalho Júnior, O. De; Correr, C. J. Efficiency and Operating Cost of Electrocoagulation System Applied to the Treatment of Dairy Industry Wastewater. *Acta Sci. Technol.* **2015**, 37 (3), 401.

(80) Horner, P.; Anderson, J. a; Thompson, M. Mobile Clarification for Re-Use of Unconventional Oil and Gas Produced Water to Reduce Costs and Minimize Environmental Footprint. In *Unconventional Resources Technology Conference, Denver, Colorado*, 12-14 August 2013; Society of Exploration Geophysicists, American

Association of Petroleum Geologists, Society of Petroleum Engineers, **2013**; pp 2098–2107.

(81) Crittenden, J. C.; Trussell, R. R.; Hand, D. W.; Howe, K. J.; Tchobanoglous, G. Water Treatment Principles and Design, 3rd ed.; John Wiley and Sons: Georgia, **2012**.

(82) Hayes, T.; Severin, B. F. Barnett and Appalachian Shale Water Management and Reuse Technologies. In *Project report by Gas Technology Institute for Research Partnership to Secure Energy for America* (RPSEA); **2012**; pp 1–125.

(83) Loganathan, K.; Chelme-Ayala, P.; Gamal El-Din, M. Pilot-Scale Study on the Treatment of Basal Aquifer Water Using Ultrafiltration, Reverse Osmosis and Evaporation/Crystallization to Achieve Zero-Liquid Discharge. J. Environ. Manage. 2016, 165, 213.

(84) He, C.; Wang, X.; Liu, W.; Barbot, E.; Vidic, R. D. Microfiltration in Recycling of Marcellus Shale Flowback Water: Solids Removal and Potential Fouling of Polymeric Microfiltration Membranes. *J. Memb. Sci.* **2014**, 462, 88.

(85) Cluff, M. A.; Hartsock, A.; MacRae, J. D.; Carter, K.; Mouser, P. J. Temporal Changes in Microbial Ecology and Geochemistry in Produced Water from Hydraulically Fractured Marcellus Shale Gas Wells. *Environ. Sci. Technol.* **2014**, 48 (11), 6508.

(86) Camarillo, M. K.; Domen, J. K.; Stringfellow, W. T. Physical-Chemical Evaluation of Hydraulic Fracturing Chemicals in the Context of Produced Water Treatment. J. Environ. Manage. 2016, 183, 164.

(87) Edzwald, J. K. Dissolved Air Flotation and Me. Water Res. 2010, 44 (7), 2077.

(88) Wilson, J. R.; Mahank, T. A. Hydrocyclone Separation for the Remediation of Contaminated Sediment. In *ASEE North Central Section Conference*; **2016**; pp 1–8.

(89) Fakhru'l-Razi, A.; Pendashteh, A.; Abdullah, L. C.; Biak, D. R. A.; Madaeni, S. S.; Abidin, Z. Z. Review of Technologies for Oil and Gas Produced Water Treatment. *J. Hazard. Mater.* **2009**, 170 (2–3), 530.

(90) Houcine, M. Solution for Heavy Metals Decontamination in Produced Water/Case Study in Southern Tunisia, in: *International Conference on Health, Safety and Environment in Oil and Gas Exploration and Production*, Kuala Lumpur,Malaysia, 20–22 March. **2002**.

(91) Bilstad, T.; Espedal, E. Membrane Separation of Produced Water. *Water Sci. Technol.* **1996**, 34 (9), 239.

(92) Hutcherson, J. R. A Comparison of Electrocoagulation and Chemical Coagulation Treatment Effectiveness on Frac Flowback and Produced Water. *Master thesis*, Colorado State University **2015**.

(93) Beery, M.; Jekel, M. Novel Sustainable Concepts in Process Design and Assessment of Seawater Reverse Osmosis Pre-Treatment, *Doctoral Dissertation,* TU Berlin, **2013**.

(94) Cogan, J. D. The Removal of Barium, Strontium, Calcium and Magnesium from Hydraulic Fracturing Produced Water Using Precipitation with Traditional and Alternative Reactant Feedstocks. *Master Thesis*, Voinovich School of Leadership & Public Affairs, Ohio University, 2016.

(95) Ulucan, K.; Kabuk, H. A.; Ilhan, F.; Kurt, U. Electrocoagulation Process Application in Bilge Water Treatment Using Response Surface Methodology. *Int. J. Electrochem. Sci.* **2014**, 9 (5), 2316.

(96) Harish R. Acharya; Acharya, H. R.; Henderson, C.; Wang, H. Cost Effective Recovery of Low-TDS Frac Flowback Water for Re-Use. *Glob. Res.* **2011**.

(97) Vieira, L. G. M.; Barbosa, E. A.; Damasceno, J. J. R.; Barrozo, M. A. S. Performance Analysis and Design of Filtering Hydrocyclones. Brazilian *J. Chem. Eng.* **2005**, 22 (1), 143.

(98) Smith, R. M. Chemical Process Design and Integration; John Wiley and Sons, **2005**.

(99) Gumerman, R.; Culp, R.; Hansen, S. Estimating Water Treatment Costs; Environmental Protection Agency: United States, **1979**.

(100) McGivney, W.; Kawamura, S. Cost Estimating Manual for Water Treatment Facilities; John Wiley & Sons, Inc.: Hoboken, NJ, USA, **2008**.

(101) Turton, R.; Bailie, R. C.; Whiting, W. B.; Shaeiwitz, J. A.; Bhattacharyya, D. Analysis, Synthesis, and Design of Chemical Processes, Fourth.; Prentice Hall, 2012.

(102) Powell Water Systems, I. Electrocoagulation Vs. Chemical Coagulation http://powellwater.com/electrocoagulation-vs-chemical-coagulation/.

(103) Yang, L.; Grossmann, I. E.; Manno, J. Optimization Models for Shale Gas Water Management. *AIChE J.* **2014**, 60 (10), 3490.

(104) ICIS Trusted market intelligence for the global chemical, energy and fertilizer industries. Indicative Chemical Prices.

(105) Rosenthal, R. E. GAMS — A User 's Guide; 2016.

(106) Onishi, V. C.; Ruiz-Femenia, R.; Salcedo-Díaz, R.; Carrero-Parreño, A.; Reyes-Labarta, J. A.; Fraga, E. S.; Caballero, J. A. Process Optimization for Zero-Liquid Discharge Desalination of Shale Gas Flowback Water under Uncertainty. J. Clean. Prod. 2017, 164.

(107) Ashoor, B. B.; Mansour, S.; Giwa, A.; Dufour, V.; Hasan, S. W. Principles and Applications of Direct Contact Membrane Distillation (DCMD): A Comprehensive Review. *Desalination* **2016**, 398, 222.

(108) Drioli, E.; Ali, A.; Macedonio, F. Membrane Distillation: Recent Developments and Perspectives. *Desalination* **2015**, 356, 56.

(109) Deshmukh, A.; Boo, C.; Karanikola, V.; Lin, S.; Straub, A. P.; Tong, T.; Warsinger, D. M.; Elimelech, M. Membrane Distillation at the Water-Energy Nexus: Limits, Opportunities, and Challenges. *Energy Environ. Sci.* **2018**.

(110) Kim, J.; Kwon, H.; Lee, S.; Lee, S.; Hong, S. Membrane Distillation (MD) Integrated with Crystallization (MDC) for Shale Gas Produced Water (SGPW) Treatment. *Desalination* **2017**, 403, 172.

(111) Lokare, O. R.; Tavakkoli, S.; Rodriguez, G.; Khanna, V.; Vidic, R. D. Integrating Membrane Distillation with Waste Heat from Natural Gas Compressor Stations for Produced Water Treatment in Pennsylvania. *Desalination* **2017**, 413, 144.

(112) Chafidz, A.; Kerme, E. D.; Wazeer, I.; Khalid, Y.; Ajbar, A.; Al-Zahrani, S. M. Design and Fabrication of a Portable and Hybrid Solar-Powered Membrane Distillation System. *J. Clean. Prod.* **2016**, 133, 631.

(113) Silva, T. L. S.; Morales-Torres, S.; Castro-Silva, S.; Figueiredo, J. L.; Silva, A. M. T. An Overview on Exploration and Environmental Impact of Unconventional Gas Sources and Treatment Options for Produced Water. *J. Environ. Manage.* **2017**, 200, 511.

(114) Lokare, O. R.; Tavakkoli, S.; Wadekar, S.; Khanna, V.; Vidic, R. D. Fouling in Direct Contact Membrane Distillation of Produced Water from Unconventional Gas Extraction. *J. Memb. Sci.* **2017**, 524, 493.

(115) Gryta, M. Fouling in Direct Contact Membrane Distillation Process. *J. Memb. Sci.* **2008**, 325 (1), 383.

(116) Lawson, K. W.; Lloyd, D. R. Membrane Distillation. *J. Memb. Sci.* **1997**, 124 (1), 1.

(117) Duong, H. C.; Cooper, P.; Nelemans, B.; Cath, T. Y.; Nghiem, L. D. Optimising Thermal Efficiency of Direct Contact Membrane Distillation by Brine Recycling for Small-Scale Seawater Desalination. *Desalination* **2015**, 374, 1.

(118) Hitsov, I.; Maere, T.; De Sitter, K.; Dotremont, C.; Nopens, I. Modelling Approaches in Membrane Distillation: A Critical Review. *Sep. Purif. Technol.* **2015**, 142, 48.

(119) Tavakkoli, S.; Lokare, O. R.; Vidic, R. D.; Khanna, V. A Techno-Economic Assessment of Membrane Distillation for Treatment of Marcellus Shale Produced Water. *Desalination* **2017**, 416, 24.

(120) Swaminathan, J.; Chung, H. W.; Warsinger, D. M.; Lienhard, J. H. Simple Method for Balancing Direct Contact Membrane Distillation. *Desalination* **2016**, 383, 53.

(121) Lokare, O. R.; Tavakkoli, S.; Khanna, V.; Vidic, R. D. Importance of Feed Recirculation for the Overall Energy Consumption in Membrane Distillation Systems. *Desalination* **2018**, 428, 250.

(122) Elsayed, N. A.; Barrufet, M. A.; El-Halwagi, M. M. Integration of Thermal Membrane Distillation Networks with Processing Facilities. *Ind. Eng. Chem. Res.* **2014**, 53 (13), 5284.

(123) Lawson, K. W.; Lloyd, D. R. Membrane Distillation. I. Module Design and Performance Evaluation Using Vacuum Membrane Distillation. *J. Memb. Sci.* **1996**, 120 (1), 111.

(124) OLI Systems, I. OLI ESP User Guide - A Guide to Using OLI ESP 8.2; **2010**.

(125) Yun, Y.; Ma, R.; Zhang, W.; Fane, A. G.; Li, J. Direct Contact Membrane Distillation Mechanism for High Concentration NaCl Solutions. *Desalination* **2006**, 188 (1–3), 251.

(126) Chen, J. J. J. Comments on Improvements on a Replacement for the Logarithmic Mean. *Chem. Eng. Sci.* **1987**, 42 (10), 2488.

(127) Manda, A. K.; Heath, J. L.; Klein, W. A.; Griffin, M. T.; Montz, B. E. Evolution of Multi-Well Pad Development and Influence of Well Pads on Environmental Violations and Wastewater Volumes in the Marcellus Shale (USA). *J. Environ. Manage.* **2014**, 142, 36.

(128) Lira-Barragán, L. F.; Ponce-Ortega, J. M.; Guillén-Gosálbez, G.; El-Halwagi, M. M. Optimal Water Management under Uncertainty for Shale Gas Production. Ind. Eng. Chem. Res. 2016, 55 (5), 1322.

(129) Al-Obaidani, S.; Curcio, E.; Macedonio, F.; Di Profio, G.; Al-Hinai, H.; Drioli, E. Potential of Membrane Distillation in Seawater Desalination: Thermal Efficiency, Sensitivity Study and Cost Estimation. J. Memb. Sci. 2008, 323 (1), 85.

(130) Song, L.; Ma, Z.; Liao, X.; Kosaraju, P. B.; Irish, J. R.; Sirkar, K. K. Pilot Plant Studies of Novel Membranes and Devices for Direct Contact Membrane Distillation-Based Desalination. *J. Memb. Sci.* **2008**, 323 (2), 257.

(131) González-Bravo, R.; Ponce-Ortega, J. M.; El-Halwagi, M. M. Optimal Design of Water Desalination Systems Involving Waste Heat Recovery. *Ind. Eng. Chem. Res.* **2017**.

(132) González-Bravo, R.; Elsayed, N. A.; Ponce-Ortega, J. M.; Nápoles-Rivera, F.; El-Halwagi, M. M. Optimal Design of Thermal Membrane Distillation Systems with Heat Integration with Process Plants. *Appl. Therm. Eng.* **2015**, 75, 154.

(133) Bamu, H.; Abdelhady, F.; Baaqeel, H. M.; El-halwagi, M. M. Optimization of Multi-Effect Distillation with Brine Treatment via Membrane Distillation and Process Heat Integration. *Desalination* **2017**, 408, 110

(134) Wang, L. Z. Water Resources Allocation: A Cooperative Game Theoretic Approach. *J. Environ. Informatics* **2003**, 2 (2), 11.

(135) Gao, J.; You, F. Game Theory Approach to Optimal Design of Shale Gas Supply Chains with Consideration of Economics and Life Cycle Greenhouse Gas Emissions. *AIChE J.* **2017**, 63 (7), 2671.

(136) Bogardi, I.; Szidarovsky, F. Application of Game Theory in Water Management. *Appl. Math. Model.* **1976**, 1 (1), 16.

(137) Dinar, A.; Ratner, A.; Yaron, D. Evaluating Cooperative Game Theory in Water Resources. *Theory Decis.* **1992**, 32 (1), 1.

(138) Dinar, A.; Hogarth, M. Game Theory and Water Resources Critical Review of Its Contributions, Progress and Remaining Challenges. Found. Trends® Microeconomics **2015**, 11 (1–2), 1.

(139) Madani, K. Game Theory and Water Resources. *J. Hydrol.* **2010**, 381 (3–4), 225.

(140) Wei, S.; Yang, H.; Abbaspour, K.; Mousavi, J.; Gnauck, A. Game Theory Based Models to Analyze Water Conflicts in the Middle Route of the South-to-North Water Transfer Project in China. *Water Res.* **2010**, 44 (8), 2499.

(141) Raquel, S.; Ferenc, S.; Emery, C.; Abraham, R. Application of Game Theory for a Groundwater Conflict in Mexico. *J. Environ. Manage.* **2007**, 84 (4), 560.

(142) Gillies, D. B. Solutions to General Non-Zero-Sum Games. In A. W. Tucker, R. D. Luce (Eds.), Contributions to the Theory of Games IV; Princeton University Press: Princeton, **1959**; pp 47–85.

(143) Shapley, L. S. A Value for N-Person Games. In A. W. Tucker, H. W. Kuhn (Eds.), Contributions to the Theory of Games II; Princeton University Press: Princeton, **1953**; pp 307–317.

(144) Hamlen, S. S., Hamlen, W. A., & Tschirhart, J. The Use of the Generalized Shapley Allocation in Joint Cost Allocation. *Account. Rev.* **1980**, 55 (2), 269.

(145) Drechsel, J.; Kimms, A. Computing Core Allocations in Cooperative Games with an Application to Cooperative Procurement. *Int. J. Prod. Econ.* **2010**, 128 (1), 310.

(146) Carrero-Parreño, A.; Reyes-Labarta, J. A.; Salcedo-Díaz, R.; Ruiz-Femenia, R.; Onishi, V. C.; Caballero, J. A.; Grossmann, I. E. Holistic Planning Model for Sustainable Water Management in the Shale Gas Industry. Ind. Eng. Chem. Res. 2018, 57 (39), 13131.

(147) Ehrgott, M. Multicriteria Optimization, 2nd ed.; Springer: Heidelberg: Germany, **2005**.

(148) Gao, J.; You, F. Shale Gas Supply Chain Design and Operations toward Better Economic and Life Cycle Environmental Performance: MINLP Model and Global Optimization Algorithm. ACS Sustain. Chem. Eng. 2015, 3 (7), 1282.

(149) Yang, L.; Grossmann, I. E.; Mauter, M. S.; Dilmore, R. M. Investment Optimization Model for Freshwater Acquisition and Wastewater Handling in Shale Gas Production. AIChE J. 2015, 61 (6), 1770.

(150) Carrero-Parreño, A.; Onishi, V. C.; Salcedo-Díaz, R.; Ruiz-Femenia, R.; Fraga, E. S.; Caballero, J. A.; Reyes-Labarta, J. A. Optimal Pretreatment System of Flowback Water from Shale Gas Production. Ind. Eng. Chem. Res. 2017, 56 (15), 4386.

(151) Carrero-Parreño, A.; Onishi, V. C.; Ruiz-Femenia, R.; Salcedo-Díaz, R.; Caballero, J. A.; Reyes-labarta, J. A. Multistage Membrane Distillation for the Treatment of Shale Gas Flowback Water: Multi-Objective Optimization under Uncertainty. Comput. Aided Chem. Eng. 2017, 40, 571.

(152) Petroleum Services Association of Canada. How many jobs does a single drilling rig create and where are they? https://www.albertaoilmagazine.com/2015/05/drilling-rig-jobs/ (accessed Mar 12, 2018).

(153) United States Department of Labor. Usual Weekly Earnings of Wage and Salary Workers https://www.bls.gov/news.release/wkyeng.toc.htm (accessed Mar 12, 2018).

(154) Urban Institute & Brookings Institution. Tax Policy Center http://www.taxpolicycenter.org/taxvox (accessed Mar 12, 2018).